

https://dspace.org/

Recovery of valuable minerals from acid mine drainage using thermally activated cryptocrystalline magnesite

Masindi Vhahangwele

2022

https://hdl.handle.net/10539/34138

Downloaded from a DSpace repository. https://dspace.org/



Recovery of valuable minerals from acid mine drainage using thermally activated cryptocrystalline magnesite

By

Vhahangwele Masindi (Pr. Sci. Nat.)

Student:	**Vhahangwele Masindi**
Student No:	747943
Course:	CIVN7019A
Program:	Master of Science in Engineering:
	Civil and Environmental Engineering
Supervisor:	**Prof John Ndiritu**
	University of the Witwatersrand
Co-supervisor:	**Prof Johannes Philippus Maree**
	ROC Water Technologies and University of Limpopo

2021

ABSTRACT

Acid mine drainage (AMD) is a biorecalcitrant and toxic wastewater matrix that causes serious environmental, ecotoxicological, carcinogenic, and socio-economic stresses. It is typically encountered in countries with strong mining industry, including South Africa, the USA, Canada, and China. In recent decades, acid mine drainage (AMD) has been a topical issue of prime concern, primarily due to the magnitude of its environmental, ecotoxicological, health, and socio-economic impacts. Mining activities are notorious for their environmental footprint and AMD is the acidic water effluent that typically originates from metal (primarily gold) and coal mines. The problem persists in numerous countries with a strong mining industry. Even though AMD has a low to very low (acid) pH, it also contains dissolved toxic metals (e.g. copper and iron), both causing detrimental effects to receiving aquatic ecosystems. Practical and cost-effective solutions for the prevention of negative impacts and particularly for its treatment at large scale has yet to be introduced. Traditionally, active (driven by frequent input of chemicals, energy, and equipment) and passive (typically based on oxidation or reduction) treatment technologies have been employed. Active systems tend to be more efficient than passive ones in contaminants removal; however, at the expense of process complexity, cost, and energy consumption. More recently, and under the circular economy concept, the recovery of valuable minerals from AMD has been a topical issue of prime interest particularly for mine dominated regions that produce highly concentrated AMD. In light of the above, AMD in South Africa is rich in elevated levels of Al, Fe, Mn and sulphate amongst miniscule levels of heavy metals, metalloids, rare earth metals and radionuclides.

This study was developed with the aim of using activated magnesite for the recovery of Al, Fe, Mn, and sulphate from AMD. Batch experimental procedures were used to fulfil the goals of this study, specifically the one factor at a time (AFAAT) whereby one factor was varied with the rest fixed. The optimised parameters include contact time, and feed stock dosage on the recovery of valuable minerals. The metals were recovered through sequential and fractional precipitation at varying pH gradients. The obtained results were analysed using the state of the art analytical techniques, such as Inductively coupled plasma mass spectrometry (ICP-MS), Gallery™ Plus Discrete Analyzer photo spectrometer, HANNA Multi-parameter probe, Inductively coupled plasma - optical emission spectrometry (ICP-OES), Fourier transform infrared spectroscopy (FTIR), X-ray diffraction (XRD), and X-ray fluorescence (XRF), which were used along with a high resolution scanning electron microscope (HR-SEM) coupled with

energy dispersive X-Ray spectroscopy (EDS). The pH Redox Equilibrium (in C language) (PHREEQC) was used to substantiate aqueous and solids experimental results. The experiments were conducted in triplicate and results were reported as mean values. The samples were analysed in an ISO/IEC 17025:2017 accredited laboratory, i.e., at Magalies Water Services Laboratory, Brits, North West, South Africa.

Findings from this study confirmed the feasibility of recovering Al, Fe, Mn and sulphate from real AMD and their relativity to solution pH. PHREEQC confirmed that prevalent species existed as di-valents, tri-valents, and oxyanions in aqueous solution. The sensitivity study registered Fe to have been recovered at pH ≥ 3 - 3.5, gypsum at pH ≥ 4 - 9, Al at pH ≥ 6.5, Mn at pH ≥ 9.5, Cu at pH ≥ 7, Zn at pH ≥ 8, Pb at pH ≥ 8 and Ni at pH ≥ 9. Essentially, greater than 99% removal efficiency was achieved for all the metals (Al Fe and Mn) for given pH regimes except for sulphate that attained 40% removal efficacy. Other metals such as Zn, Cu, Ni, and Pb were also removed from AMD. The reduction of chemical species in the treated AMD further confirmed the attenuation of chemical species. This corroborated the sludge results. The experimental results corroborated the geochemical modelling and characterisation results. The fate of chemical species were verified using a synergy of HR-SEM equipped with EDS and PHREEQC amongst other analytical techniques. Lastly, but not least, the PHREEQC geochemical model suggested that chemical species were removed as (oxy)-hydroxides, (oxy)-hydro-sulphates, and metals hydroxides. Ca and SO_4^{2-} were removed as gypsum ($CaSO_4 \cdot 2H_2O$) and Pb, Fe, and Al as hydroxyl sulphate minerals. Mg formed a complex of $MgSO_4$ in solution and it was removed as $Mg(OH)_2$ at pH ≥ 9.5. Overall, this study proved the pragmatism and feasibility of recovering valuable minerals from AMD. Finally, feasible and practical avenues for minerals harvesting from AMD for potential valorisation and beneficiation were confirmed and scientifically proven. Future research studies should focus on the enhancement of the purity of minerals recovered from AMD and the beneficiation of the product water for drinking purposes.

Keywords: Acid mine drainage; thermal activation; cryptocrystalline magnesite; treatment; sequential recovery; and PHREEQC geochemical model.

TABLE OF CONTENTS

ABSTRACT i
LIST OF FIGURES vi
LIST OF TABLES viii
DECLARATION ix
ACKNOWLEDGEMENT x
ABBREVIATIONS AND ACRONYMS xi
PUBLICATION OUTPUTS xii
CHAPTER ONE 1
1.1 Background information 1
1.2 Problem statement 4
1.3 Aim and specific objectives 5
1.3.1 Aim of the study 5
1.3.2 Specific objectives 5
1.4 Significance of the study 5
1.5 Structure of the thesis 6
CHAPTER TWO 7
LITERATURE REVIEW 7
2.1 Introduction 7
2.2 AMD formation pathway 8
2.2.1 Physicochemical characteristics 11
2.2.1.1 Physical properties 12
2.2.1.2 Chemical properties 12
2.3 Ecotoxicological impacts 14
2.4 Abatement techniques 15
2.4.1 Utilisation of covering materials 16
2.4.2 Stabilization using alkaline materials 16
2.4.3 Passivation or microencapsulation 16
2.4.4 Bactericide application 17
2.4.5 Control of oxygen and water ingression 17
2.4.6 Backfilling of voids and opencast trenches 18
2.4.7 Application of abatement techniques in practice 18

2.4.7 Beneficiation of tailings 19
2.5 Treatment technologies 21
2.5.1 Active processes 21
2.5.2 Passive processes 23
2.5.2.3 Advantages and disadvantages of AMD treatment systems 24
2.5.3 Hybrid processes 25
2.5.4 Integrated or multi-staged approach 26
2.6 Mechanisms for contaminants removal, recovery and synthesis 32
2.6.1 Precipitation/oxidation process 32
2.6.2 Adsorption/ion exchange process 34
2.6.3 Filtration 36
2.6.4 Bio- and-phyto-remediation 36
2.7 Geochemical modelling 37
2.8 AMD beneficiation and valorisation 38
2.8.1 Water and drinking water reclamation 39
2.8.2 Recovery of valuable minerals 39
2.8.3 Synthesis of valuable minerals 40
2.8.4 Irrigation with AMD 40
2.8.5 Co-treatment of municipal wastewater 41
2.8.6 Recovery and production of sulphuric acid 41
2.9 Factors hampering AMD valorisation and beneficiation 42
2.9.1 Purity of the recovered material as a limiting factor 42
2.9.2 Quantity of the recovered material 43
2.9.3 Conditions suitable for minerals recovery 43
2.10 Summary of the literature review 44
CHAPTER THREE 45
MATERIALS AND METHODS 45
3.1 Acquisition of the samples 45
3.2 Optimisation of the recovery of chemical species 45
3.3 Quality control and quality assurance 47
3.4 Characterisation 48
3.4.1 Characterisation of aqueous samples 48
3.4.2 Characterisation of solid samples 48

3.5 Geochemical modelling 49
CHAPTER FOUR 50
RESULTS AND DISCUSSIONS 50
4.1 Feed and processed products quality 50
4.2 Effect of pH on the removal levels of chemical species 51
4.3 Simulation of the effect of pH and dosage on the recovery of chemical species 52
4.4 Sensitivity analysis 53
4.5 Simulation of the precipitation potential with PHREEQC 54
4.6 Treatment of AMD using activated magnesite 55
4.7 Solid characterisation 56
4.7.1 Map spectrums for elemental composition 56
4.7.2 Morphological properties 58
4.7.3 Elemental composition analysis 61
4.7.4 Spot analysis using HR-SEM-EDS 68
4.8 Mineralogical composition 82
4.9 Chemical species-functional groups using FTIR 83
4.10 PHREEQC modelling of saturation index of all the chemical components 84
CHAPTER FIVE 86
RECOMMENDATION AND CONCLUSIONS 86
5.1 Conclusions and lessons learnt 86
5.2 Recommendations 87
REFERENCES 89

LIST OF FIGURES

Figure 2.1: Acid mine drainage effluent from underground shaft in Witwatersrand basin. 10
Figure 2.2: A schematic illustration of the AMD treatment process and products analysis. 20
Figure 2.3: Schematic illustration of a typical AMD active treatment train, along with the techniques for the recovered minerals and the reclaimed water analyses. 23
Figure 2.4: The schematic illustration of the AMD treatment process and products analysis.24
Figure 2.5: The schematic illustration of the hybrid treatment process. 26
Figure 2.6: Schematic of atypical integrated (multi-stage) AMD treatment system. 27
Figure 2.7: An illustration of different adsorption mechanisms on an adsorbent. 35
Figure 4.1: The effect of feedstock dosage (i.e. activated magnesite) on pH and chemical species removal (Conditions: 1000 mL solution, 250 rpm shaking speed, ≤32 μm particle size, 60 min reaction, 26 °C temperature). 51
Figure 4.2: Simulation of the effect of feedstock dosage (i.e. activated magnesite) on pH and chemical species levels using PHREEQC geochemical model (Water Q4 database). 53
Figure 4.3: The sensitive dosage (i.e. activated magnesite) and its effects on pH and chemical species levels (Conditions: 1000 mL solution, 250 rpm shaking speed, ≤32 μm particle size, 60 min reaction, 26 °C temperature). 53
Figure 4.4: The simulation of the mineral phases to be recovered from AMD using activated magnesite by PHREEQC geochemical model (water Q4 database). 54
Figure 4.5: The map sum spectrum of the elemental composition of activated magnesite and recovered elements at different pH ranges from the treatment of real AMD with specified dosages of activated magnesite. 58
Figure 4.6: FESEM images of the morphological properties of activated magnesite (a), and minerals recovered at different pH (pH from ≥ 3 to ≥ 10.5 [b-h]) at 1 μm and 100 nm.....59
Figure 4.7: The FESEM image and mapping of (a) the feed material (activated magnesite) and (b) product mineral at pH = 3. 61
Figure 4.8: The FESEM image and mapping of (c) material recovered at pH = 3.5 and (d) product mineral recovered at pH = 4. 63
Figure 4.9: The FESEM image and mapping of (e) material recovered at pH≤6.5 and (f) product mineral recovered at pH ≤ 8.....65

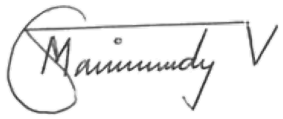
Figure 4.10: The FESEM image and mapping of (g) material recovered at pH≤9.5 and (h) mineral recovered at pH ≤ 10.5.....67
Figure 4.11(a): The SEM-EDS showing the spot analysis image, and the relevant EDS spectra (Wt. %) of the feedstock which was used for minerals recovery. 69
Figure 4.11(b): The SEM-EDS showing the spot analysis image, and the relevant EDS spectra (Wt. %) of the recovered mineral at pH = 3. 71
Figure 4.11(c): The SEM-EDS showing the spot analysis image, and the relevant EDS spectra (Wt. %) of the recovered mineral at pH≤3.5. 72
Figure 4.11(d): The SEM-EDS showing the spot analysis image, and the relevant EDS spectra (Wt. %) of the recovered mineral at pH≤4. 74
Figure 4.11(e): The SEM-EDS showing the spot analysis image, and the relevant EDS spectra (Wt. %) of the recovered mineral at pH≤6.5. 76
Figure 4.11(f): The SEM-EDS showing the spot analysis image, and the relevant EDS spectra (Wt. %) of the recovered mineral at pH≤8. 77
Figure 4.11(g): The SEM-EDS showing the spot analysis image, and the relevant EDS spectra (Wt. %) of the recovered mineral at pH≤9.5. 79
Figure 4.11(h): The SEM-EDS showing the spot analysis image, and the relevant EDS spectra (Wt. %) of the recovered mineral at pH≤10.5. 81
Figure 4.12: The mineral composition of minerals recovered at different pH ranges (pH ≤3 to pH≤10.5). 82
Figure 4.13: The information on the functional groups of feedstock and recovered materials. 83
Figure 4.14: The saturation indices (SI) of mineral phases which were recovered from AMD at different pH ranges using PHREEQC geochemical model.....……85

LIST OF TABLES

Table 2.1: Indicative volumes of AMD generated in mining fields situated in several regions of South Africa. 11
Table 2.2: The chemical composition of acid and neutral mine drainages. 13
Table 2.3: Different piloted technologies, their advantages, and disadvantages 29
Table 2.4: Different alkaline materials used for the precipitation of metals from AMD. 32
Table 2.5: Precipitation of metals at varying pH gradients using calcined magnesite. 33
Table 3.1: Examined parameters and values for the recovery of valuable minerals from AMD. 46
Table 3.2: The analytical instruments which were used to determine the physical and chemical parameters of water samples. 48
Table 3.3: The equipment used to determine the properties of the raw and recovered minerals. 49
Table 4.1: The physico-chemical characteristics of feed water, product water and their respective dosages. 50
Table 4.2: The physico-chemical properties of raw and treated AMD. 55

DECLARATION

I, **Vhahangwele Masindi**, hereby declare that this dissertation submitted for the Master of Science in Civil and Environmental Engineering at the University of Witwatersrand by me is my own work, that it has not been submitted for any degree or examination at this or any other institution, and that all the sources I have used or quoted have been indicated and duly acknowledged by complete references.



ACKNOWLEDGEMENT

I would like to express my whole-heartily thanks to respective individuals who in one way or another participated and prolonged their valuable support during planning and completion of this dissertation.

Firstly, I would like to thank God who has always been wonderful to me. I would also like to express my deep appreciation and gratitude to my principal and co-supervisor, Prof John Ndiritu and Prof Jannie Maree, respectively, for their patient guidance and unwearyingly mentorship and consideration they provided to me, all the way from the start of this MSc degree through to its completion. I am certain that this dissertation would have not been possible without their support, understanding and encouragement.

The funding received from the Council for Scientific and Industrial Research (CSIR) towards my MSc in Civil and Environmental Engineering played a significant role in ensuring that I complete this qualification. Their financial support and assistance is profoundly acknowledged and appreciated. The National Research foundation for funding the conference to Finland is also acknowledge for their financial support. Without their financial assistance, some of the milestones were not going to be viable.

My greatest profound heartfelt appreciation and deepest gratitude goes to my family, colleagues, and friends for their moral support, guidance and wisdom. Without them, none of this could have been accomplished.

Lastly, but not least, I would like to thank the laboratory staff at the University of Pretoria (UP), Magalies Water (MW) and the Council for Scientific and Industrial Research (CSIR) for their endless effort and dedication towards ensuring that my samples are timeously analysed and characterised.

ABBREVIATIONS AND ACRONYMS

Abbr.	Meaning	Abbr.	Meaning
AMD	Acid mine drainage	EC	Electrical Conductivity
EDS	Energy-dispersive spectroscopy	TDS	Total Dissolve Solids
XRD	X-ray powder diffraction	HR	High Resolution
XRF	X-ray fluorescence	WHO	World Health Organisation
SEM	Scanning electron microscopy	FB	Focused Beam
RSA	Republic of South Africa	BDL	Below Detection Limit
GDP	Gross Domestic Products	UF	Ultra Filtration
ARD	acid rock drainage	MF	Micro Filtration
NMD	neutral mine drainage	NF	Nano Filtration
AGP	acid generation potential	RO	Reverse Osmosis
ANP	acid neutralisation potential	MD	Membrane Distillation
AFAAT	one-factor-at-a-time	UN	United Nations
ICP-OES	Inductively Coupled Plasma Atomic Emission Spectroscopy		
ICP-MS	Inductively Coupled Plasma Mass Spectroscopy		
EPA	Environmental Protection Agency		
FTIR	Fourier-transform infrared spectroscopy		
NIST	National Institute Standards and Technology		
EPA	Environmental Protection Agency		
PHREEQC	pH Redox Equilibrium (in C language)		
LMIC	Low and Middle Income Communities		
CSIR	Council for Scientific and Industrial Research		

NB: Please refer to the periodic table for chemical elements.

PUBLICATION OUTPUTS

Published papers

Manuscript

Masindi, V., Ndiritu, J. G. & Maree, J. P. 2018. Fractional and step-wise recovery of chemical species from acid mine drainage using calcined cryptocrystalline magnesite nano-sheets: An experimental and geochemical modelling approach. **Journal of Environmental Chemical Engineering**, 6**,** 1634-1650.

Conference proceedings

Masindi, V. and Ndiritu, J. G. 2018. Fractional and sequential recovery of inorganic contaminants from acid mine drainage using cryptocrystalline magnesite. The 13th International Mine Water Association Congress – "Mine Water & Circular Economy – A Green Congress". IMWA 25-30 june 2017 – Mine Water & Circular Economy" Lappeenranta, Finland, ISBN 978-952-335-065-6, Wolkersdorfer, Christian; Sartz, Lotta; Sillanpää, Mikka & Häkkinen, Antti (eds).

Paper under review

V Masindi, S Foteinis, P Renforth, J Ndiritu, JP Maree, M Tekere, E Chatzisymeon. (2021). Challenges and possible avenues for the treatment, beneficiation, and valorization of acid mine drainage: A review. Draft ready for submission.

Draft paper

Masindi, V., Ndiritu, J. G. & Maree, J. P. 2021. Fate of Al, Fe, Mn and sulphate post their sequential recovery using activated magnesite. Draft ready for submission.

CHAPTER ONE

INTRODUCTION

1.1 Background information

Post-industrial revolution, ubiquitous mining of valuable minerals for myriads of industrial application gained immense attention and massive momentum. This has contributed to economic growth of different countries and afield. Primarily, the observed progress was underpinned to notable impacts of mining activities towards job creation, poverty alleviation and enhancement of the through-put rate for gross domestic products (GDP) (Tutu et al., 2008). Albeit, the legacy of mining activities results in numerous secondary impacts and devastating effects that degrade the environment and its suitability to foster life. In the Republic of South Africa (RSA), intensive mining of coal and gold for myriads of industrial application has gained much attention (Masindi, 2016, Masindi et al., 2019a). In counter of its much-needed benefits, vicious impacts that led to the wake of serious environmental problems that require urgent attention to curtail their potential ecological impacts and footprints commenced to teeth-up. Of prime concern is the ruthless generation of acidic and metalliferous drainage known as acid mine drainage (AMD) (Park et al., 2019, Rambabu et al., 2020). This effluent stream results from the oxidation of sulphide bearing minerals on contact with water and oxygen. In this case, pyrite (FeS_2) will be used as an example to illustrate the formation of AMD as denoted below (Eqn. 1.1-1.4) (Simate and Ndlovu, 2014, Kefeni et al., 2018):

$$2FeS_{2(s)} + 7O_{2(g)} + 2H_2O \xrightarrow{\text{bacteria}} 2Fe^{2+}_{(aq)} + 4H^{+}_{(aq)} + 4SO^{2-}_{4(aq)} \quad (1.1)$$

$$4Fe^{2+}_{(aq)} + O_{2(g)} + 4H^{+}_{(aq)} \rightarrow 4Fe^{3+}_{(aq)} + 2H_2O_{(l)} \quad (1.2)$$

$$FeS_{2(s)} + 14Fe^{3+} + 8H_2O \rightarrow 15Fe^{2+} + 2SO^{2-}_{4(l)} + 16H^{+} \quad (1.3)$$

$$Fe^{3+}_{(aq)} + 3H_2O_l \rightarrow Fe(OH)_{3(s)} + 3H^{+}_{(aq)} \quad (1.4)$$

The formation of AMD is meticulously mediated by iron and sulphur oxidising bacteria hence leading to a self-perpetuating reaction as denoted in Eqn. 1.1 – 1.4. This microbial community is characterised of Thiobacillus ferrooxidans, ferrobacillus sulphooxidans and T. thiooxidans (Baker and Banfield, 2003, Sheoran et al., 2011c). The outlined reactions (Eqn. 1.1-1.4) summarise the conversion of Fe(II) to Fe(III) and sulphate formation including acidity production. The acidic nature of the product water encourages the dissolution of metals from the surrounding rocks and lithologies. This leads to high electrical conductivity (EC) due to elevated levels of total dissolved solids (TDS). According to documented studies, AMD has

been reported to be predominated by Al, Fe, Mn and sulphate amongst traces of other chemical species such as Cu, Zn, Ni, Pb, Co, Cr, As, rare earth metals, and radionuclides but this is site and geology dependent. The composition of AMD can drastically vary but this is primarily due to the weathered rocks and lithologies and the surrounding mineral phases (Sheoran et al., 2011c, Simate and Ndlovu, 2014, Kefeni et al., 2017b, Skousen et al., 2017, Park et al., 2019).

The mine drainage formation concept depends on the principle of acidity and alkalinity, where, the product drainage is dependent on those factors and the underlying geology. The drainage which results from an area that is rich in base minerals such as limestone and magnesite will be circum-neutral. However, if the drainage results from alkalinity free region, the product effluent will be acid mine drainage (AMD) (Sheoran et al., 2011c, Simate and Ndlovu, 2014, Nordstrom et al., 2015b, Kefeni et al., 2017b). The discharge of this effluent to different receiving ecosystems has posed numerous ecological impacts and renders the environment unfit to perform its intrinsic values. As reported in ecotoxicological studies (Neculita et al., 2008, Netto et al., 2013, Talukdar et al., 2016), chemical species in AMD can result to numerous effects towards living organisms. It can also affect the food security in a given country and afield due to contamination of water resources. Aquatic life will also diminish due to high acidity and toxic chemical species, including the deposition of "yellow boy" at the bottom of riverine ecosystem hence affecting the habitat of benthic organisms. The magnitude of its ecological, social and economic impacts justifies the need to come-up with pragmatic and prudent technologies to treat AMD and curtail its ecological impacts (Zumarán Farfán et al., 2003, Naidoo, 2014, Park et al., 2014, Simate and Ndlovu, 2014, Truter et al., 2014, Nordstrom et al., 2015b, Jain et al., 2016).

In light of what has been mentioned above, a wide array of technologies has been developed for the management of AMD. This includes abatement of its generation and its treatment post generation (Naidu et al., 2019, Park et al., 2019). These treatment technologies include active, passive, hybrid and integrated technologies. Over numerous decades, these initiatives have been employed for the treatment of AMD. The advantage was with their good ability in removing contaminants but the generation of sludge that incurs additional costs on disposal becomes problematic and renders most technologies undesired. These technologies rely on different mechanisms such as precipitation, filtration, ion exchange, adsorption, phytoremediation and freeze crystallization (Nleya et al., 2016, Kefeni et al., 2017b, Fernando et al., 2018, Agboola, 2019, Neculita and Rosa, 2019, Park et al., 2019). Lately, although in

response to conventional challenges, majority of technologies are focusing on minerals recovery using different approach (Buzzi et al., 2013, Masindi et al., 2019a).

The filtration techniques have significantly contributed in the reclamation of drinking water but they generate brine which becomes an ecological issue of concern. In addition, the technique require a lot of energy to purify water with limited recovery at time (Agboola, 2019). Adsorption and ion exchange have been effective in removing contaminants but their selectivity and limitation of quick saturation in high concentration limit its application (Masindi et al., 2019a). Phytoremediation has also received massive attention but the challenges with their limited efficacy due to high sensitivity and demands for space and adequate time limit its application (Rojas et al., 2014, Gu, 2018, Kiiskila et al., 2019). However, precipitation has received massive attention recently. This is attributed to the ability to be independent of concentration and high efficacy in removing metals at different pH levels as a benign approach. To fulfil that, different alkalinity generating materials (Ca, Mg, and Na) such as lime, limestone, hydrated lime, magnesite, periclase, brucite, soda ash, and caustic soda amongst others (Masindi et al., 2017a). Different researchers have employed these materials to recover valuable minerals from AMD and valorised them (Kefeni et al., 2017b, Masindi et al., 2019a).

Specifically, Hedrich and Johnson (2014) investigated the use of bio-reactors for the recovery of minerals from AMD and its holistic treatment whilst Akinwekomi et al. (2017a) demonstrated the feasibility of recovering Fe (III) and Fe(II) from AMD and explore its facile use in the synthesis of magnetite. Seo et al. (2017) evaluated the use of hydrated lime, soda ash and caustic soda for the recovery of Fe, Al, and Mn in AMD by sequential selective precipitation with pH control. A study by Oh et al. (2016) reported that sodium sulphide has the potential to selectively recover Cu and Zn in drainage discharged from an operating mine. Park et al. (2015) investigated the recovery of metals from acid mine drainage through electro-reactions.

The Republic of South Africa has been perceived to be well-endowed by natural resources such as magnesite. This mineral has been documented to have high alkalinity. Geologically, it has been documented to comprise the cryptocrystalline nature (Masindi, 2020). A study by Masindi et al. (2015a) reported that a maximum pH of ≈ 10.2 can be reached using cryptocrystalline magnesite. It has been successfully evaluated for the treatment of acid mine drainage in both coal and gold mine effluents (Masindi et al., 2015a, Masindi et al., 2017a). However, it has not been explored for sequential recovery of metals from AMD. Therefore, this study explored

sequential recovery of chemical from AMD using the thermo-mechano-chemically activated cryptocrystalline magnesite. The fate of chemical species was further determined using the state-of-art and advanced analytical instruments. Results from the laboratory experiments were complemented with PHREEQC geochemical modelling.

1.2 Problem statement

In order to safeguard the community and minimize ecotoxicological effects associated with different waterborne contaminants, the regulatory frameworks require water to comply with different water quality guidelines, specifications, and standards. This ensures that water which is fit for a defined purpose and end-use is produced (SABS, 2015, EPA, 2017, WHO, 2017). According to the United Nations (UN) report, majority of people in low- and middle-income communities (LMIC) lack safe water that is suitable for utilisation. This also affects the food security in those countries since water is a fundamental resource in agricultural production (The United Nations., 2018). South Africa is a water scarce country due to it being located between arid to semi-arid regions. The ever-increasing contamination of the environment with AMD further compounds the water availability challenges and it has been an issue of prime concern. This is mainly caused by the toxicological effects posed by chemical species present in AMD. According to documented studies, AMD has been reported to be predominated by Al, Fe, Mn and sulphate amongst traces of other chemical species such as Cu, Zn, Ni, Pb, Co, Cr, As, rare earth metals, and radionuclides. These chemical species can cause harm to living organisms on exposure. With reference to pot assays, eco-toxicological studies and epidemiological reports, contaminants embodied in AMD can pose carcinogenic, teratogenic and mutagenic effects to living organism from different compartment of the environment (Seo et al., 2010, Talukdar et al., 2016, Liao et al., 2017, Talukdar et al., 2017). As such, these chemical species need to be managed prior to release in the environment. A wide array of active and passive technologies have been developed to remove contaminants from AMD; however, the new focus is mainly on minerals recovery (Sahoo et al., 2013, Simate and Ndlovu, 2014, Park et al., 2019). This is usually done in an attempt to advocate the concept of circular economy and minimize ecological footprints of mining activities. This study, therefore, intends to explore the use of activated cryptocrystalline magnesite for the treatment of AMD.

1.3 Aim and specific objectives

1.3.1 Aim of the study

The overall aim of this study was to explore sequential recovery of valuable minerals from acid mine drainage using activated cryptocrystalline magnesite.

1.3.2 Specific objectives

To fulfil the main objectives of this study, the following specific objectives were pursued:

- To assess the chemical characteristics of acid mine drainage before and after contacting different dosages of calcined cryptocrystalline magnesite;
- To determine the physicochemical properties of calcined cryptocrystalline magnesite and the recovered mineral resources using different analytical techniques;
- To optimise the optimum dosage for fractional and sequential recovery of metals and minerals from AMD;
- To use PHREEQC geochemical model to numerically model the process to complement the laboratory tests and to inform about the mechanisms thereof; and
- To assess the quality of product water against different water quality guidelines, standards, and specifications.

1.4 Significance of the study

The extraction, exploitation, and processing of metalliferous ores from underground and surface mineral reserves played an indispensable role in advancing the economy of the country (Masindi, 2016). However, mining and related activities could potentially, contaminate the soils, sediments and water, in many cases, leaving a legacy of environmental impacts long after mine closure. Often, metal-rich leachates and surface runoffs that result from the weathering of sulphide rich minerals could potentially alter the physical and chemical compositions of the receiving environments (streams, rivers, and groundwater) (Aaron et al., 2014, Park et al., 2019). Eventually, toxicological effects can affect living organisms that live in those streams, and in some cases, almost all species are lost from the receiving environment at least for some kilometres downstream (Zumarán Farfán et al., 2003). The proposed study will play a significant role in recovering valuable minerals from AMD; thereby minimizing potential environmental impacts and footprints associated with AMD. Specifically, this study explores the possibility of using the lixiviates generated by sulphide mining in the AMD as a source of

economic interest elements, estimating the available metal reserves and discussing the economic gains that would result from the recovery of this potential source of critical raw materials and other economic interest elements. This will foster the concept of circular economy due to its unique ability to recover minerals that can be beneficiated to harness some economic returns.

1.5 Structure of the thesis

This document comprises of five (5) chapters integrated together to form a thesis. The chapters are assembled in a way that they give information of specific component of the thesis, of which, chapter 1- 5 are detailed as follows:

Chapter One (1): This chapter gives a detailed background on the focus of the study, problems that are encountered in the area of study and the objectives to address the identified problem in the study area including the significance of the proposed study.

Chapter Two (2): This chapter focuses on the literature review. It unpacks the science behind AMD and informs the readers about the progress and status quo as it pertains the recovery of metals and sulphate from AMD. Thenceforth, it will also elucidate the formation, ecological problems, toxicity and existing technologies for AMD treatment and management.

Chapter Three (3): This chapter gives insights on the materials and methods which were used to achieve the outlined objectives of this study. Specifically, enumerates analytical techniques, instruments, and quality control procedures which were utilised and followed during the experiments.

Chapter Four (4): This chapter infers a detailed discussion on the results and discussions which were obtained from the reported methodology and experimental studies. It will, to a larger extent, endeavour to cover the enumerated objectives of this study in relation to the findings. Quality control procedures and complementary findings will also be reported.

Chapter Five (5): Finally, this chapter concludes on key findings of this study in relation to the outlined main and specific objectives of this study. Thenceforth, the identified gaps are enumerated as recommendation for future research avenues. This will then be used to guide future research in areas that were unveiled from the findings of this study. Subsequently, the references for the used scientific studies will be included as the last section of the thesis.

CHAPTER TWO

LITERATURE REVIEW

This in-depth literature review meticulously give insights into the state-of-art on existing and newly developed technologies that have been used for abatement and treatment of AMD. However, emphasis will be cascaded towards metals recovery since this is the main focus of this novel study. Thenceforth, it will also elucidate the formation, hydrogeology and environmental implications of acid mine drainage (AMD).

2.1 Introduction

Coal and gold mining has been historically perceived as the backbone of the economy of both developed and particularly developing countries and the main driver of economic growth for the latter (Haldar, 2018, Masindi et al., 2021). Due to its high calorific value, coal has been mined, towards using it for power generation, for more than 140 years (Andrić et al., 2015), while gold has been mined and used for jewellery since ancient times (Tutu et al., 2008). Revenue generated from coal and gold mining largely contribute to job creation and to gross domestic product (GDP) growth, thus also reinforcing, in the short-term at least, social welfare (Ramontja et al., 2011, Masindi, 2016, Ahokpossi et al., 2018, Shengo et al., 2019); albeit with huge environmental impacts, since mining activities are notorious for their environmental footprint (Omotehinse and Ako, 2019). In addition, during and in the aftermath of mining, by-products or waste minerals, such as overburden and metalliferous materials, can lead to the production of drainage streams, grossly contaminating the receiving environment with metalliferous and acidic drainage (Tutu et al., 2008). Specifically, if not properly stored and managed, mining tailings will generate leachates, through seepages or interaction with precipitations (typically rainwater), leading to the production of very acidic and metalliferous drainage, popularly known as acid mine drainage (AMD) or acid rock drainage (ARD) (Shu et al., 2017, Kotsiopoulos and Harrison, 2018, Park et al., 2019). Shafts in abandoned or active mines can also lead to AMD production, if not properly covered/managed. When AMD reaches different receiving environments, it negatively affects them, leading to alteration of pH, changing

the osmotic properties of the waterbodies, and increasing the dissolved irons among others (Tutu et al., 2008, Bologo et al., 2012, Masindi et al., 2017a).

Apart from directly affecting the water quality, the minerals contained in AMD can also settle at the bottom of the receiving water bodies, such as streams, thus also affect the ability of the ecosystem to harbour benthic organisms (Hogsden and Harding, 2012, Torres et al., 2014). According to literature, huge volumes of AMD are produced daily, for example, the coal, and gold mines in the western basin and Mpumalanga coal fields in South Africa produces enormous volumes of acid mine drainage into the environment (Hobbs and Cobbing, 2007, Bologo et al., 2012, Masindi, 2016, Masindi, 2018). This perpetually contaminates the environment and diminishes its suitability to foster life and render its intrinsic values (Equeenuddin et al., 2010, Chalkley et al., 2019, Masindi et al., 2019a).

Studies informs that the AMD problem will persist in South Africa and other countries afield hence calling for better management practices if mining still continues. Moreover, it seems like AMD will be generated long into the future since some countries like South Africa, heavily relies on electricity generated from combustion of coal. Almost 80-90% of the electricity is fossil fuel-based and this is anticipated to increase since the population is drastically increasing (Masindi et al., 2017c). In light of that, there is an urgent need for interventions to be put in place to ensure sustainable management of this product stream. The produced 735 ML/day of AMD can supply three provinces, i.e. Northwest, Gauteng, and Mpumalanga, in South Africa. This shows high economic viability and feasibility of minerals recovery. The reclaimed water can be used for drinking purposes and agricultural processes and alleviate the water challenges (Simate and Ndlovu, 2014, Masindi, 2018, Masindi et al., 2019a, Akinwekomi et al., 2020).

2.2 AMD formation pathway

AMD is mainly formed by the weathering of sulphide-rich and sulphide -bearing minerals, which are typically encountered in coal, copper, and gold deposits (Sheoran et al., 2011b, Blowes et al., 2013, Amos et al., 2015, Nordstrom et al., 2015b). Such minerals include FeS_2, Fe_xS_x, FeAsS, $(Fe,Ni)_9S_8$, $CuFeS_2$, Cu_2S, CuS, MoS_2, ZnS, NiS, and PbS, among others, and they are typically exposed to the atmosphere through mining activities (e.g. surface or deep mines, waste piles, and tailings). Iron sulfide

minerals (typically pyrite) are the main source of AMD formation, with other sulphide minerals only contributing to a limited extent (Sheoran et al., 2011a, Sheoran et al., 2011b, Simate and Ndlovu, 2014, Amos et al., 2015, Nordstrom et al., 2015b, Nleya et al., 2016, Kefeni et al., 2017b). The underlying reason for AMD formation is the oxidation of suphide in the presence of air and water, as shown in equation (2.1) (Masindi et al., 2015a):

$$4FeS_2 + 15O_2 + 14H_2O \xrightarrow{\text{microorganisms}} 4Fe(OH)_3 + 8H_2SO_4 \qquad (2.1)$$

The reaction is catalysed by certain microorganisms, particularly Fe-based bacteria (e.g. acidithiobacillus (acidic) and thiobacillus (basic pH)) and S-based bacteria (e.g. sulfolobus (acidic) and desulfovibrio (circum-neutral-basic)) (Johnson et al., 2002, Baker and Banfield, 2003, Hallberg, 2010, Nordstrom et al., 2015b).

In general, the chemical reactions that govern AMD formation are described in equation (2.2) to (2.5) (Kefeni et al., 2015a, Kefeni et al., 2015b, Masindi et al., 2016b, Masindi et al., 2018c):

$$2FeS_2 + 7O_2 + 2H_2O \rightarrow 2Fe^{2+} + 4{SO_4}^{2-} + 4H^+ \qquad (2.2)$$

$$4Fe^{2+} + O_2 + 4H^+ \rightarrow 4Fe^{3+} + 2H_2O \qquad (2.3)$$

$$4Fe^{3+} + 12H_2O \rightarrow 4Fe(OH)_3 + 12H^+ \qquad (2.4)$$

$$FeS_2 + 14Fe^{3+} + 8H_2O \rightarrow 15Fe^{2+} + 2{SO_4}^{2-} + 16H^+ \qquad (2.5)$$

Where, equation 2.2 demonstrates the oxidation of the sulphide ($S2^-$) to sulphate (SO_4^{2-}), ferrous iron (Fe^{2+} or Fe (II)), and acidity (H^+), when exposed to air (O_2) and water (H_20). Ferrous iron will then be oxidised to ferric iron (Fe^{3+} or Fe (III)) and hydrogen, as shown in equation 2.3. Thenceforth, in equation 2.4 the hydrolysis of Fe(III), in the presence of water, is shown, which leads to the formation of ferric hydroxide ($4Fe(OH)_3$) or yellow-boys (Figure 2.1) and acidity (H^+). These reactions typically occur spontaneously and are also catalyzed by microorganisms that obtain energy by oxidation reactions, as shown in Equation 2.1. Finally, Equation 2.5 shows how the oxidation of additional pyrite by ferric iron occurs. The net effect of these reactions is the release of H^+, which lowers the pH and maintains the solubility of the ferric ion and other metals contained in the AMD. Overall, the abovementioned chemical reactions, which govern AMD formation, are well-known and relatively

simple; however AMD composition can vary depending on local characteristic, such as climatic conditions, water quality, existence of microorganisms, and local geology, among others (Sheoran et al., 2011a, Sheoran et al., 2011b, Simate and Ndlovu, 2014, Amos et al., 2015, Anawar, 2015, Masindi et al., 2016a, Masindi et al., 2018c). These reactions affect the physicochemical characteristics of the receiving water matrices, affecting the pH, colour, and leading to the formation of "yellow –boy", among others, as shown in **Figure 2.1**.



Figure 2.1: Acid mine drainage effluent from underground shaft in Witwatersrand basin. (a) and (b): Initially the effluent is colourless with the "yellow–boy" (i.e. the yellowish-orange deposits at the bottom of the effluent discharges) shown in the nearby aquatic ecosystem, (c) after oxidation by atmospheric air in the presence of sulphide minerals and waterborne bacteria and the effluent gradually turns red.

Once formed, AMD typically finds its way to receiving waterbodies through: (i) flooding of mines (primarily abandoned) from precipitation and groundwater seeping, (ii) open surface mining activities, (iii) seepage from mine residue deposits, (iv) mine water losses, and (v) sewage and storm water reticulation effluents and (vi) drainages (Johnson and Hallberg, 2005, Sheoran et al., 2011b, Masindi et al., 2017a, Park et al.,

2019). In several regions of South Africa around 1100 m^3 of AMD are being daily released (Table 2.1), highlighting the serious nature and extent of the problem (Maree et al., 2013). To reduce the flow of water into the underground mine area and also curtail AMD releases to the environment, various engineering interventions can be employed, such as storage of mine waste and improved mine closure practices (Parbhakar-Fox and Lottermoser, 2015), as will be discussed in Table 2.1.

Table 2.1: Indicative volumes of AMD generated in mining fields situated in several regions of South Africa (Hobbs and Cobbing, 2007, Bologo et al., 2012, Masindi, 2016, Masindi, 2018)

Region	**Indicative AMD volume (ML day^{-1})**
Mpumalanga Coalfields	200
KwaZulu Natal Coal mining sites	10
Okiep Copper District	5
Witwatersrand Basins	
• Eastern (Springs)	120
• Central (Boksburg)	90
• Western	60
• Far West Rand	160
KOSH	50
Evander	30 (coal mine drainage)
	10 (gold mine drainage)
Total AMD	735

2.2.1 Physicochemical characteristics

AMD physicochemical characteristics largely vary, depending on the host minerals and local geology, which, along with the local climatic conditions and bacterial concentrations, will dictate the final type of mine drainage to be formed, giving it distinctive physical and chemical properties (Sheoran et al., 2011b, Amos et al., 2015, Nordstrom et al., 2015b).

2.2.1.1 Physical properties

Depending on the predominant elements in its matrix, AMD physical properties can grossly vary, making it distinctive at a spatial level. The colour is among the most distinctively physical properties of AMD, since this can range from colourless, blackish, greenish, bluish, and reddish, principally depending on the dissolved chemical species in its matrix. In most instances, AMD is reddish in colour and this is mainly linked to the oxidation of Fe(II) to Fe(III). On the other hand, the greenish colour is mainly linked to the presence of copper in its matrix; however, this is not the typical case. The presence of bluish colour is attributed to Fe(II), while white and black colour suggest the predominance of Al(III) and Mg, respectively. For example, in South Africa the majority of AMD originates from the oxidation of pyrite and arsenopyrite, which results to a reddish colour, whilst in streams with pH in the range of 5 to 6.5, orange-yellow ferric iron-rich sediments are formed (i.e. the yellow-boy shown in Figure 2.1a and b) (Cheng et al., 2009, Zhao et al., 2012, Amos et al., 2015, Masindi et al., 2018c). Overall, the oxidation of minerals species from different geological materials leads to their colouring, which imparts colour to receiving waterbodies. Moreover, sulphate imparts a salty or bitter taste to water, while the presence of AMD accelerates the erosion rate of pipes. Hardness and total dissolved solids also increase, leading to bad taste, skin dryness, scum in water and high soap consumption, among others (SABS, 2015, EPA, 2017, WHO, 2017).

2.2.1.2 Chemical properties

AMD chemical composition depend on a wide range of factors, including the formation conditions, local geological setting, underlying geology, hydrogeology, and mineral phases being mined. As such, the chemical composition of the resultant mine drainage is bound to drastically vary and thus also making it distinctive at a spatial level (Sracek et al., 2004, Sheoran and Sheoran, 2006, Natarajan, 2008, Peretyazhko et al., 2009, Sheoran et al., 2011c, Zhao et al., 2012, Nordstrom et al., 2015b). Based on the existing body of knowledge, AMD can be classified as acid mine drainage, circumneutral drainage, and basic drainage (Madzivire et al., 2010, Madzivire et al., 2011, Nordstrom et al., 2015a). This classification is based on the pH value of the drainage, typically in the range 2 to 12, (Madzivire et al., 2010, Madzivire et al., 2011). The pH influences the drainage chemical composition, with metals predominating the acidic pH and base

metals the basic pH (Langmuir, 1997). Specifically, with reference to Masindi et al. (2017a) and other authors (Maree et al., 2013, Akinwekomi et al., 2016, Akinwekomi et al., 2017b, Akinwekomi et al., 2020), AMD has been reported to be predominated by metals and sulfate. On the other hand, Madzivire et al. (2010) and Nordstrom et al. (2015b) reported that the circumneutral to basic drainage (or both popularly known as neutral mine drainage (NMD)) are rich in metals, oxyanions (e.g. sulfate and metalloids), and base metals. However, the metal concentrations in NMD are much lower than in AMD, since metals precipitate at high pH values, which also suggests that metals can be removed from AMD with an increase in pH (Masindi et al., 2018c).

The mean chemical properties of AMD and NMD are listed in Table 2.2 and it is clear that in both cases the chemical species concentrations are well above the prescribed limits for water intended for human consumption or for other defined uses, such as irrigation (SABS, 2015, EPA, 2017, WHO, 2017).

Table 2: The chemical composition of acid and neutral mine drainages.

Element	Types of mine drainages		References
	Acid mine drainage	Neutral mine drainage	(Maree et al., 1999, Maree et al., 2004a, Maree et al., 2004c, Madzivire et al., 2010, Madzivire et al., 2011, Pope and Trumm, 2015, Masindi et al., 2016a, Masindi et al., 2017a, Masindi et al., 2017d, Masindi et al., 2019a, Park et al., 2019, Masindi et al., 2021)
	Units (mg L^{-1})	Units (mg L^{-1})	
pH	2 - 4	5.5 – 9.5	
Al	500	0.016	
Fe	8000	0.074	
Mn	100	2.5	
SO_4^{2-}	4000-80000	4600	
Cu	0.4	-	
Ni	0.21	0.21	
Pb	0.10	-	
Zn	0.2	0.16	
Ca	450	540	
Mg	400	860	

The values shown in Table 2.2 suggest the possibility of valorizing these effluents through water reclamation and metals recovery. Nonetheless, Tutu et al. (2008) reported that there are notable levels of radionuclides in drainages emanating from gold

mining activities; however, this was not the case in coal mining drainage. As shown in Table 2, NMD drainage has elevated levels of sulphate, Mg, and Ca. This can be attributed to its elevated pH, which is above the precipitation potential of many metals in water. Hardness in NMD is also high, due to the elevated levels of Mg and Ca. This is primarily linked to dissolution of carbonates during the formation of the drainage, leading to alkaline product water. As such, the only elements that could possibly be recovered from NMD are sulphate and possibly Mg and Ca, depending on their concentration, by means of softening techniques such as soda ash softening (Madzivire et al., 2010, Madzivire et al., 2011, Masindi et al., 2014, Masindi et al., 2018a, Masindi et al., 2019a). On the other hand, AMD has a huge potential for minerals recovery and synthesis, due to the presence of elevated levels of Fe, Al, Mn and sulphate (Table 2.2). For example, it has been shown that AMDs from coal mine areas are rich in Fe, Al, Mn and sulfate, hence the recovery of Fe and sulfate minerals can be viable (Akinwekomi et al., 2017b, Akinwekomi et al., 2020). As such, here focus is placed on AMD. Overall, apart from the beneficiation of NMD and particularly AMD, their valorization is also possible through water reclamation.

2.3 Ecotoxicological impacts

It has been well-documented that AMD chemical composition is responsible for a number of social (Singh et al., 2020), economic (Hengen et al., 2014, Favas et al., 2016, Singh et al., 2020), and ecological impacts (Netto et al., 2013, Talukdar et al., 2016, Chalkley et al., 2019). Among them, the chemical species contained in the AMD matrix pose devastating effects on living organisms, such as plants and animals, and affect the agricultural industry and food security. Pollutants, and particularly toxicants contained in AMD can cause teratogenic, carcinogenic, and mutagenic effects to living organisms (in biosphere) on exposure (Jooste and Thirion, 1999, Balistrieri et al., 2007, Ivask et al., 2015, Chu et al., 2018). As such, AMD can affect organisms living in different spheres and environmental compartments, i.e. soil (terrasphere), water (aquasphere/hydrosphere), and air (atmosphere).

Ecotoxicological studies and assays have reported various conditions that are associated with elements present in AMD (Netto et al., 2013). In detail, acidity in AMD can lower the pH of receiving ecosystems, thus possibly killing or forcing species to migrate, if possible. Typically, fish and plants will die due to lack of tolerance in low pH, while

also the ecological conditions are affected. Among others, the chemical species in AMD affect plants via changing their osmotic conditions, while even though the majority of those species can serve as nutrients for plants, their elevated concentrations cause toxic effects. These toxic effects are typically measured using the lethal concentration (LC, e.g. LC_{10}, LC_{20}, LC_{50}, and LC_{100}) and lethal dosage (LD e.g. LD_{10}, LD_{20}, LD_{50}, and LD_{100}), and have been widely reported in the literature, focusing on pot assays, aquarium studies, and toxicological tests, among others (Jooste and Thirion, 1999, Balistrieri et al., 2007, Sobral et al., 2013, Ivask et al., 2015, Chu et al., 2018, Doyi et al., 2018, Hu et al., 2019, Zhang et al., 2019).

Furthermore, exposure to toxicants contained in AMD can alter plants' metabolic activities, homeostasis, and induce toxic symptoms, as well as destabilise the salt balance (Yadav, 2010, Vardhan et al., 2019). Furthermore, metals, metalloids, anions, and radioactive materials in AMD can bio-accumulate in living organisms and eventually bio-magnify through the food chain (Simate and Ndlovu, 2014, Vigneri et al., 2017, Vardhan et al., 2019, Yuan et al., 2019). In addition, chemical species, including heavy metals, contained in AMD are known to cause skin lesions, hyperpigmentation, cancer, upper respiratory, pulmonary, gastrointestinal and cardiovascular failure, along with nerve damage, sensory loss in the peripheral nervous system, hypertension, gastrointestinal, irritation, nausea, vomiting, diarrhea, kidney and multiple organ failure, which can be fatal (SABS, 2015, EPA, 2017, WHO, 2017). As such, there is a pressing need to limit and manage the produced AMD quantities to safeguard human health and the environment. To this end, various AMD pollution abatement and/or treatment techniques have been employed and more recently the beneficiation of such streams has been also studied, as discussed below.

2.4 Abatement techniques

Several technologies have been proposed to prevent the formation of AMD, focusing in active and abandoned mine sites, with the underlying goal being to limit the main factors that lead to AMD formation (Hughes and Gray, 2011, Sahoo et al., 2013, Kefeni et al., 2017b, Park et al., 2019). These include oxygen (O_2), water, and microorganisms, which are required for the oxidation of pyrite and of other metals contained in AMD (Sheoran et al., 2011a, Sheoran et al., 2011c, Amos et al., 2015). Over the past decades, AMD formation has been hindered through the elimination of at least one of those

factors, typically by preventing water and oxygen from reacting with sulphide minerals or by covering sulphide minerals with inert materials to prevent the oxidation reaction to take place (Sahoo et al., 2013, Pozo-Antonio et al., 2014, Kefeni et al., 2017b). However, in the long-term the sustainability of such systems, which are described below, is challenging. Specifically, the main AMD abatement techniques include:

2.4.1 Utilisation of covering materials

This technique makes use of materials with limited to low water permeability, typically clay minerals (e.g. bentonite) and polymeric plastic materials, to cover the exposed minerals and prevent their oxidation from taking place. However, these cover materials can react with the covered minerals and are also exposed to weather extremes and environmental conditions, which lead to their degradation thus reducing their insulation capacity. In addition, to form the required thick non-permeable layers, large amounts of these materials are required, but this comes at the expense of the cost and sustainability of this technique (Zipper and Skousen, 2014, Park et al., 2019).

2.4.2 Stabilization using alkaline materials

This approach involves the addition of alkaline materials on sulphide rich tailings, minerals extraction voids, and other geological settings that are conducive for the formation of AMD. These materials hinder the production of acidic and metalliferous drainage since they increase the pH and also lead to metals precipitation. In most cases tailings and sulphide rich minerals are mixed with alkaline materials such as brucite, periclase, lime, limestone, dolomite, and soda ash as a mean of source neutralization and curtailing the formation of acidic drainage (Skousen, 2014, Tripathy, 2014). This technique is simple to apply and effective for AMD abatement; however, it is also associated with drawbacks. Specifically, the neutralization potential of such materials reduces over time, hence leading to the formation of acidic drainage (Tripathy, 2014). As such, static tests for acid generation potential (AGP) and acid neutralisation potential (ANP) are used to overcome this problem (Xenidis et al., 2002, Skousen et al., 2019)., with the PHREEQC geochemical model typically employed (Simunika et al., 2013).

2.4.3 Passivation or microencapsulation

This technique is based on the use of hydrophobic coating materials to prevent the reactive Sulphide fractions from oxidizing. Organic materials and their derivatives,

such DETA, sodium aleate, phospholipids, and humic substances are typically used due to their high hydrophobicity (Moodley et al., 2018, Park et al., 2019). However, similarly to covering materials environmental conditions, substances from the outside and from covered material, and organisms (e.g. bacteria) can degrade microencapsulation materials rendering them unable to isolate the covered material from the air and water thus leading to AMD formation (Villain et al., 2013).

2.4.4 Bactericide application

This abatement technique is based on the use of substances aimed to impede the biological activities of the bacterial communities which are harbored in tailings and mining voids. The main focus is to limit the bacteria that oxidise sulfur, such as acidithiobacillus (acidophile), thiobacillus (basic pH) and other sulphur based bacteria (e.g. sulfolobus (acidic) and desulfovibrio (circumneutral to basic), thus preventing sulfate production and hampering AMD formation (Kim et al., 1999). The main drawback of bactericides application is that environmental conditions can limit their activity, thus not being able to prevent sulfur oxidation, and therefore the monitoring of their levels and their timely and frequent addition play an important role towards this end (Park et al., 2019).

2.4.5 Control of oxygen and water ingression

This concept involves preventing permeability of water and the rate of flooding of sulphide bearing rocks and minerals and the eventual decant volumes of AMD. This option is usually considered because pumping and treating AMD water is costly and requires the use of raw materials, which are even getting depleted (Tripathy, 2014). As such, it is imperative to reduce the volume of water, which is to be pumped and treated. The pumping of clean uncontaminated water from deepest aquifer and preventing the contamination of surface aquifers also aids in preventing the contamination of water and the filling of the voids. This prevents the perpetual effects of AMD due to elimination of water, which is a fundamental component of AMD formation (Tripathy, 2014, Park et al., 2019). This technique is ineffective during rainfall since rain water can always finds its way to the voids. A rise in ground water level diminishes the application of this approach.

2.4.6 Backfilling of voids and opencast trenches

Mining activities entail the removal of minerals from different stratas and lithologies, thus leaving voids or trenches that are exposed to water and air and therefore are prone to AMD formation. As such, voids and trenches can be filled with the extracted materials or alkaline materials to prevent the formation of AMD. The latter prevent AMD formation due to in-situ neutralisation and include lime, fly ash, alkaline tailings, and alkaline waste materials, which typically have been used for backfilling (Akcil and Koldas, 2006, Sahoo et al., 2013, Pozo-Antonio et al., 2014, Kefeni et al., 2017b, Park et al., 2019). Similarly, to covering materials, backfilling materials are prone to erosion from weather and other environmental factors. Villain et al. (2013) evaluated the effects of backfilling and sealing the waste rock on water quality at the Kimheden open-pit mine, northern Sweden highlighted that this technique is effective and viable. Gitari et al. (2008) evaluated the use of coal fly ash for mine void backfilling and column studies that simulate the neutralisation potential suggested the feasibility of increasing the pH and attenuate inorganic contaminants in the product mine water.

2.4.7 Application of abatement techniques in practice

The abovementioned abatement techniques have been found promising in preventing AMD formation. However, they are, in general, expensive to apply and are vulnerable to failure in the long run. Therefore, the mining industry, which has largely also not adopted the principles of circular economy, has not been willing to adopt them at large scale. This is mainly attributed to the deficiency of minerals mining and long-term effects of AMD forming due to weathering and other natural processes. This prevents mining of minerals from waste materials hence presenting secondary challenges of waste materials in a form of tailing. This hampers the concept of circular economy and valorization of waste materials. Modern research initiatives focus on the recovery of minerals resources from AMD and product wastes hence fostering circular economy and closed-loop mining initiatives. This process favors the cradle to grave concept while the current focus of science is on the cradle-to-cradle approach where resources are circulated in a closed-loop to foster sustainable development (Pozo-Antonio et al., 2014, Kefeni et al., 2017b, Park et al., 2019).

2.4.7 Beneficiation of tailings

Tailings from coal and gold mining can be valorized and beneficiated, particularly in the context of circular economy which is a concept that has gained momentum in the past few years. Similarly, to other wastewater streams, such as municipal wastewater (Mavhungu et al., 2020), it is possible to valorize AMD effluents through water reclamation. However, the main drawback of AMD, i.e. its high metal content, if viewed under the circular economy concept could provide opportunities for its beneficiation through metals recovery (Akinwekomi et al., 2020). Specifically, AMD contains residues and fractions of various minerals that have commercial value and therefore their recovery can be both economically viable and at the same time provide a treatment solution. For example, recently Si has been recovered from mine tailing and used for the synthesis of geo-polymer bricks and other related minerals (Obenaus-Emler et al., 2020). Other minerals contained in AMD including pyrite, calcites, and sulphides can be recovered and thus foster the concept of circular economy (Oliveira et al., 2016, Taha et al., 2017, Figueiredo et al., 2019, Shengo et al., 2019, Skandrani et al., 2019).

This merely minimize the formation of AMD but water from the reclamation process could lead to the production of acid mine drainage from the tailings. Moreover, the heterogeneous nature of tailings hampers the feasibility minerals recovery since sophisticated equipment and technically advanced engineering system are required for this. Tailings are mainly taken for re-mining, mainly to ensure that the footprints of mining activities are minimized via eco-sound initiatives that are considered as green initiatives (Taha et al., 2017, Shengo et al., 2019, Skandrani et al., 2019). In developing countries, particularly the low and middle-income countries (LMIC), artisanal mining is very prevalent and informal miners expose themselves to very dangerous toxicants in the tailings from coal and gold mining. This then induce numerous morbidity and mortality to miners. This also increases the degree of pollution if the tailings material is not properly managed. In light of that, methods such as the use of top covers, application of bactericides, passivation, encapsulation, organo-stabilization, and co-disposal are utilized to prevent the generation of AMD to the environment (Park et al., 2019). Tailings also poses huge risk to surface and ground water resources. Contamination by tailings also degrades the soil and its biodiversity due to alteration of the physico-chemical properties of the soil. Such soil could then be unsuitable for

various activities including agriculture, land development for residential purposes and establishment of economic zones, rangeland, and wildlife activities. Furthermore, land contaminated by tailings from acid mine drainage is no longer suitable for utilization since its classification drops to a very vulnerable state that requires intensive rehabilitation and restoration.

A schematic illustration of the AMD treatment process and products analysis is shown in Figure 2.2.

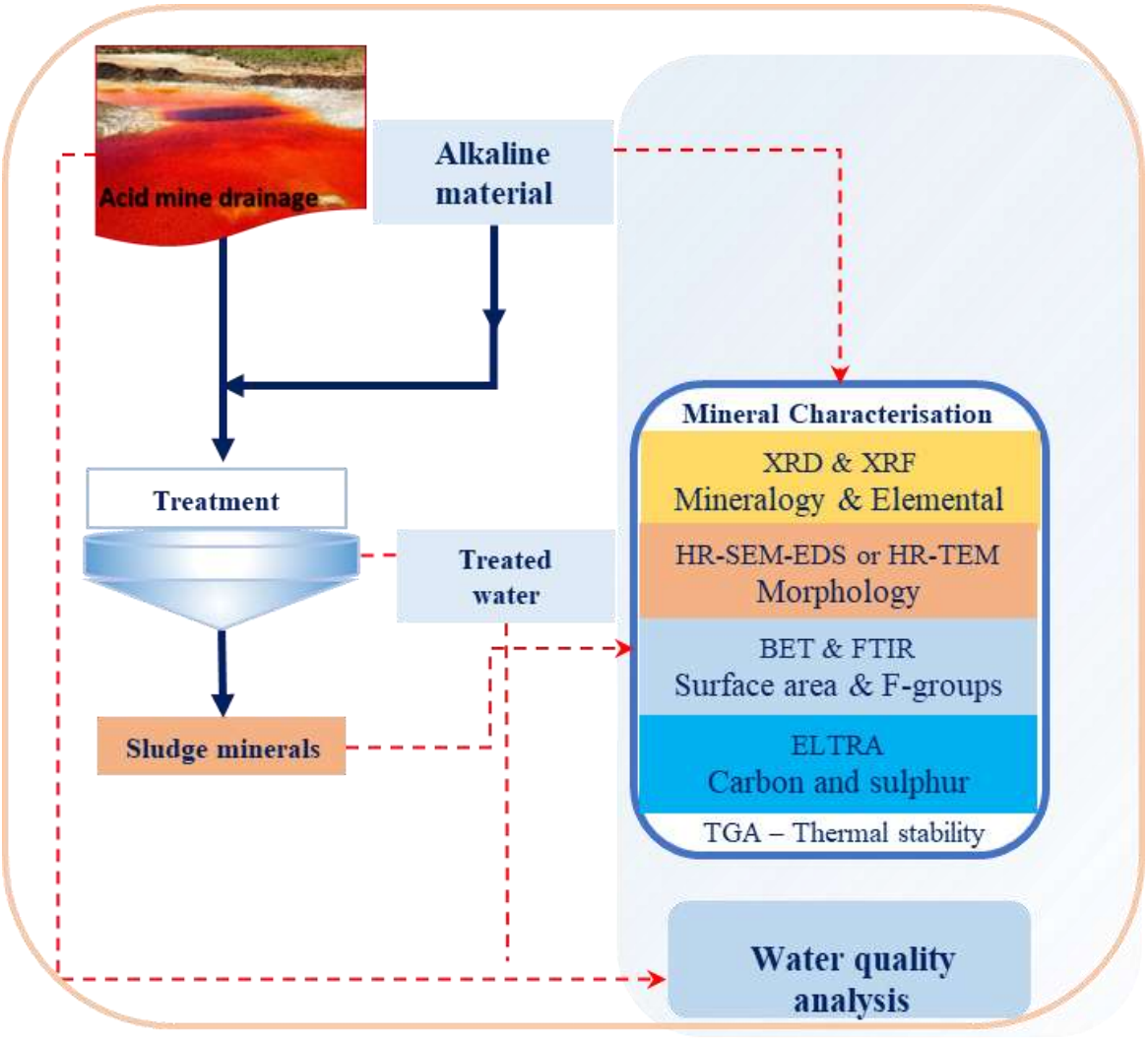


Figure 2.2: A schematic illustration of the AMD treatment process and products analysis.

As illustrated in Figure 2.2, the treatment of AMD requires a sophisticated process and materials characterisation. This is mainly done to determine the fate of chemical species post the chemical reactions. Different techniques and methods are utilised to determine the process of contaminants attenuation and their fate.

2.5 Treatment technologies

After generation, AMD is treated typically by active or passive systems, while hybrid approaches, where active and passive systems are combined have also been proposed (Simate and Ndlovu, 2014, Nleya et al., 2016, Kefeni et al., 2017b, Park et al., 2019). Below, the strengths and weaknesses of each treatment approached are summarised and discussed. Active treatment is considered more reliable than passive; however it requires infrastructure, such as tanks, mixers, and pumps, regular operation and maintenance along with regular chemical and energy input to operate (Naidu et al., 2019). As such, active treatment is perceived less eco-friendly than passive treatment (Skousen et al., 2017). On the other hand, passive treatment typically does not require frequent operation and maintenance (O&M), as well as power and chemical input, and therefore is less expensive and more suitable for remote locations, albeit is not as efficient as active treatment (Naidu et al., 2019). To overcome the limitations of both systems, hybrid treatment has been proposed, where passive and active treatments are combined under a multi-stage process making use of different mechanisms (Sheoran and Sheoran, 2006, Sheoran et al., 2011c, Pozo-Antonio et al., 2014, Simate and Ndlovu, 2014, Nleya et al., 2016, Kefeni et al., 2017b, Skousen et al., 2017, Park et al., 2019).

2.5.1 Active processes

Active processes are typically based on the frequent energy, chemical, and other material inputs to drive the treatment process. Due to the acidic nature of the mine effluents, alkaline chemicals, such as $Ca(OH)_2$, CaO, NaOH, Na_2CO_3, and NH_3, MgO, and $Mg(OH)_2$ are used, while energy and infrastructure is also required. As such, active treatment tends to be expensive, while material and energy input leads to high environmental footprints. Apart from the use of alkaline agents, filtration and adsorption technologies are also included in active treatment. Different filtration techniques such as ultra-filtration (UF), micro-filtration (MF), nano-filtration (NF), reverse osmosis (RO), and membrane distillation (MD), have been employed for AMD treatment, whereas adsorption techniques typically entail the use of different natural and synthetic materials such as activated carbon, clay minerals and other synthetic compounds for AMD treatment (Xingyu et al., 2013, Hong et al., 2014, Masindi et al., 2015b). Specifically, Masindi et al. (2017a) compared the use of different alkaline

materials for the treatment of AMD and identified that different materials achieve different levels of AMD treatment via metals precipitation and adsorption, with lime and calcined magnesite being the most promising materials. Similar results were reported in Potgieter-Vermaak et al. (2006). Furthermore, Kefeni et al. (2018) explored the use of Fe-based minerals for AMD treatment, which were found promising for metals and sulphate attenuation through adsorption and other mechanisms. Various filtration techniques have also been explored (Al-Zoubi et al., 2010, Sierra et al., 2013, Aguiar et al., 2018, Lopez et al., 2018, Singh et al., 2020). However, membrane fouling was a limiting factor, while the need for pre-treatment further constrains on the feasibility of filtration for AMD treatment (Kefeni et al., 2017b, Masindi, 2017b, Agboola, 2019, Rambabu et al., 2020). Finally, the retentate, typically brine, generation is another drawback, for which management is costly and can lead to large environmental footprints. The above concerns on filtration application for AMD treatment have led to the research and development of Membrane Distillation (MD) for AMD treatment. MD is perceived as an emerging technology to treat AMD, brine, and retentate. It mainly softens the water using temperature different temperature gradients through semi-permeable membranes (Amaya-Vías et al., 2019, Foureaux et al., 2019, Ryu et al., 2019). Overall, active processes are typically employed in active mines, rather than in abandoned ones, and are perceived as a promising treatment approach to treat AMD and also supply water. A typical AMD active treatment train, along with the analytical techniques employed for water and mineral analyses are shown in **Figure 2.3**.

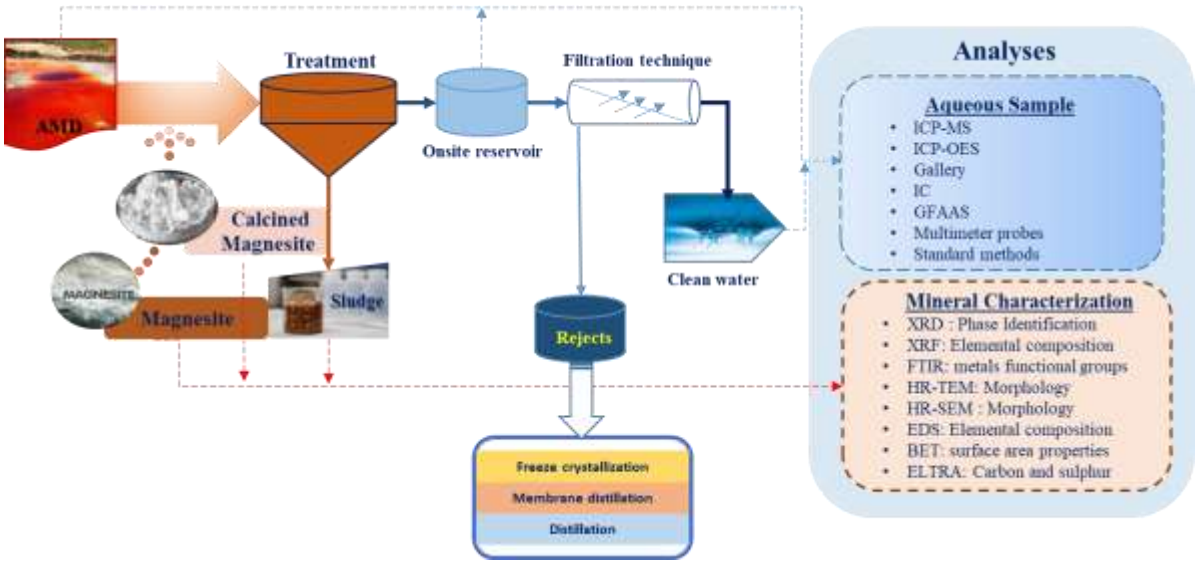


Figure 2.3: Schematic illustration of a typical AMD active treatment train, along with the techniques for the recovered minerals and the reclaimed water analyses.

2.5.2 Passive processes

Passive treatment processes are typically employed in abandoned mines and areas where the effluent requires minor, rather than major treatment. Wetlands have been traditionally used for AMD passive treatment, by removing contaminants and neutralising the pH through bioremediation and/or phytoremediation. More recently, apart from aerobic and anaerobic wetlands, anoxic limestone drains, vertical flow wetlands, open limestone channels, and alkaline leach beds have also been employed (Sheoran et al., 2010, Skousen et al., 2017). Because frequent materials and energy inputs are not required, passive treatment is considered more environmentally friendly than active treatment (Skousen et al., 2017). However, different mechanisms play a pivotal role in passive AMD treatment with bioremediation and phytoremediation, i.e. contaminants are sorbed as nutrients by plants and bio-accumulate in different parts of plants (Nguegang et al., 2021), used due to their high treatment efficiency. For example, Kiiskila et al. (2019) evaluated the remediation of acid mine drainage-impacted water by Vetiver grass and it was found promising for the removal of metals and oxyanions. Moreover, if neutralisation materials, such as limestone, are used, AMD will be neutralised and metals will precipitate. Nonetheless, the key challenge in passive systems is their sustainability in a long run, primarily due to blockages from precipitates, armouring of the reactive materials, and channelling. Wetlands (Figure 2.4) and limestone drains are two widely used passive systems.

Specifically, wetlands can be aerobic or anaerobic. Aerobic wetlands are floral systems, which can be lined or unlined. They are primarily filled with soil or limestone gravel, in the latter case pulverised to the desired particle size to enhance performance. Through these systems, metals oxidation and precipitation (e.g. iron, manganese, and other metals) from AMD is naturally achieved (Rambabu et al., 2020). Wetland plants also absorb nutrients contained in AMD, which they use for their growth, but this depends on affinity and tolerance. Anaerobic wetlands are also employed to neutralize acidity and reduce metals as sulphide; however, in this case due to oxygen deficiency. Anaerobic reactions consume H^+, hence the reduction in acidity. Anaerobic wetlands are mainly filled with organic matter, such as compost, and underlain by limestone

gravel. Water percolates through the organic matter to the lime bed, thus achieving anaerobic conditions. This encourages metals to precipitate as sulphides. Furthermore, organic matter aerobic decomposition, achieved by different microorganisms contained in the organic matter, consumes the dissolved oxygen leading to the production of alkalinity and H_2S (Skousen et al., 2017, Ben Ali et al., 2019, Rambabu et al., 2020).

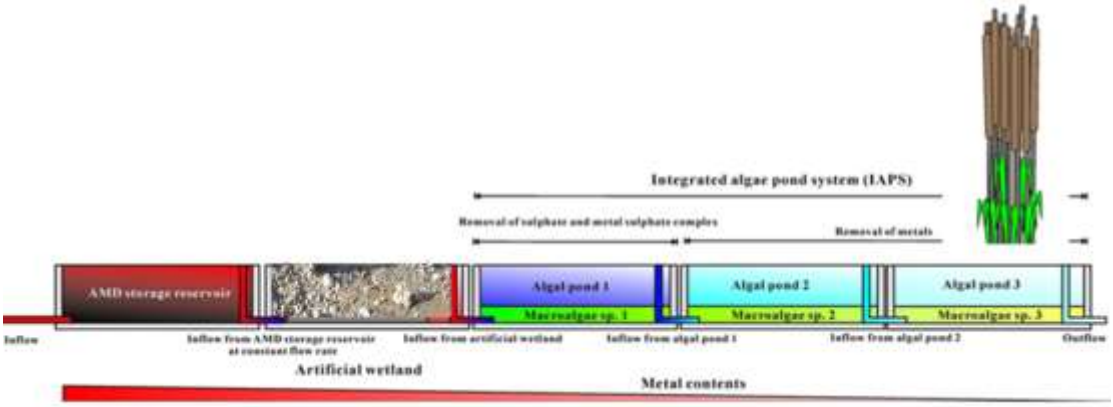


Figure 2.4: The schematic illustration of the AMD treatment process and products analysis.

Anoxic limestone drains or channels consist of buried limestone gravel systems, where the AMD flows through and is anaerobically treated. However, if oxygen or aluminum are present within the channel, then iron and aluminum hydroxides that could clog the system can be developed, causing its failure. Alkalinity producing systems can also be a combination of an anaerobic wetland and an anoxic limestone drain. Other types of passive treatment systems include various limestone treatment configurations, ranging from limestone ponds to open limestone channels in which water flows down a steep slope with limestone riprap. These systems oxidize and precipitate metals and add alkalinity to the water (Gazea et al., 1996, Jung et al., 2014, Skousen et al., 2017, Skousen et al., 2019, Rambabu et al., 2020).

2.5.2.3 Advantages and disadvantages of AMD treatment systems

Overall, passive treatment systems are typically used in remote locations, such as abandoned mines since they are simple to operate because they do not require electrical power, machinery, and addition of chemicals to operate. Their maintenance is fairly simple, while they do not largely impose on the aesthetic quality of the area that they

are installed on, since they are natural and can support plants and local wildlife. They are also far less expensive than the active alternatives.

However, they are also associated with many drawbacks, compared to active systems, since: i) they might not treat the AMD effluent to a high standard due to design issues or weather extremes (e.g. low winter temperatures) , ii) blockages can be frequent, thus regular monitoring is required,, iii) they cannot be employed in circular economy concepts, since resource recovery is very difficult, and iv) highly mineralised sludge is produced, which makes its use or its beneficiation practically unfeasible. To reduce the effects of the disadvantages of both active and passive systems, hybrid systems which combine both of these processes have been examined recently.

2.5.3 Hybrid processes

The term hybrid literary refers to the offspring of two plants or animals of different species/varieties. As such, in this context, hybrid refers to the integration of active with passive processes for AMD treatment. Typical hybrid processes include the use of neutralisation with alkaline media and wetlands (bioremediation or phytoremediation using plants or microorganisms respectively) for the synergistic removal of contaminants from AMD (Groudev et al., 2008, Moodley et al., 2018, Naidu et al., 2019). Hybrid treatment systems are typically effective under certain flow and acidity conditions. The schematic illustration of the hybrid-AMD treatment process is shown in **Figure 2.5**. It should be noted that even though this process appears promising (Nleya et al., 2016), further research is required to find out if hybrid systems are suited for large-scale applications.

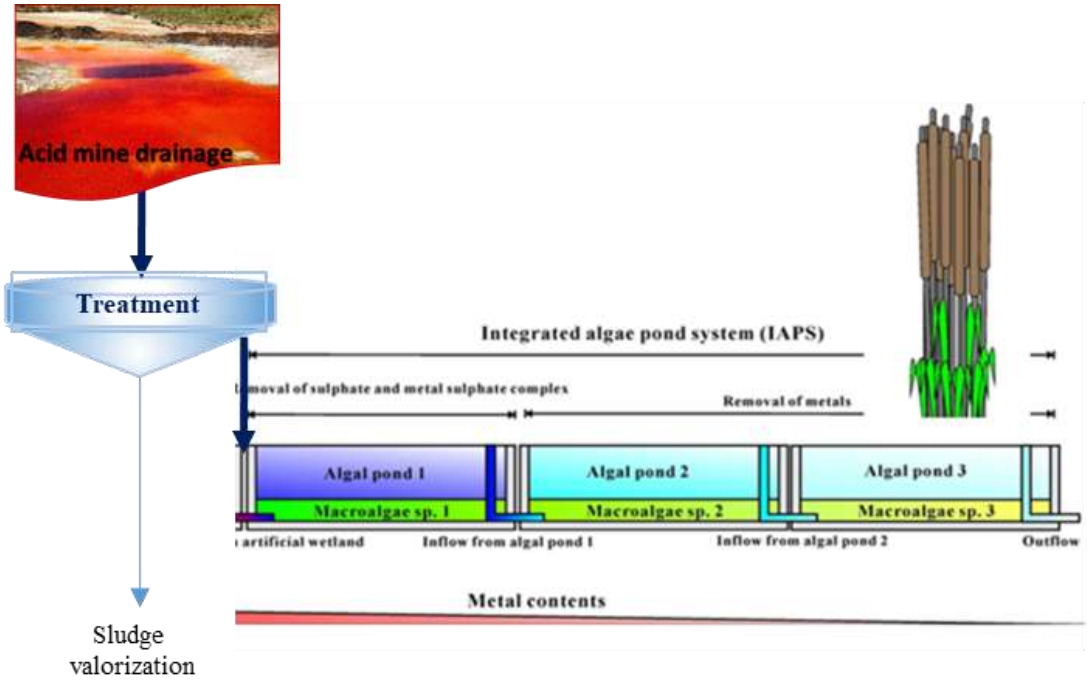


Figure 2.5: The schematic illustration of the hybrid treatment process.

2.5.4 Integrated or multi-staged approach

Apart from hybrid systems, the treatment of mine drainage can also follow an integrated approach, where minerals are recovered step-wise, i.e. at different stages. As such, contaminants are removed at different stages, using different mechanisms. In most cases, integrated systems are based on the synergistic effects of precipitation, adsorption, and filtration for the removal of contaminants from AMD and the recovery of valuable minerals at different stages. Integrated systems can be used for the valorisation and beneficiation of mine drainage, i.e. harbouring the circular economy concept, and therefore focus is placed on such systems. A typical integrated AMD treatment process, including AMD beneficiation (metals recovery) is shown in **Figure 2.6**. Some of the main proposed integrated technologies, for potential industrial applications, are discussed below.

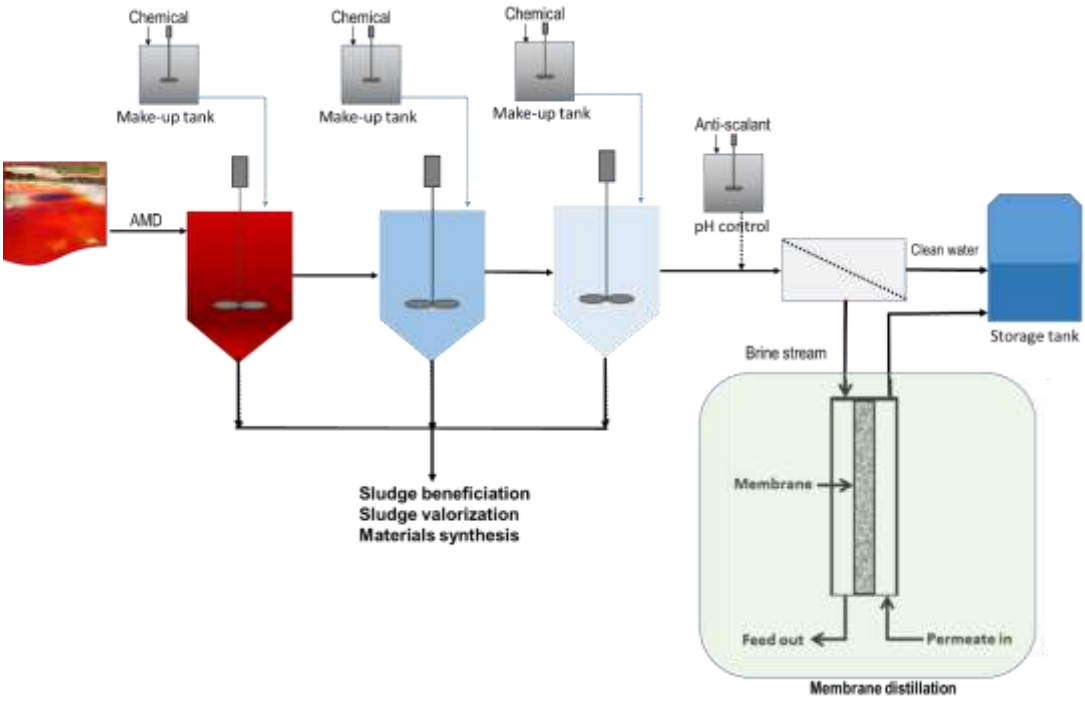


Figure 2.6: Schematic of atypical integrated (multi-stage) AMD treatment system.

Karakatsanis (2010) proposed the High Recovery Precipitating Reverse Osmosis (HiPRO) treatment plant (daily capacity 15 ML) for the treatment of circumneutral mine drainage (rich in sulphate and notable amount of Fe and Mn), making use of lime addition, ozonation, sand filtration, ultrafiltration, and reverse osmosis (RO), for gypsum and sludge recovery, the latter having a number of industrial applications, and drinking water reclamation. A few years later, the Magnesite Softening and Reverse Osmosis (MASRO) system (daily capacity 3.5 KL) was proposed for AMD treatment (Masindi et al., 2019a). This integrated system uses thermally activated (calcined) magnesite for AMD neutralisation, followed by minerals precipitation and then effluent is softened using lime and soda ash for sulphate and magnesium removal. The softened effluent is then purified by means of RO to reclaim drinking water, while the RO retentate was also treated by Membrane Distillation (MD). Apart from drinking water reclamation, important minerals were also recovered, including Fe-based minerals, gypsum, and limestone. However, the generated sludge from the Mg-reactor should be properly managed (Masindi, 2017b, Masindi et al., 2017d, Masindi et al., 2018a, Masindi et al., 2019a). Another integrated system is the Tshwane University of Technology Magnesium Barium Alkali (TUT MBA), which employs magnesium for AMD neutralisation and metals removal, apart from sulphate which is then removed

using barium, i.e. barium sulphate is formed. Similarly to MASRO, the sludge produced in the magnesium reactor, which is highly mineralised and heterogeneous, is costly to manage (Bologo et al., 2012). Regarding that system, Masindi (2017a) reported similar results for the integrated use of magnesite and barium for sulphate removal from AMD.

Another promising integrated process is the Council for Scientific and Industrial Research alkali-based-calcium (CSIR ABC) process. This process entails the neutralisation of AMD with lime and the subsequent treatment of the product water with barium carbonate, to attenuate the residual sulphate. To minimise costs and make the process self- sustaining minerals were recovered from the produced sludge and re-fed to the system (Geldenhuys et al., 2003, Maree et al., 2004b, Hlabela et al., 2007). In that regard, the GypSlim process was proposed to recover sulphur from the product waste (Nengovhela et al., 2007). Finally, the SAVMIN process, which utilises lime neutralisation to remove metals as hydroxides, gypsum precipitation, and ettringite formation, has been recently proposed, with the added benefit of water reclamation and mineral (sulphuric acid and gypsum), recovery (Abdrakhmanova et al., 2019). Biological based processes, such as the Rhodes BioSure process and THIOPAQ process, have also been proposed; however their primary focus was solely AMD treatment, and not minerals recovery. This is the case for other sulphate technologies, such as the EARTH ion exchange process and GYP-CIX (Simate and Ndlovu, 2014). Overall, even though effective solutions for AMD treatment, with water reclamation and minerals recovery have been proposed and tested, more research is required towards this end. A summary on the main integrated process for AMD treatment and water/minerals reclamation/recovery, along with their main advantages and disadvantages is shown in **Table 2.3**.

.

Table 2.3: Different piloted technologies, their advantages, and disadvantages

Technology	**Advantages**	**Disadvantages**	**References**
CSIR ABC	Treat water to limit Recovery of sulphate	Generation of hazardous, heterogeneous and highly mineralised sludge. Require precise barium dose to balance the stoichiometry and residual barium.	(Mulopo, 2015)
CSIR MAS	Treat water to limit Recover gypsum and lime Brine free Good for discharge purposes	Toxic sludge in Mg-reactor High cost due to CO_2 ingression	(Masindi et al., 2018a)
CSIR MASRO	Treat water to limit Recover Fe-based minerals Recover gypsum and lime	Cost intensive Generation of brine	(Masindi et al., 2019a)
CSIR MASROE	Treat water to limit Recover valuable minerals such as gypsum	Cost intensive Generation of brine Generation of Fe-sludge for beneficiation	(Masindi, 2017b)
SAVMIN process	Treat water to limit Recover valuable minerals	Hazardous sludge Generation of toxic sludge Sophisticated process	(Abdrakhmanova et al., 2019)

TUT MBA	Recover valuable minerals such as barium sulphate Reclamation of product water that can meet the discharge limits Recover barium using GYP-SLIM for re-use.	Generation of hazardous, heterogeneous and highly mineralised sludge. Require precise barium dose to balance the stoichiometry and residual barium.	(Bologo et al., 2012)
ROC technology	Reclaim drinking water from acid mine drainage using filtration Recover valuable minerals from brine using freeze technique Recover Fe-based minerals for the synthesis of goethite, hematite and magnetite Generate zero-liquid into the environment.	Cost intensive Still at pilot scale Sophisticated process that requires high level skills. Challenges with the synthesis of Fe-based minerals.	(Zvinowanda et al., 2014)
HiPRO	Can reclaim drinking water from the treatment process. Can synthesize gypsum from the treatment process Brine free and zero-liquid-discharge	Cost intensive Hazardous sludge from the ozonation process	(Karakatsanis, 2010)

EARTH	Uses ion exchange column. It can recover uranium and sulphate The sulphate can be used to produce ammonium sulphate	Cost intensive Generation of toxicants from ion exchange regenerates Requires acid for operation.	(Simate and Ndlovu, 2014)
CSIR BOF-SRO	Reclaim drinking water Recover gypsum	Voluminous sludge rich in Fe Require high dosage of BOF slag Generation of brine which is difficult to dispose	(Masindi et al., 2017d)

2.6 Mechanisms for contaminants removal, recovery and synthesis

Different mechanisms for the removal of contaminants from AMD have been used through the years, with the main treatment processes including:

- Precipitation/oxidation/coagulation
- Adsorption/ ion exchange
- Filtration
- Bio- and phyto-remediation

A brief introduction on each process, along with their limitations in terms of minerals recovery and factors that hamper their application for minerals recovery and synthesis is given below.

2.6.1 Precipitation/oxidation process

These mechanisms rely on the use of alkaline chemicals to increase the pH or oxidants to convert metals to insoluble state, hence leading to precipitation, with the prevalently used chemical species being oxides, hydroxides, sulfides, and carbonates (Blais et al., 2008, Lewis, 2010). Specifically, the addition of alkaline chemicals lead to the precipitation of the contained chemical species in AMD as hydroxides, sulfides and carbonates sulfides (Lewis, 2010), with the underlying mechanism being nucleation, followed by crystallization and settling (Blais et al., 2008). This also depends on the saturation levels of the solution. The solution can be under-saturated, saturated, and over-saturated. This also influences the homogeneity of the substance formed from the chemical reaction (Blais et al., 2008, Fu and Wang, 2011).. The removal of metals as hydroxides can be denoted by the following equation (Masindi et al., 2018a):

$$M^{n+} + nOH^{-} \rightarrow M(OH)_n \downarrow \quad (2.5)$$

A wide array of alkaline materials has been examined for precipitation of metals from AMD, as shown in **Table 2.4**.

Table 2.4: Different alkaline materials used for the precipitation of metals from AMD.

Mineral	Name	Formula	Reference
Mg-based	Amorphous magnesite	$MgCO_3$	(Masindi et al., 2014)
	Periclase	MgO	(Magagane et al., 2019)
	Brucite	$Mg(OH)_2$	(Bologo et al., 2012)
	Magnesium bicarbonate	$Mg(HCO_3)_2$	(Akinwekomi et al., 2016)

Ca-based	Limestone	$CaCO_3$	(Maree and Du Plessis, 1994)
	lime	CaO	(Geldenhuys et al., 2003)
	Hydrated lime	$Ca(OH)_2$	(Mulopo, 2016)
Na-based	Soda ash	Na_2CO_3	(Akinwekomi et al., 2017b)
	sodium hydrosulfide	NaHS	(Wang et al., 2013)
	Caustic soda	NaOH	(Mirbagheri and Hosseini, 2005)
Ammonia	anhydrous ammonia	NH_3	(Viadero et al., 2006)
	Ammonium hydroxide	NH_4OH	(Maila et al., 2014)
Tailings	Ca, Mg, Ca, Na, etc.	Ca, Mg, Na	(Kastyuchik et al., 2016)

As shown in Table 2.4, Ca, Mg, and Na based materials are typically used for AMD neutralisation. Tailings from the mining and processing of these materials also contain some neutralisation capacity, hence they can be used for AMD neutralisation. AMD chemical composition influences the type of reagents (alkaline chemicals) that need to be used for the recovery of chemical species, while these reagents also influence the recovered chemical species and their use thereafter (Blais et al., 2008).

As reported in Silva et al. (2019), Fe(III) can be recovered from AMD, processed, and then employed for pigments production. Similarly, Akinwekomi et al. (2017b) highlighted the use of Na_2CO_3 and NaOH for the recovery of Fe(III), Fe(II) and Al(III) from AMD at varying pH values and explore its use for the synthesis of goethite, hematite and magnetite. Calcined cryptocrystalline magnesite has been also explored for the recovery of metals, at different pH gradients, from AMD (Masindi et al., 2018c), and the optimal pH values for the recovery of each metal are shown in **Table 2.5**. This concept can be very effective for metals and minerals recovery; however, since there is no distinct line to segregate metal precipitation, the purity of the recovered material could be adversely affected.

Table 2.5: Precipitation of metals at varying pH gradients using calcined magnesite.

Element	**pH range**	**Reference**
Al	4.5	(Masindi et al., 2018c)
Fe (III)	3.5	
Fe (II)	8.5	
Cu	6.5	
Mn	9.5	

Ni	8	
Pb	6.5	
Zn	8	

2.6.2 Adsorption/ion exchange process

This process relates to a surface phenomenon in colloidal science and chemistry. It refers to mechanisms in which contaminants migrate in aqueous solutions and get adsorbed onto surfaces using different forces. This solid-water interface process is governed by numerous processes, which include the migration of pollutants from solutions to the surface that is oppositely charged. More so, other mechanisms such as isomorphous substitution, ion exchange, surface complexation and precipitation may play a critical role in the attenuation of contaminants from aqueous solutions (**Figure 2.7**). This also depends on the oxidation states of chemicals, since the surface charge of chemical species depends on the pH of the aqueous system (Sparks, 1995, Langmuir, 1997). This process has been widely explored for the removal of chemical species from aqueous solution, with its main strengths being (Sen Gupta and Bhattacharyya, 2012, Yadav et al., 2019, Zhou et al., 2019, Kalita and Baruah, 2020):

- The material required to drive the process, such as activated carbon, are readily available and often low-cost.
- Adsorbents have high adsorption capacities and they can be re-used for adsorption process for numerous cycles.
- Simplicity in operation and ease of application.

However, this process has also numerous drawbacks, including:

- Quick saturation leads to poor performance in highly concentrated solutions.
- High selectivity and affinity hamper its utilisation in the decontamination of multi-charged wastewaters, such as AMD.
- Regenerates from the regeneration process require proper handling and disposal and this incurs additional disposal costs.
- This process has been proven to be effective in less concentrated solutions, compared to AMD, and it is mainly used as a polishing technique.

- Regenerants are highly mineralised and heterogeneous, due to multi-mechanisms that utilize different techniques, hence making it difficult to recover pure and high quality minerals.

This process has been widely employed for the removal of anionic and cationic contaminants, making use of materials such as activated carbon (Tran et al., 2017b, Tran et al., 2020), zeolites (Westholm et al., 2014, Adam et al., 2019), clay minerals (Ngulube et al., 2017), and ion exchange resins (Zhu et al., 2017), amongst others. The commercially used chemicals include activated carbon, anthracite, zeolite, and bentonite clay. For AMD treatment, Zhang (2011) reported the adsorption of Pb(II), Cu(II) and Zn(II) from simulated AMD using dairy manure compost, while Motsi et al. (2009) explored the adsorption of heavy metals from AMD using natural zeolite, among others.

Different mathematical models and techniques have been employed to identify and describe the mechanisms that govern contaminants removal from aqueous solutions. Specifically, the adsorption isotherms, kinetics, and thermodynamics are used to determine the mechanisms governing the removal of pollutants (Tran et al., 2020). The point of zero charge or zeta potential is used to highlight the relationship between the types of pollutants and capacity (Tran et al., 2017a).

The key challenge in the adsorption/ion exchange process is poor selectivity to species of homogenous charge and hence it finds little applicability in the circular economy concept.

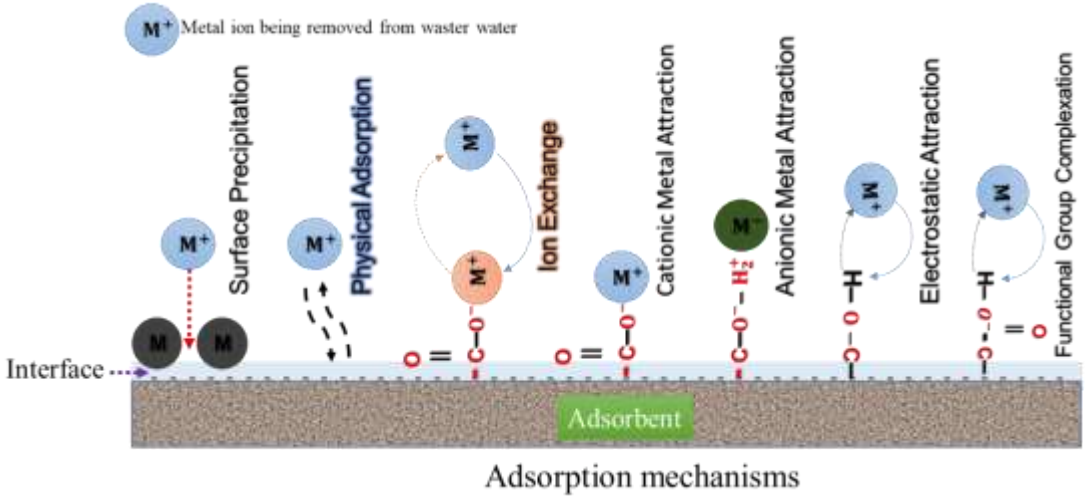


Figure 2.7: An illustration of different adsorption mechanisms on an adsorbent.

2.6.3 Filtration

This is a membrane driven process, where compounds are filtered out using a semi-permeable membrane. Primarily, membrane filtration utilises pressure, concentration gradients, and flux for the removal of contaminants from aqueous solutions. Membrane filtration has gained much application for seawater desalination, drinking water reclamation, and grey water re-use. As such, membranes with different perforations, efficiency, and performance have been developed and they include microfiltration (MF), ultrafiltration (UF), nanofiltration (NF), reverse osmosis (RO) and membrane distillation (MD) (Fu and Wang, 2011, Agboola et al., 2014, Shahrin et al., 2019). Membrane processes have been widely employed for the removal of bacteria, microorganisms, particulates, and natural organic material, which can impart color, tastes, and odors to water and react with disinfectants to form disinfection by-products. Recently, it has been increasingly applied in the removal of metals from raw, retentate, and brine streams in industrial applications. The pores of different filtering media range from as low as 0.001 to as high as 1000 microns. Cations, anions, suspended solids, and organic matters are effectively removed using membrane technologies. Several researchers have explored the use of membranes for AMD treatment (Agboola, 2019). Lopez et al. (2018) evaluated the use of NF for the removal of heavy metals and sulphates from AMD. However, challenges include membrane fouling, pre-treatment requirements, high energy demand, generation of brine, and high costs(Agboola, 2019). Nonetheless, the brine itself can act as new source for minerals recovery. As such, different techniques such as freeze crystallization and distillation have been employed for salts recovery from brine and highly concentrated solutions. MD can also be used for brine treatment due to its temperature driven nature. Moreover, this can be used in waste heat for industrial application where heat is generated as waste (Osman et al., 2019).

2.6.4 Bio- and-phyto-remediation

Phyto-bio-remediation relies on the use of plants and other biological species for the removal of contaminants from different wastewater and soil matrices. This process has been proved to be effective in different applications such as AMD treatment and land rehabilitation. For example, Bwapwa et al. (2017) assessed the bioremediation of AMD using algae strains and highlighted the feasibility of recovering adsorbed metals due to the ability of algae to hyper-accumulate and hyper-absorb (semi-)metals. Kiiskila et al. (2020) reported the metabolic response of vetiver grass (Chrysopogon zizanioides), after being subjected to AMD, while the

efficiency of the same plant for AMD treatment, on a multiscale long-term study, has been also reported in the literature (Kiiskila et al., 2019).

However, it is also very sensitive to numerous environmental indicators, such as plants tolerance to varying conditions, including chemical species concentration, pH and temperature. Specifically, in terms of AMD treatment the following drawbacks have been highlighted in the literature (Ali et al., 2013, Syranidou et al., 2017, Wang et al., 2017, Gu, 2018, Asad et al., 2019):

- Poor performance in concentrated solutions
- Long residence time for effective removal of contaminants
- Requires intensive monitoring
- Requires large land area and a closely controlled environment
- Very difficult to recover minerals post the absorption process
- Disposal of plants can pose secondary toxicity

2.7 Geochemical modelling

In line with the fourth industrial revolution (4IR), modelling and computer simulations have emerged as valuable tools used to: i) gain insight into geochemical processes, ii) interpret laboratory experiments and field data and iii) make predictions of long-term behaviour of chemical components in a system under investigations. In recent decades, the ever-growing concern surrounding the discharge of highly polluted effluents and wastewater streams has encouraged the development of pollution probability scenarios and design management strategies to curtail the impacts associated with mining activities. Moreover, due to the complexity of the underlying process and the time-scales involved, it is often not feasible to adequately conduct realistic laboratory experiments to observe the long-term behaviour of environmental systems. As such, geochemical models are primarily employed to predict future and potential scenarios, as well as, to interpret and predict complex and long-term environmental processes. As such, in the design perspective, geochemical modelling can be applied to effectively optimise remediation efforts, identify crux parameters in environmental management, and help effectively design techniques to prevent the release of ecological contaminants in different settings, such as the mines. Albeit, this initiative cannot be a substitute for experimental studies, rather modelling is a valuable predictive tool that can be used to bridge the gap between laboratory assays, field observations, and long-term behaviour of geochemical systems. A prevalent model has been the PHREEQC (PH REdox EQuilibrium

(in C language)), which is a widely used public-domain geochemical modelling software available from the United States Geological Survey (USGS) (Parkhurst, 1995). In addition, the Geochemical Modelling Code is widely used to model the processes involving the interaction of different minerals and aqueous interface, simulating processes such as adsorption, desorption, neutralization and speciation, amongst others (Parkhurst, 1995, Parkhurst and Appelo, 1999, Zhang and Luo, 2007, Tiruta-Barna, 2008, Wissmeier and Barry, 2010). This model is mainly used as a complementary tool to substantiate experimental results. Wissmeier and Barry (2010) evaluated the use of variably saturated flow into PHREEQC for the simulation of biogeochemical reactions in the vadose zone. Luo et al. (2020) employed PHREEQC geochemical model as a post-remediation study for the distribution and mobilization of heavy metals at an acid mine drainage-affected region in South China. This technique could indicate minerals phases that can be recovered from AMD when using different techniques as highlighted above.

2.8 AMD beneficiation and valorisation

AMD contains valuable compounds that can be reclaimed, recovered, and synthesized using different approaches (Table 2.8). These compounds can render AMD a valuable resource, thus ensuring that the environmental footprint attributed to its treatment can be minimised. This can be achieved through the concept of circular economy, suggesting that AMD can be perceived as a resource and not a waste material (Masindi et al., 2019b, Silva et al., 2019). Specifically, AMD valorisation is achieved through water, even drinking water, reclamation (Masindi, 2017b, Masindi et al., 2017d, Masindi et al., 2018a, Masindi et al., 2019b, Masindi et al., 2021), while its beneficiation can be achieved through the synthesis and recovery of valuable minerals (Silva et al., 2012, Masindi et al., 2019b). However, the main challenge of AMD beneficiation lies in the minerals cross-contamination during recovery, due to the presence of sensitive chemical species that easily precipitate, co-precipitate and co-adsorb, hence contaminating the resultant product. To enhance precision of the minerals recovery and enable AMD valorisation, geochemical tools such as PHREEQC (PH REdox EQuilibrium (in C language)) can be utilised to predict the formation of acid mine drainage and product minerals after treatment with different chemicals such as limestone, lime, periclase, brucite, soda ash, caustic soda, and different alkaline medias.

2.8.1 Water and drinking water reclamation

The dissolved solids in AMD, apart from being contaminated themselves also cause high electrical conductivity. As such, by removing these dissolved solids and recovering them (AMD beneficiation), the treated effluent can be further treated to reclaim water, even to drinking water standards. Various processes have been used to reclaim drinking water, but filtration has been identified as the most promising for drinking water reclamation from AMD (Qu et al., 2009, Agboola, 2019). Other processes, such as adsorption and precipitation, pose secondary pollution and are selective in their efficacies. Specifically, adsorption has an overall low treatment efficiency but precipitation manages to reclaim water suitable for discharge or irrigation (Fosso-Kankeu et al., 2020). However, due to the high content of dissolved metals and hardness of the water, filtration experiences challenges of scaling, fouling and damage due to different chemicals and pH (Nleya et al., 2016, Masindi et al., 2017d, Masindi et al., 2018a, Agboola, 2019). As such, different AMD pre-treatment technologies have been examined. Specifically, Aguiar et al. (2018) successfully explored the treatment of AMD by nano-filtration, focusing on membrane fouling, chemical cleaning, and membrane ageing, with the final goal of reclaiming drinking water was reclaimed. Andrade et al. (2017) evaluated the use of ultrafiltration (UF)-nanofiltration (NF) for the treatment of wastewater from gold mines using a hybrid approach (two-phase treatment process) to prevent fouling, however at the expense of process cost . Ricci et al. (2015) reported the feasibility of using a sequence of microfiltration (MF), nano-filtration (NF) and reverse osmosis (RO) to recover sulfuric acid, separate noble metals, and produce high quality reuse water from wastewater emanating from gold mining. The driving mechanisms were pressure-oxidation process for the highlighted wastewater stream.

2.8.2 Recovery of valuable minerals

Valuable minerals that can be recovered from AMD typically include metals and gypsum. However, the co-contamination of the recovered minerals from AMD has been an issue of prime concern, since this affects their purity, suggesting the need for specific treatment approaches (Lewis, 2010, Nleya et al., 2016, Fernando et al., 2018, Agboola, 2019, Ben Ali et al., 2019). Specifically, Ricci et al. (2015) proposed the use of microfiltration (MF) and nano-filtration (NF) to produce sulfuric acid and separate and recover noble metals from gold mine drainage. The entire process was governed by pressure-oxidation modality (Agboola, 2019). The recovery of Fe(II) and Fe(III) species has been also widely explored (Mohan and Chander,

2006, Chen et al., 2014, Yan et al., 2015, Akinwekomi et al., 2017b). Mohan and Chander (2006) evaluated the use of lignite for sorption of Fe(II)/(III), Mn, Zn and Ca, with the adsorbed minerals being recovered as regenerants, albeit a quick saturation was observed.

2.8.3 Synthesis of valuable minerals

Fe, Mn, Zn, sulfate and other chemical species contained in AMD make it a viable source for (semi-) metals recovery. Specifically, Fe(III) and Fe(II) have been recovered from AMD towards the synthesis of goethite, hematite and magnetite (**Figure 2.7**) (Akinwekomi et al., 2017b, Akinwekomi et al., 2020). Goethite can be used for pigments in the clays, the paint and coatings industry, and it has been also used as an adsorbent for (semi-) metals (Mohan and Pittman Jr, 2007, Basu et al., 2015). Hematite has been employed in pigments synthesis, removal of (semi-) metals and oxyanions, and shielding of radiation, amongst other applications (Phuan et al., 2017, Duuring et al., 2018, Bhateria and Singh, 2019). Similarly, magnetite can be used in ferro-fluid technology, storage of information, photo-degradation for organic contaminants, photo-anode, catalyst, biomedicine, controlled drug delivery, removal of water contaminants and magnetic nanoparticles formation (Wei and Viadero Jr, 2007, Akinwekomi et al., 2017b, Kefeni et al., 2017a, Bui et al., 2018).

2.8.4 Irrigation with AMD

In water-scarce agricultural areas, AMD-contaminated streams, primarily enriched with elevated trace metal, have been used for irrigation. However, these trace metal concentrations eventually leach to the soil and agricultural produce, degrading both the ecosystem and impacting human health. Specifically, in a case study in Potosí, Bolivia the risk of ecotoxicological contamination was identified when AMD-contaminated irrigation water, with trace metal concentrations well above the United Nations Food and Agriculture Organization (UNFAO), Canadian, and Australian guidelines for irrigation water, was used in potato cultivation (Garrido et al., 2009). As a result, Cu, Pb and Zn concentrations exceeded i) the Dutch, Canadian, and German guidelines for agricultural land, implying high secondary risks and ecotoxicological concerns, and ii) the commercially-sold vegetable guidelines in the grown potatoes, suggesting that the agricultural products produced in this region may represent a potential health risk to subsistence farmers and other consumers (Garrido et al., 2009).

On the other hand, Jovanovic et al. (2004) reported that crop irrigation with gypsiferous mine water may create an opportunity to produce crops during the dry winter season on farms in

South Africa, such as in Mpumalanga. Specifically, soil water and salt balances indicated that considerable amounts of mine water can be used and considerable masses of salts can be removed through precipitation of gypsum in the soil profile and therefore with appropriate management, water and salt runoff and salt leaching can be intercepted, thereby minimizing the impact on groundwater (Jovanovic et al., 2004). This has been further corroborated by Hentati et al. (2014).

2.8.5 Co-treatment of municipal wastewater

Keefer and Sack (1983) examined the use of mineral resources recovered from AMD, i.e. Fe, for the treatment, i.e. removal of phosphate and turbidity, from municipal wastewater and results were promising. The synergistic approaches can also play an important role in the management of wastewater streams. Specifically, Hughes and Gray (2013) evaluated, at bench-scale, the potential co-treatment of AMD with municipal wastewater (MWW), using the activated sludge process (plug-flow and sequencing batch reactors) and examined three scenarios: (1) adding raw AMD to the activated sludge aeration tank, (2) pre-treating AMD prior to adding to the aeration tank by mixing with digested sludge and (3) pre-treating AMD by mixing with screened MWW. Pre-mixing AMD with screened MWW was the best process option in terms of AMD neutralization and metal removal; however, significant MWW alkalinity was consumed, suggesting an alkali supplement may be necessary (Hughes and Gray, 2013). Strosnider et al. (2011) examined, at bench-scale, the passive co-treatment of high-strength AMD and MWW and results indicated that this could be a viable approach to improve water quality with minimal use of fossil fuels and refined materials.

2.8.6 Recovery and production of sulphuric acid

Martí-Calatayud et al. (2014) evaluated the recovery of sulfuric acid (SO_4^{2-}) from AMD by means of a 3-compartment electrodialysis (ED), where SO_4^{2-}, free from Fe(III) species, was obtained in the anodic compartment as a result of the co-ion exclusion mechanism in the membranes. The difference in the pH and SO_4^{2-} values between the membrane phase and the external electrolyte promotes the dissociation of complex species inside the membranes, which impede the transport of Fe(III) and sulfates in the form of complex ions towards the anodic and cathodic compartment, respectively.

The current efficiency values of the anion-exchange membrane at different current densities were approximately constant with time. However, the increase in the recovery of acid decreases

as the current increases. This result is explained by the shift in the equilibrium at the membrane/solution interface as more SO_4^{2-} ions cross the anionic membrane and, by the enhancement of the dissociation of water when the limiting current density is exceeded. The main limitation of the process is related to an abrupt increase in the cell voltage due to the formation of precipitates at the surface of the cation-exchange membrane. Sulphuric acid and acid recovery from the metal barren solution was evaluated using Dowex MSA-1 ion exchange resins. The results showed that sulphuric acid can be recovered by the resins via the acid retardation process, and could subsequently be upgraded to near market values of up to 70% sulphuric acid using an evaporator. Water of re-usable quality could also be obtained in the acid upgrade process Hatch and Dillon (1963), (Nleya et al., 2016).

2.9 Factors hampering AMD valorisation and beneficiation

The concept of circular economy in AMD treatment has been well advocated, with advancements being made in water reclamation and minerals synthesis and recovery; however, a number of factors hamper its application (Parbhakar-Fox and Lottermoser, 2015, Kefeni et al., 2017b, Lèbre et al., 2017, Masindi, 2017b, Masindi et al., 2018a, Masindi et al., 2019a, Naidu et al., 2019, Park et al., 2019, Rambabu et al., 2020, Masindi et al., 2021). The main limitations for introducing the circular economy concept in AMD treatment are discussed below.

2.9.1 Purity of the recovered material as a limiting factor

Due to its nature, AMD is highly mineralised and heterogeneous, in terms of its waterborne chemical composition, which makes the recovery of high-grade minerals difficult. The main challenge is the cross-contaminations from minerals contained in AMD. For example, it has been reported that the fractional and sequential recovery of mineral resources from AMD encounters massive challenges due to very fine discrepancies, of pH and those overlapping regions of minerals precipitation (e.g. Fe and Al recovery contaminates each other), which can grossly affect the purity of recovered minerals (Akinwekomi et al., 2017b, Masindi et al., 2018b, Masindi et al., 2018c, Akinwekomi et al., 2020). Therefore, the recovery of pure minerals from AMD has yet to be reported, as impurities persist across the recovered minerals (Kefeni et al., 2017a, Kefeni et al., 2017b, Kefeni and Mamba, 2020). For example, the gypsum piles produced from AMD processing are contaminated with Fe, when lime is used.

2.9.2 Quantity of the recovered material

AMD is rich in Fe and S, as its main elements, followed by intermediate concentrations of Al and Mn, and traces of other elements. Fe concentration and S concentrations can be as high as 20000 ppm and 80 000 ppm, respectively, while Al and Mn can reach values as high as 500 ppm and 200 ppm, respectively, while trace levels of Zn, Cu, Cd, Co, Pb, Cr, As, and Hg, among others, can be found (Akinwekomi et al., 2017b, Masindi, 2017b, Masindi et al., 2019a, Akinwekomi et al., 2020). Other elements can exist in AMD matrices, but typically only at trace levels. As such, Fe and S are the main metals that can be recovered from AMD in large quantities. For example, 50 kg of Fe-based minerals were recovered from 3.5 KL AMD when this was treated with 25 kg of calcined cryptocrystalline magnesite (Masindi et al., 2019a). Gypsum is also recovered, attributed to the large S concentrations. However, due to its low quality it has found little use for industrial applications and therefore processes, such as the GYPSLIM, have been proposed for S recovery from gypsum wastes (Maree et al., 2013). The large Fe and S concentrations can be explained by the fact that the genesis of AMD is from the oxidation of pyrite, arsenopyrite and other Fe-based sulphide minerals. The other chemicals species are impurities, which are incorporated to coal and gold matrices during deposition processes. Gypsum can also be recovered in elevated levels due to sulphate being present in high concentration. The gypsum piles are prevalent in South Africa but they are not usable due to low grade product that fails to meet industrial specifications.

2.9.3 Conditions suitable for minerals recovery

Mine drainage is typically very acidic by nature, but if it occurs in an environment which is rich in carbonates (e.g. dolomites, limestone, magnesite and clay minerals) it will have circumneutral to basic pH, giving it a variable composition since the predominant elements will be sulphate and base metals. As such, AMD is more conducive for metals recovery and sulphate as well. Essentially, acidic pH conditions in AMD can enable the recovery of metals in a step-wise fashion, with the following pH sequence being suggested: Fe can be recovered at pH ≥ 3 - 3.5, gypsum at pH ≥ 4 - 10, Al at pH ≥ 6.5, Mn at pH ≥ 9.5, Cu at pH ≥ 7, Zn at pH ≥ 8, Pb at pH ≥ 8, Ni at pH ≥ 9, Mg at pH>10, and Ca at pH>12 (Masindi et al., 2018c). Furthermore, in real operations, minerals synthesis is complex, requiring also complex processes such as co-precipitation. For instance, magnetite production requires the co-precipitation of Fe(III) and Fe(II), thus cannot be typically pursued in a linear process. Furthermore, the temperature of approximately 80 °C and 700 °C are required for the synthesis

of goethite and hematite, respectively. The synthesis of magnetite at100 ℃ cannot also be achieved using one linear reaction, suggesting the need for a stage-wise approach, where gypsum and calcium carbonate can also be recovered (Akinwekomi et al., 2020).

2.10 Summary of the literature review

The literature review informs that AMD can be a viable re-source from which valuable minerals such as goethite, hematite and magnetite can be synthesized. Drinking water can also be reclaimed from AMD. Gypsum, limestone and dolomite can be synthesized from the treatment process. This could make this system self-sustainable, if the revenue generated from the reclaimed, recovered and synthesized products can off-set the running costs and the ecological and other impacts of the treatment process. Amongst the value recovery technology, precipitation has been identified as the main technique for minerals recovery but for drinking water reclamation, filtration technologies are better. Challenges associated with minerals recovery and AMD valorisation are the generation of heterogeneous sludge, the costs associated with minerals recovery and feasibility considering the complex composition of AMD. Adsorption has been identified as an unviable technology for minerals recovery and beneficiation due to quick saturation of the sorbents and regeneration requirement, which is unselective. For the future, studies should focus on sequential and fractional recovery of valuable minerals from mine drainages using different techniques. Future studies also need to include integrated approaches for minerals recovery from AMD.

In light of this findings of the literature review, the objectives of this study which aims at recovering minerals from AMD will seem viable and a game changer in the valorisation of AMD. This will effectively address the concept of circular economy and minimisation of ecological footprints of AMD treatment and their disposal process.

CHAPTER THREE

MATERIALS AND METHODS

In this chapter, acquisition of the samples, experimental configurations, optimisation studies, and analytical techniques used to fulfil the goals and objectives of this study are meticulously explained. The quality control procedures and simulation conditions applied in the experiments are also described in this section.

3.1 Acquisition of the samples

The pulverised magnesite (≤32µm particles) which is thermally activated (calcined) at 1050 ℃ was procured from Sterkfontein Carbonates Pty (Ltd), Republic of South Africa. The samples came in 25 kg bags and stored in a designated area until use for the recovery experiments. The real field AMD samples were obtained from a coal mine in Mpumalanga province, South Africa. Grab samples were collected in the flowing stream from the coal handling facility. The samples were filled to the top of the container to avoid air ingression. The samples were stored in 25 L bottles of High-Density Polyethylene (HDPE) containers. The containers were tightly closed to prevent further oxidation and precipitation of metals, and kept at 4°C until utilisation for metals recovery experiments. Before utilisation, the AMD samples were filtered through Whatman® Grade 1 filter paper. This was done to remove suspended solids and debris. In-situ analysis, i.e, pH, EC and TDS, were done using a multimeter probe as described below whilst ex-situ analysis were done in an accredited lab using the state of the art analytical instruments as described below.

3.2 Optimisation of the recovery of chemical species

To acquire an in-depth understanding of the factors influencing the recovery of Al, Fe, Mn and sulphate including traces of other metals from AMD matrices, the effect of activated magnesite dosage was evaluated. pH and activated magnesite dosage were used as the main indicators for this analysis. Sixty (60) minutes of reaction time was used for the optimisation studies and as this had been found appropriate in previous studies (Masindi et al., 2015a, Magagane et al., 2019). To precisely denote the effect of the parameters under study, ambient room temperature and pH for AMD were considered for AMD matrices since this would be applied for scaled up systems. Effective mixing was achieved by means of an overhead stirrer at 650 rpm. To study the effect of feedstock dosage on pH and metals recovery, the one-factor-at-a-time (OFAAT)

method was used, i.e. first the grams of activated magnesite were varied while keeping the contact time, temperature and supernatant pH parameter fixed, as shown in **Table 3.1**. This enabled an in-depth understanding of the factors that influence the recovery of Al, Fe, Mn and sulphate from AMD.

Table 3.1: Examined parameters and values for the recovery of valuable minerals from AMD.

Number	Target pH	Initial pH
Units	-	-
1	2.5	2.5
2	3	2.5
3	3.5	3
4	4	3.5
5	6.5	4
6	8	6.5
7	9.5	8
8	10.5	9.5

Specifically, the effect of the dosage of each effluent was examined by considering solid-liquid (Activated magnesite: AMD) ratios. The dosage sensitivity analysis and effect of pH were examined by mixing activated magnesite with AMD feed solution for 60 minutes of equilibration. All experiments were performed in triplicate and results are reported as mean values.

The sensitivity of the system was done using pH as an indicator by varying the amount of activated magnesite introduced into the beakers. The pH was varied by adding a small fraction of activated magnesite until a desired pH was reached using stabilisation time interval of 30 minutes. This time interval was determined in a previous study by Masindi et al. (2016a). Specifically, measured fractions (grams) of activated cryptocrystalline magnesite were added into different volumetric flask that contained AMD. The mixtures were agitated for 60 minutes at 650 rpm as denoted in **Table 3.1**. Post equilibration, the mixtures were filtered through a 0.45 µm pore nitrocellulose filter membrane for characterisation. The filtrates were preserved by adding two drops of concentrated HNO_3 to prevent aging and immediate precipitation of Al, Fe and Mn, and refrigerated at 4ºC prior to analysis. The respective pH values of samples

before and after agitation were recorded. A separate set was left un-acidified for sulphate analysis.

The percentage removal of chemical species (Al, Fe, Mn and sulphate) from AMD using activated cryptocrystalline magnesite was determined using Eqn. 3.1.

$$\text{Percentage removal (\% removal)} = \left(\frac{C_i - C_e}{C_i}\right) \times 100 \quad (3.1)$$

Where, C_i is the initial concentration and C_e is the final concentration. This precisely and effectively denotes the efficacy of the system in recovering chemical species from the activated magnesite-AMD solution. The computed figures were used to determine the effectiveness of the identified dosage in relation to the percentage of the chemical species which were removed at a given pH range.

3.3 Quality control and quality assurance

In analytical environmental chemistry, quality assurance is essential. This is mainly done to ensure the repeatability, reproducibility and validity of the obtained results. This study therefore included quality control and quality assurance to ensure the generation of trustworthy and valid results. The quality control and quality assurance process in this study comprised undertaking all the experiments in tri-plicate and reporting the obtained results as mean values. The data was considered acceptable when percentage difference within triplicate samples and percent error were below or equal to fifteen percent (≤15%). Furthermore, analytical values which were noted to be below the detection limit (BDL) were managed following the Environmental Protection Agency (EPA) guideline. To further reinforce the validity of the results, the National Institute of Standards and Technology (NIST) aqueous standards were employed to assure the accuracy of the analysis (Wei and Viadero Jr, 2007). Lastly, but not least, the results for selected samples was further validated using the inter-laboratory analysis approach. All the aqueous samples were characterised in an ISO/IEC 17025:2017 accredited laboratory, i.e., Magalies Water Services Laboratory, Brits, North West, South Africa. The solid samples were characterised at the University of Pretoria (XRF and XRD) whilst the other indicators (morphological properties, elemental mapping, and metals-functional groups) were analysed at the Council for Scientific and Industrial Research (CSIR), the state-of-the-art materials characterisation, testing, and analytical facility for nano-materials.

3.4 Characterisation

3.4.1 Characterisation of aqueous samples

Analytical instruments that were used to determine the physical and chemical parameters of the examined water samples are listed in **Table 3.2**. It should be noted that the total dissolved solids (TDS) were measured at 180 °C while the electrical conductivity (EC) and pH were measured at 25 °C.

Table 3.2: The analytical instruments which were used to determine the physical and chemical parameters of water samples.

Parameters	**Analytical equipment**
Al, Fe and Mn	The inductively coupled plasma mass spectrometry (ICP-MS), X-Series 2, ICP-MS, supplied by Thermo scientific, from Hanna-Kunath-Str. 11 28199 Bremen, Germany. The ICP-MS was equipped with ASX-520 Auto sampler.
Cu, Ni, Pb, and Zn	The inductively coupled plasma - optical emission spectrometry (ICP-OES), 5110 ICP-OES vertical dual view, Agilent technologies Australia, Made in Malaysia. The ICP-OES was equipped with Agilent SPS 4 Auto sampler.
Sulphate	The Gallery™ Plus Discrete Analyzer. Gallery plus photo spectrometer, Automated chemistry analyzer, Supplied by Thermo Fisher scientific, Made in Vantaa, Finland.
pH, EC, and TDS	The HANNA Multi-parameter probe. Model: HI-9828 Multi-parameter water quality portable meter was utilized.

Techniques shown in **Table 3.2** were used to characterize the aqueous samples before and after the interaction of activated cryptocrystalline magnesite and AMD.

3.4.2 Characterisation of solid samples

For the characterization of activated magnesite and recovery of valuable minerals at different pH ranges, the state-of-the art analytical instruments were used as demonstrated in Table 3.1. In particular, the morphological properties, surface functional groups, elemental composition, and minerals phases of the recovered minerals were explicitly measured. To this end, Fourier transform infrared spectroscopy (FTIR), X-ray diffraction (XRD), X-ray fluorescence (XRF),

were used along with a high resolution scanning electron microscope (SEM) that was coupled with energy dispersive X-Ray spectroscopy (EDS) (**Table 3.3**).

Table 3.3: The equipment used to determine the properties of the raw and recovered minerals.

Parameter	**Equipment**	**Model**
Mineralogical composition	XRD	PANalytical Aeris powder diffractometer with a PIXcel detector and fixed divergence- and receiving slits with Fe filtered Co-Kα radiation (λ=1.789Å). Phases were identified using X'Pert High-score plus software.
Elemental composition	XRF	The Thermo Fisher ARL Perform'X Sequential XRF instrument with Uniquant software.
Morphology properties and spot-analysis	SEM-EDS	Auriga Cobra FIB-FESEM (Model: Sigma VP FESEM with Oxford EDS Sputtering System, Make: Carl Zeiss, Supplier: Carl Zeiss, USA).
Functional groups	FTIR	Perkin-Elmer Spectrum 100 Fourier Transform Infrared Spectrometer (FTIR) equipped with a Perkin-Elmer Precisely Universal Attenuated Total Reflectance (ATR) sampling accessory equipped with a diamond crystal.

Techniques shown in **Table 3.3** were used to determine the fate of chemical species post the interaction of AMD and activated cryptocrystalline magnesite.

3.5 Geochemical modelling

To complement the experimental results and determine the aqueous species and mineral phases that are more likely to be synthesized from the interaction of activated cryptocrystalline magnesite and AMD, geochemical modelling was applied. The primary aim was to determine speciation and calculate the saturation indices (SIs) of the mineral phases, based on compositions and pH. To fulfill that objective, PH REdox EQuilibrium (in C language) (PHREEQC) geochemical model along with the WATEQ4F chemical speciation model were used (Masindi, 2016). Furthermore, the chemical species which were more likely to precipitate were determined using the modelled SI index whereby, SI values lower than unity (< -1) denote an under saturated solution, SI values equal to unity (= 1) denote a saturated solution and, SI values higher than unity (> 1) denote a supersaturated solution.

CHAPTER FOUR

RESULTS AND DISCUSSIONS

This chapter presents the results which were obtained from the experiments carried out to meet the objectives of this study. The results were obtained using the methodologies described in Chapter 3. This section corroborates results from a laboratory study and PHREEQC geochemical modelling. The used AMDs were collected from the beginning of the experiments and post optimisation studies to check the efficacy of the material, as such, there might be some variations in the water quality of AMD used for optimisation and for the performance verification at optimum conditions.

4.1 Feed and processed products quality

The physico-chemical characteristics of feed water, product water and their respective dosages are summarised in **Table 4.1**.

Table 4.1: The physico-chemical characteristics of feed water, product water and their respective dosages.

Parameters	**AMD**	**Effect of dosage on pH and chemical species**						
pH	2.5	3	3.5	4	6.5	8	9.5	10.5
Volume (mL)	5000	5000	4500	4200	4000	3700	3600	3100
Dosage (g)	Nil	23	23.6	24.1	31.1	31.3	40.1	57.1
Al (mg/L)	450	180	150	50	BDL	BDL	BDL	BDL
Fe^{3+} (mg/L)	9000	600	500	450	400	BDL	BDL	BDL
Mn (mg/L)	125.9	110	100	90	70	10	0.5	BDL
SO_4^{2-} (mg/L)	18000	14500	14000	13900	13500	9000	8000	4500
Cu (mg/L)	2	2	2	2	1.5	BDL	BDL	BDL
Ni (mg/L)	3	2.8	2.5	2.4	2.3	2	BDL	BDL
Pb (mg/L)	2	2	2	2	1.5	BDL	BDL	BDL
Zn (mg/L)	6	6	5	4	3	2	BDL	BDL

NB: Volume is for AMD and dosage for activated magnesite. BDL stand for below the detection limit.

As shown in **Table 4.1**, the physico-chemical properties showed the effect of dosage on pH and chemical species in AMD. Specifically, there was a congruent relationship between dosage

and pH. Chemical species were observed to decrease with an increase in dosage of the feedstock, i.e. activated cryptocrystalline magnesite. The pH was observed to increase from 2.5 to 10.5 at 57.1 g in 3100 mL of AMD. Similarly, the obtained results were also reported by Petrilakova et al. (2014). Thenceforth, from **Table 4.1**, it can be seen that Fe precipitated at pH 3 – 3.5, Al at pH 6.5 and Mn at pH 9.5, with sulphate precipitating from pH 3.5-10.5. Albeit, the concentration of Cu, Ni, Pb, and Zn were very minute and their recovery would not be economically viable.

4.2 Effect of pH on the removal levels of chemical species

To gain insight into the minerals recovery efficacy, the effect of dosage on pH and chemical species removal was examined and the results are shown in **Figure 4.1**.

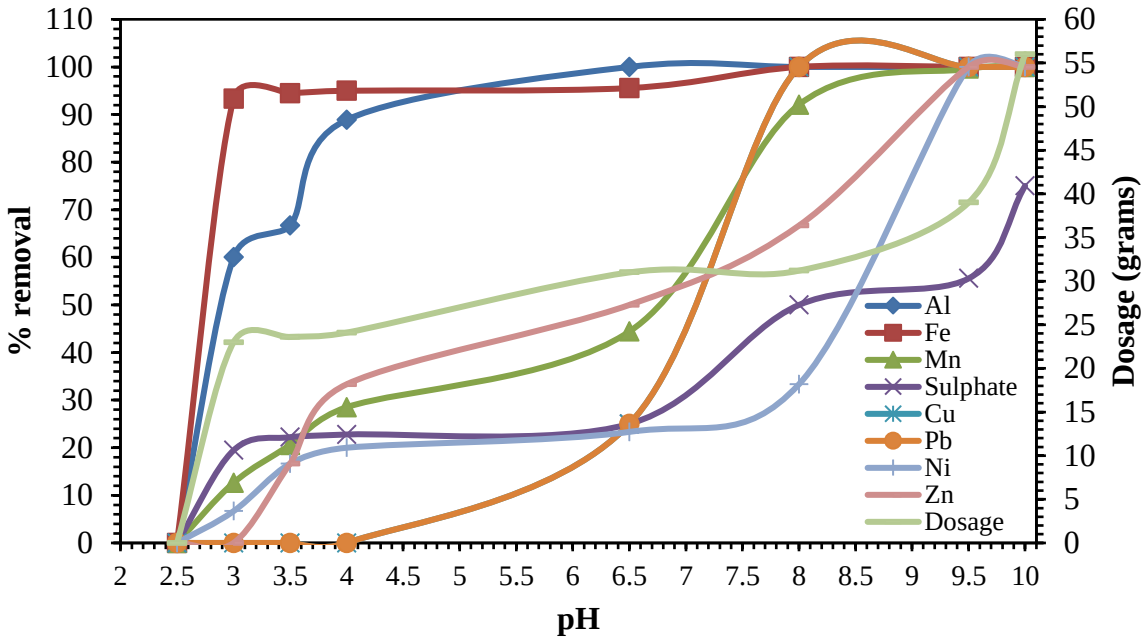


Figure 4.1: The effect of feedstock dosage (i.e. activated magnesite) on pH and chemical species removal (Conditions: 1000 mL solution, 250 rpm shaking speed, ≤32 µm particle size, 60 min reaction, 26 °C temperature).

The results revealed close relationship between dosage and pH, and this further influenced the removal of metals. The effect of pH on the removal of metals has been widely reported in literature (Simate and Ndlovu, 2014). An increase in dosage increased the pH from 2.5 for the feed water to 10.5 with a dosage of 55 g of activated magnesite. Such increase in pH is attributed to the addition in alkalinity (OH^-) during the dissolution of Mg and Ca from activated magnesite matrices. As shown in Figure 4.1, magnesite achieved 99% removal efficiency of

Fe at pH > ≈ 4, Al-species at pH > ≈ 6, and Mn removal was observed to be >99% at pH > ≈ 9. These results of this study are consistent with those obtained by other researchers (Wei and Viadero Jr, 2007, Seo et al., 2017). This indicates the pH that is suitable for fractional and sequential recovery of chemical species from AMD. Furthermore, it was observed that Cu precipitated at pH ≤7, Zn at pH ≤9.5, Pb at pH ≤8, and Ni at pH ≤9.5. The findings of this study were congruent to findings reported by Park et al. (2013). To this end, approximately ≥99% removal efficiency was achieved for chemical species except for sulphate which attained an attenuation of about 70%. Albeit, the levels of Cu, Ni, Pb and Zn were observed to be insignificant due to their minute concentrations in AMD; as such, there is no economic metal recovery potential for them, thus leaving Al, Fe, Mn and sulphate as the recoverable elements.

4.3 Simulation of the effect of pH and dosage on the recovery of chemical species

To further assess the recovery of chemical species from AMD, PHREEQC geochemical model was used to simulate the effect of dosage on pH and chemical species attenuation. The results are shown in **Figure 4.2**.

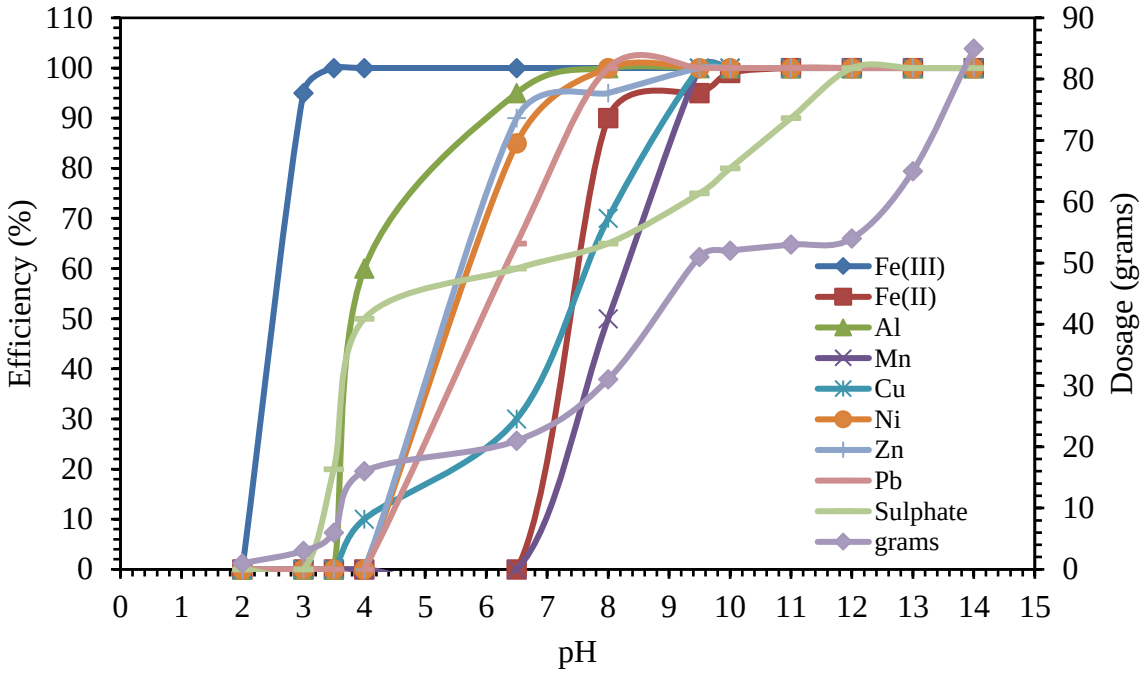


Figure 4.2: Simulation of the effect of feedstock dosage (i.e. activated magnesite) on pH and chemical species levels using PHREEQC geochemical model (Water Q4 database).

As shown in **Figure 4.2**, findings from PHREEQC geochemical model simulation denoted the feasibility of Fe(III) to have been recovered at pH ≥ 3.5, Fe(II) at pH ≥ 10, Mn at pH ≥9.5, Zn

at pH ≥10, Cu at pH ≥9.5 whilst Ni and Pb at pH ≥8. The recovery of sulphate was observed to be feasible from pH 4 -12. The obtained results corroborate the findings which were reported from the laboratory experiment and from previous studies. A slight variation was observed with dosages but the chemical species attenuation was observed to be similar hence strengthening the validity of the laboratory results.

4.4 Sensitivity analysis

To gain insight into the effect of sensitive dosage on the recovery of minerals from AMD, the effect of dosage on pH and chemical species reduction was investigated and the results are shown in **Figure 4.3**.

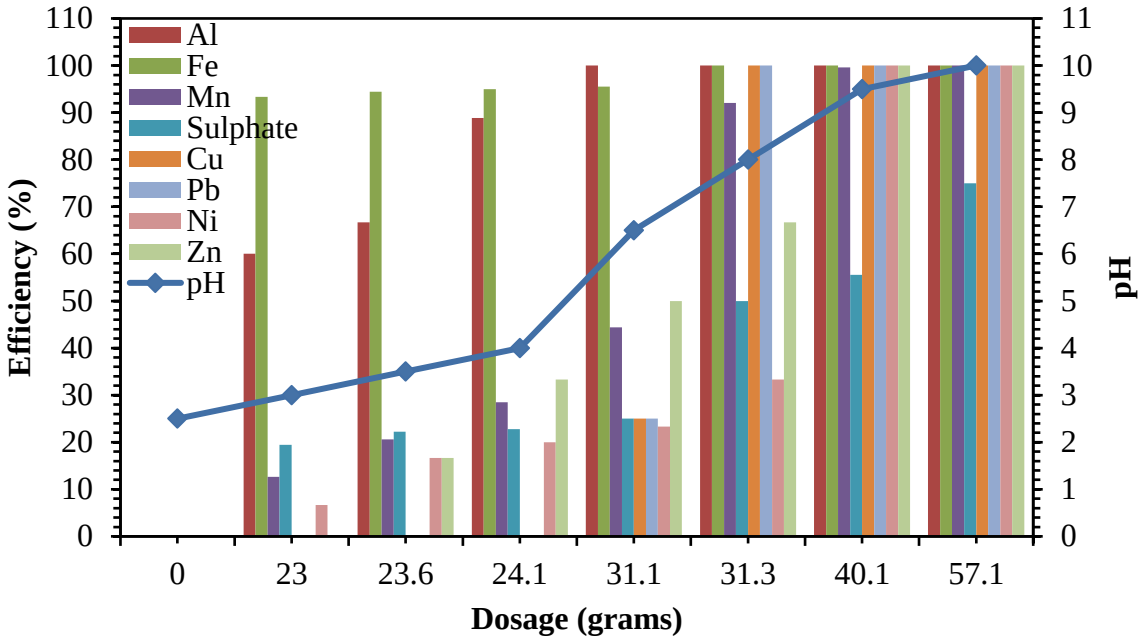


Figure 4.3: The sensitive dosage (i.e. activated magnesite) and its effects on pH and chemical species levels (Conditions: 1000 mL solution, 250 rpm shaking speed, ≤32 µm particle size, 60 min reaction, 26 °C temperature).

As shown in **Figure 4.3**, the sensitivity analysis of activated magnesite on the recovery of chemical species from real AMD is observed. Specifically, an increase in dosage led to an increase in pH and the reduction in the concentrations of chemical species. In particular, the pH increased from 2.5 to 10 using 0 – 57.1 grams of activated magnesite. An increase in dosage increased the alkalinity of the system via the addition of hydroxyl groups (OH-group). This has corroborated results reported in Figure 4.1 and PHREEQC geochemical modelling. As expected, at Fe^{3+}/Fe^{2+} were recovered at pH ≥ 3 and ≥8, respectively, Al at pH ≥ 6.5, Cu and

Pb at pH ≥ 7.5 and, lastly, Ni and Zn at pH ≥ 9. The results obtained in this study are consistent with findings reported in other studies and afield (Oh et al., 2016, Akinwekomi et al., 2017b, Seo et al., 2017, López et al., 2019, Naidu et al., 2019, Akinwekomi et al., 2020).

4.5 Simulation of the precipitation potential with PHREEQC

The simulation of the mineral phases recovered from AMD using activated magnesite by PHREEQC geochemical model (water Q4 database) was performed, and the results are shown in **Figure 4.4**.

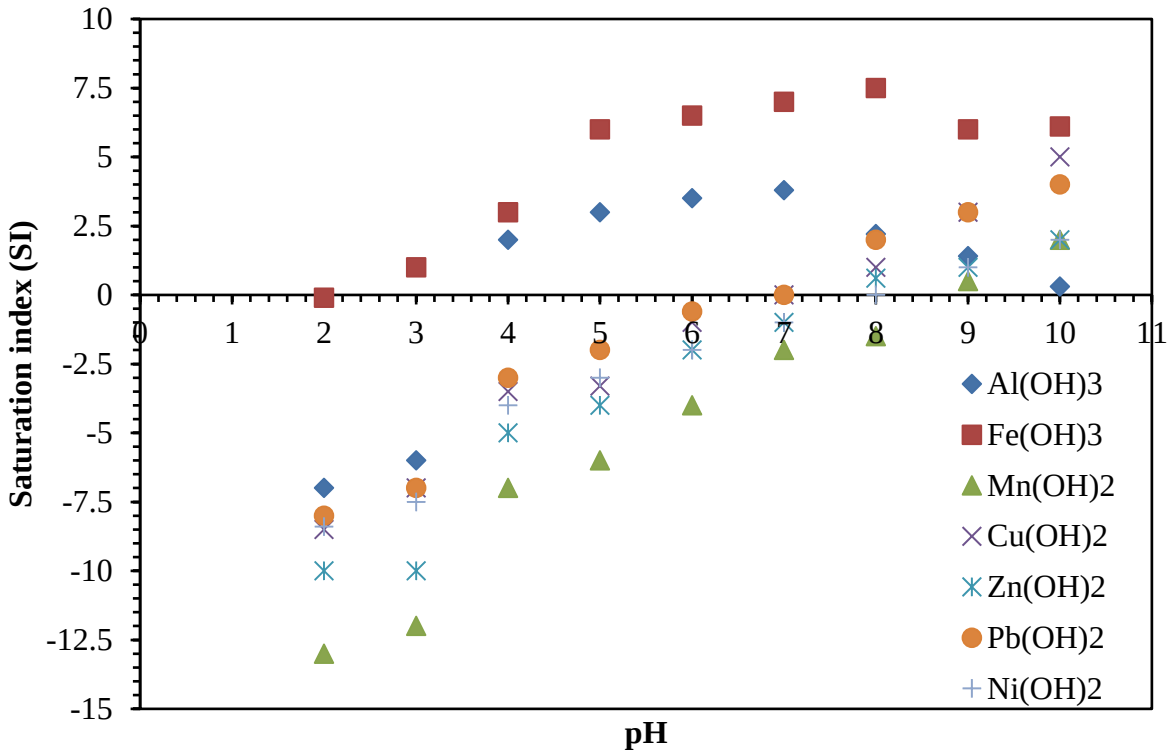


Figure 4.4: The simulation of the mineral phases to be recovered from AMD using activated magnesite by PHREEQC geochemical model (water Q4 database).

The obtained results revealed that Fe minerals will be recovered at pH ≥ 3.5, Al at pH ≥ 4.5, Cu at pH ≥ 7, Zn at pH ≥ 8, Pb at pH ≥ 8, Mn at pH ≥ 9, and Ni at pH ≥ 9. This has confirmed that different mineral phases could be recovered at different pH gradient using activated magnesite. Metals were predicted to precipitate as oxy-hydroxides and sulphate as gypsum and Al-Fe-oxy-hydrosulphates. The chief mechanisms which were governing the recovery of different mineral phases were precipitation as the alkalinity in the system increases due to Ca and Mg in the aqueous system. Thenceforth, the reported PHREEQC geochemical model results are congruent to laboratory assays hence confirming that the obtained results are valid.

4.6 Treatment of AMD using activated magnesite

To assess the overall performance of activated magnesite on real AMD treatment, the physico-chemical composition of raw and treated AMD are shown in **Table 4.2**. Due to variation in geological conditions and sampling dates, the AMD used for final treatment at optimised conditions was slightly different from the AMD which was used in optimisation studies. Based on our previous findings, 60 minutes of mixing was used in this study (Masindi et al., 2015a).

Table 4.2: The physico-chemical properties of raw and treated AMD.

Parameters	**Units**	**Limits**	**Raw AMD**	**Treated AMD**	**%**
pH	-	9.5	2.57	10.10	-293.00
Conductivity (EC)	mS/cm	150	1700.00	2200.00	-29.41
Aluminium (Al)	mg/L	0.5	200.00	0.24	99.88
Iron (Fe)	mg/L	0.3	1800.00	0.32	99.98
Manganese (Mn)	mg/L	0.1	98.00	0.30	99.69
Calcium (Ca)	mg/L	30	622.00	737.00	-18.49
Magnesium (Mg)	mg/L	30	495.00	1638.00	-230.91
Nickel (Ni)	mg/L	0.1	1.30	0.02	98.15
Zinc (Zn)	mg/L	0.1	3.70	0.02	99.46
Copper (Cu)	mg/L	0.01	0.24	0.02	90.42
Lead (Pb)	mg/L	0.01	0.20	0.04	82.00
Sulphate (SO_4)	mg/L	200	13166.00	8200.00	37.72

NB: Limit is the department of water and sanitation guideline for irrigation water (Department of Water Affairs and Forestry, 1996).

AMD was characterised of high acidity (low pH), and high EC. The initial AMD pH was ≈ 2.57 and the predominant chemical species were sulphate, Fe, Al, Mn, Ca and Mg. Minute levels of Cu, Ni, Pb and Zn were also found to be present. Practically, the levels which are recoverable are sulphate, Al, Fe, and Mn due to their significant concentrations as compared to the rest. High levels of Fe and sulphate denote that the current AMD could be the product of pyrite weathering (Tabelin et al., 2017a). The feed AMD comprised chemical species which were above the maximum allowed limits (MAL) for irrigation (Department of Water Affairs and Forestry, 1996) indicating that this effluent is not suitable for discharge to any receiving

environment. The presence of Ca implies the feasibility of $CaSO_4$ precipitation. The treatability index of AMD is very high denoting high treatment cost but the recovery of valuable metals could make it viable. After treatment of real AMD with activated magnesite, the levels of Al, Fe and Mn were observed to have reduced significantly, approximately 99% removal efficacy. Albeit, the levels of Ca and Mg were observed to have increased but this could be due to their dissolution. Similarly, treatment has increased the EC and TDS of the AMD. The pH increased to 10.10 making it suitable for precipitation of metals as oxy-hydroxides. In light of the above, the treatment of AMD for discharge and minerals recovery could be viable using activated magnesite. However, further treatment to meet all the water quality limits for Ca, Mg, sulphate and EC would be required.

4.7 Solid characterisation

This section presents the characterisation results of activated magnesite and recovered minerals. This will be used to determine the fate of inorganic contaminants post the AMD treatment and the viability of their recovery. This section will highlight different minerals phases that are recovered at different pH ranges.

4.7.1 Map spectrums for elemental composition

The utilized FE-SEM instrument was equipped with an Energy-dispersive X-ray spectroscopy (EDS) detector, which was used towards identifying the Wt. % spectrum and elemental composition of the feed and recovered elements. The results are shown in **Figure 4.5**.

As shown in **Figure 4.5**, the feedstock was found to comprise of Mg, O, and C as its major elements, whilst low concentrations of Si, Al, and Ca were also identified. This composition denotes a clear representation of the calcined magnesite since residual carbon from CO_2 emission should remain. The step-wise and fractional mixture of AMD and activated magnesite led to the recovery of different chemical species at different pH. This could be linked to the precipitation of different elements at different pH as shown in the water quality results and PHREEQC geochemical simulations. The interaction of real AMD with activated magnesite led to an increase in the level of Fe and S at pH ≥3. Furthermore, at pH ≥3.5, the level of S was observed to increase whilst Fe, O and Mg remained the same. This denoted that sulphate is being scavenged from the aqueous solution. At pH ≥ 4, the S and Ca level drastically increased and this could be linked to the formation of gypsum during the chemical reaction. The level of Fe was reducing hence denoting that it has been depleted from the aqueous system as confirmed

by the water quality analysis. Thenceforth, at pH ≥6, the level of Al was observed to increase in the sludge hence denoting that this pH is conducive for the removal of Al from real AMD. Conversely, the level of S and Ca were observed to reduce as compared to pH ≥ 4. The mixture activated magnesite and real AMD at pH ≥ 8 further confirmed the attenuation of a different chemical species, specifically, Mg, S, Ca, and Al. This could be explained to the fact that Al precipitates at pH ≥ 6 – 8, Mg ≥ 8 – 10, and S ≥ 4- 10. At pH ≥ 9.5, Mn stepped-up to the precipitation sequence; however, it was accompanied by S, Ca, and Mg. The literature has confirmed that Mg precipitates at pH ≥ 8-10. Lastly, but not least, pH 10 denotes the precipitation of Mg as the key element. Therefore, results from this study explicitly confirm that different elements and chemical species precipitate at different pH gradients. Furthermore, as discussed above, activated magnesite contributes to the removal of contaminants from the real AMD matrix. According to PHREEQC geochemical model simulations, Fe and Al were removed as oxy-hydrosulphates, oxy-hydroxides and carbonates due to residual carbonate in the matrices of activated magnesite. Explicitly, the formation of carbonates, oxy-hydroxides and oxy-hydrosulphates are apparent in the obtained sum spectrum results (Wt. %). As a result, the recovered materials appear to be rich in minerals that could possibly be harvested for beneficiation hence confirming that a sequential recovery of elements from the real AMD could be feasible if it adequately offsets the running costs and environmental impacts of resource recovery.

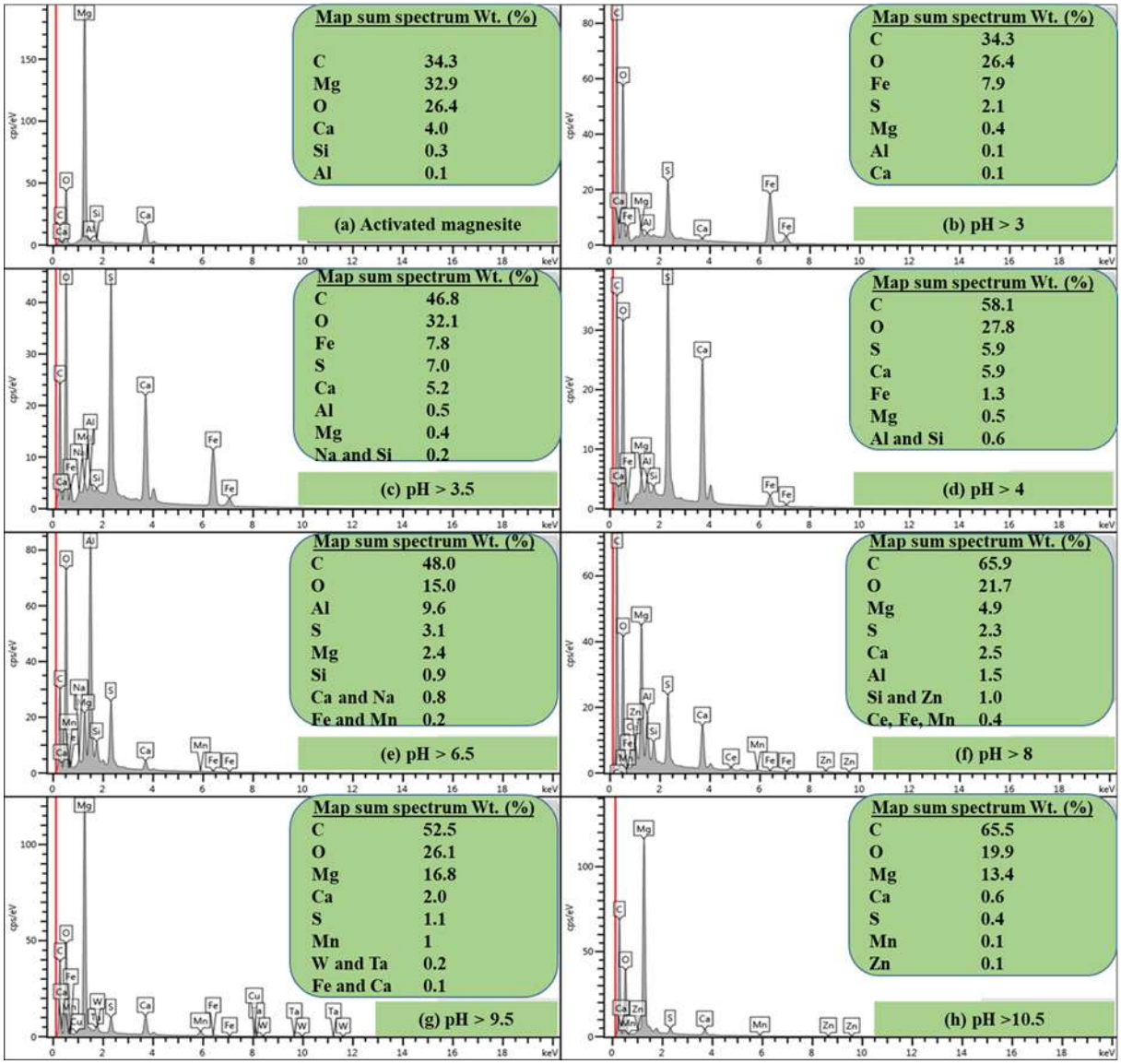


Figure 4.5: The map sum spectrum of the elemental composition of activated magnesite and recovered elements at different pH ranges from the treatment of real AMD with specified dosages of activated magnesite.

4.7.2 Morphological properties

The morphological properties of activated magnesite and minerals recovered at different pH (pH from ≥ 3 to ≥ 10.5 are shown in **Figure 4.6**. As mentioned in section 3.4, a high-resolution Focused Ion Beam Scanning Electron Microscope (FIB FESEM) instrument was used to identify the morphological characteristics of the feed and product materials. In particular, the Auriga Cobra FIB FESEM instrument was used for obtaining images in this study. The primary aim was to acquire clear, ultra-high resolution, and low electrostatically distorted images that reveal pristine morphology of the minerals under study (**Figure 4.6**).

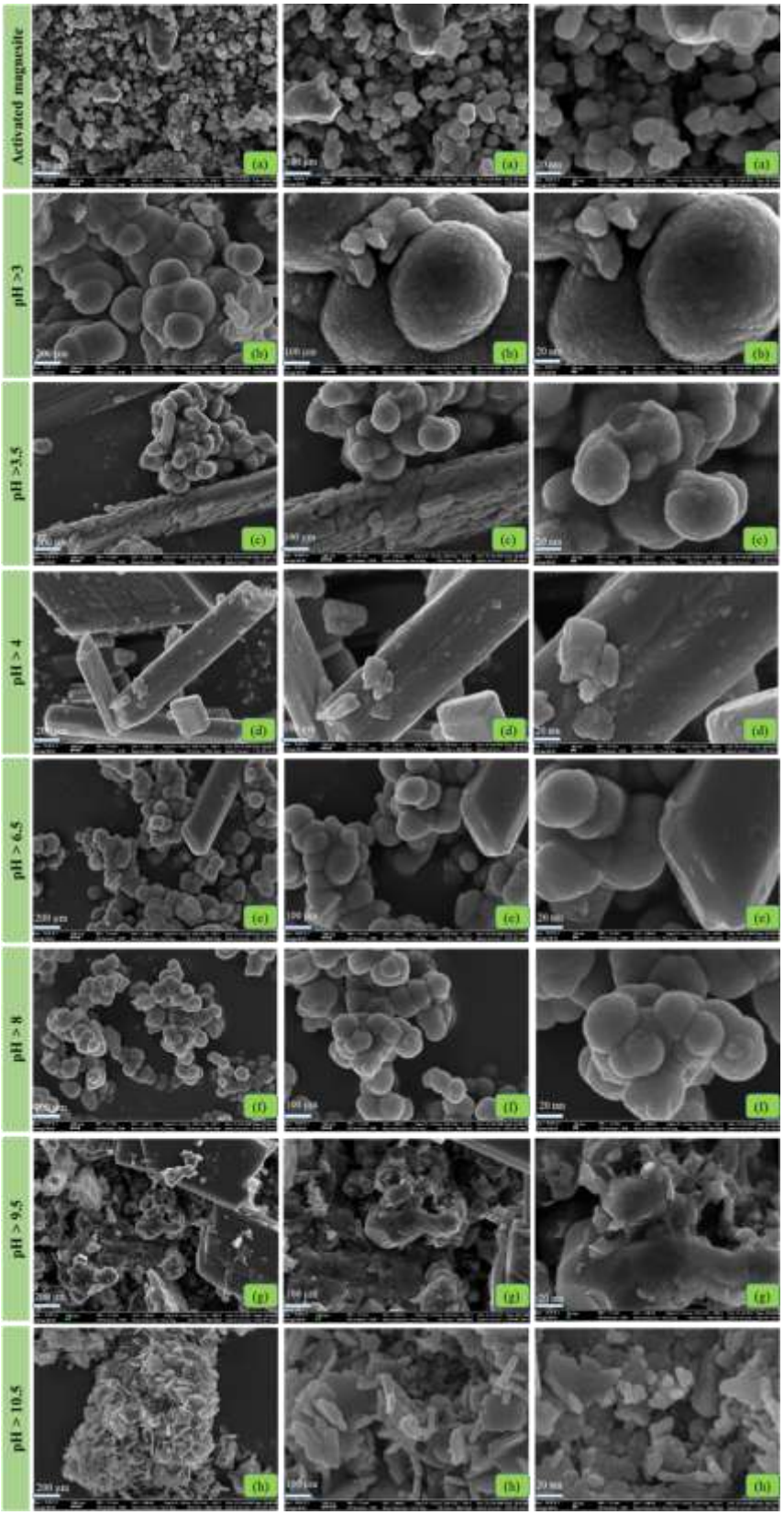


Figure 4.6: FESEM images of the morphological properties of activated magnesite (a), and minerals recovered at different pH (pH from ≥ 3 to ≥ 10.5 [b-h]) at 1 μm and 100 nm.

As shown in **Figure 4.6(a),** the calcined cryptocrystalline magnesite comprised of particles with octagonal leafy-like structure and sheets with varying sizes. Interestingly, the morphological properties were observed to be the same at different magnifications (1 μm and 100 nm). The surface was observed to be homogenous in nature hence indicating that the material is the same through-out. The obtained results corroborates what has been reported for calcined magnesite and its derivatives (Zeng et al., 2009, Wang et al., 2011, Stolzenburg et al., 2015, Ramakokovhu et al., 2020). At pH ≥3 (**Figure 4.6b**), the recovered mineral was observed to comprise of spherical material inter-connected in a rod-like fashion. This was consistent in different magnifications. According to the map sum spectra, the material recovered at pH ≥3 is rich in Fe hence denoting that this material with spherical properties could potentially be Fe, but this will be confirmed by the SEM mapping results. Furthermore, **Figure 4.6(c)** demonstrated the presence of rod-like and spherical structures on the recovered material. The predominant structures were the rods at this stage. This could explain the presence of Fe and S. According to **Figure 4.5(c),** pH ≥ 3.5 fosters the precipitation of Fe, Ca, and S, and this explicitly denotes the feasibility of gypsum and Fe-oxyhydroxide precipitation. Thenceforth, results shown in **Figure 4.6(d)** demonstrated the presence of rod-like and spherical structures on the material. The predominant structures were the rods and trapezium shaped structures. Rods denote gypsum from S and Ca whilst spherical structures denote Fe-based minerals. According to **Figure 4.5(d),** pH ≥ 4 encourages the precipitation of Fe, Ca, and S, and this explicitly denotes the feasibility of gypsum and Fe-oxyhydroxide precipitation. In **Figure 4.6(e),** pH ≥ 6.5, the SEM image demonstrated the presence of rod-like and spherical structures on the recovered material. The predominance of these structures further confirms that Fe and S are still precipitating at this stage. This could explain the presence of Fe and S. According to **Figure 4.5(e),** the pH ≥ 4 - 10.5 create a conducive environment for the precipitation of Ca, and S as gypsum. **Figure 4.5 (f - g)** demonstrated the presence of rod-like structure and spherical particles. This could solely be explained by the formation of calcium sulphate (gypsum), Al-oxyhdrosulphate and Mg. Lastly, **Figure 4.5 (h)** demonstrated leafy-like structures distributed across the surface of the recovered material. This confirms that the material is homogenous across the surface. Overall, the rod-like structures from a Ca and S rich system mainly demonstrate the formation of gypsum (Strydom et al., 1995, Tolonen et al., 2015, Schug et al., 2017) whereas the spherical particles demonstrate the formation of Fe-based minerals (Frost et al., 2005, Zhang et al., 2010, Ristić et al., 2013, Akinwekomi et al., 2020).

4.7.3 Elemental composition analysis

Herein, the HR-FE-SEM and the corresponding EDS elemental mapping images for the feed and recovered minerals are given and discussed. The primary aim is to invoke and gain an in-depth understanding and verify the elemental composition obtained by the EDS element appraisals. In particular, the EDS element analysis revealed the existence of Mg, O, and Ca, in activated magnesite as the feed and real AMD-elements in the recovered mineral. This section focuses on the discussion of FESEM-EDS elemental mapping. In **Figure 4.7(a),** the FESEM-EDS layered images of the feed material and their respective elements are shown.

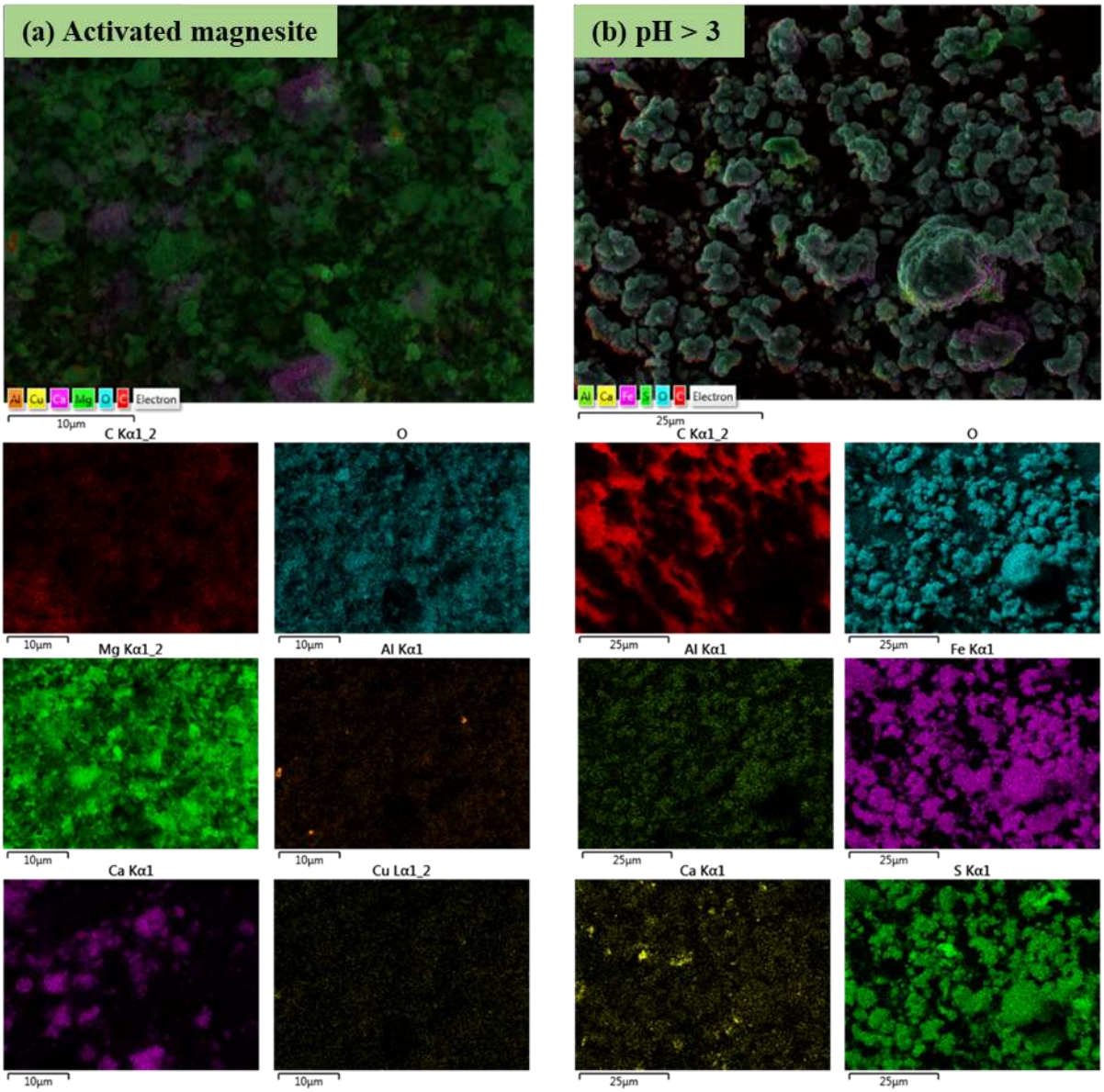


Figure 4.7: The FESEM image and mapping of (a) the feed material (activated magnesite) and (b) product mineral at pH = 3.

As shown in **Figure 4.7a**, raw magnesite was observed to contain C, O, Mg, and Ca as major components and traces of Al and Cu. Availability of Ca and Mg denotes that this material could contribute to the addition of hydroxyl groups in aqueous solution hence increasing the pH of the AMD. An increase in pH plays a significant role in the addition of alkalinity in water hence fostering the precipitation of chemicals species. In light of that, there is a clear indication that Ca in activated cryptocrystalline magnesite could dissolve in AMD and precipitate sulphate as gypsum whilst Mg will form $MgSO_4$ complex in solution. This has been confirmed by PHREEQC geochemical modelling. Thenceforth, a clear illustration of potential chemical reactions that may take place could be demonstrated as follows (Eqn. 4.1-4.5) (Name and Sheridan, 2014):

$$MgSO_4 + Ca(OH)_2 + 2H_2O \rightarrow CaSO_4.2H_2O + Mg(OH)_2 \quad (4.1)$$

$$CaO + H_2O \rightarrow Ca(OH)_2 \quad (4.2)$$

$$Ca(OH)_2 \rightarrow Ca^{2+} + 2OH^- \quad (4.3)$$

$$Fe^{m+} + MOH^- \rightarrow Fe(OH)_m \quad (4.4)$$

$$Ca^{2+} + SO_4^{2-} + 2H_2O \rightarrow CaSO_4.2H_2O \quad (4.5)$$

Essentially, base metals (Mg and Ca) which are prevalent in activated cryptocrystalline magnesite play an indispensable role in the supernatant pH mainly after dissolution and this contributes to the attenuation of chemical species through precipitation as metals hydroxide as indicated by equation 4.4 and 4.6.

$$M^{n+} + nOH^- \rightarrow M(OH)_n \downarrow \quad (4.6)$$

The obtained results are consistent with the PHREEQC geochemical modelling results. The dissolution of base cations may be represented by the following equations (Masindi et al., 2017b):

$$MgO + H_2O \rightarrow Mg^{2+} + 2OH^- \quad (4.7)$$

$$CaO + H_2O \rightarrow Ca^{2+} + 2OH^- \quad (4.8)$$

This may lead to an increase in the pH of the aqueous system with the subsequent precipitation of chemical species. Explicitly, an increase in pH of the product water may be due to dissolution of Ca and Mg as shown by the EDS results (Section 4.7.2). **Figure 4.7b** shows the presence of C, Al, Fe, Ca and S. The presence of C may be explained by the feedstock which was used. Magnesite comprises of carbonate and Mg on its matrices, however, after contacting AMD, the

product mineral was observed to comprise Al, Fe, Ca and S. This denotes the potential formation of gypsum as calcium sulphate and the precipitation of Fe and Al from AMD. These findings could be explained by the reduction of Fe and S in feed AMD. As shown in Figure 4.6, magnesite comprised the nano-sheet and the product mineral at pH ≤3 comprised the spherical particles. Akinwekomi et al. (2017b) reported Fe-minerals to comprised spherical nano-particles. The morphological properties and elemental mapping of minerals recovered at pH = 3.5 and = 4 are shown in **Figure 4.8**.

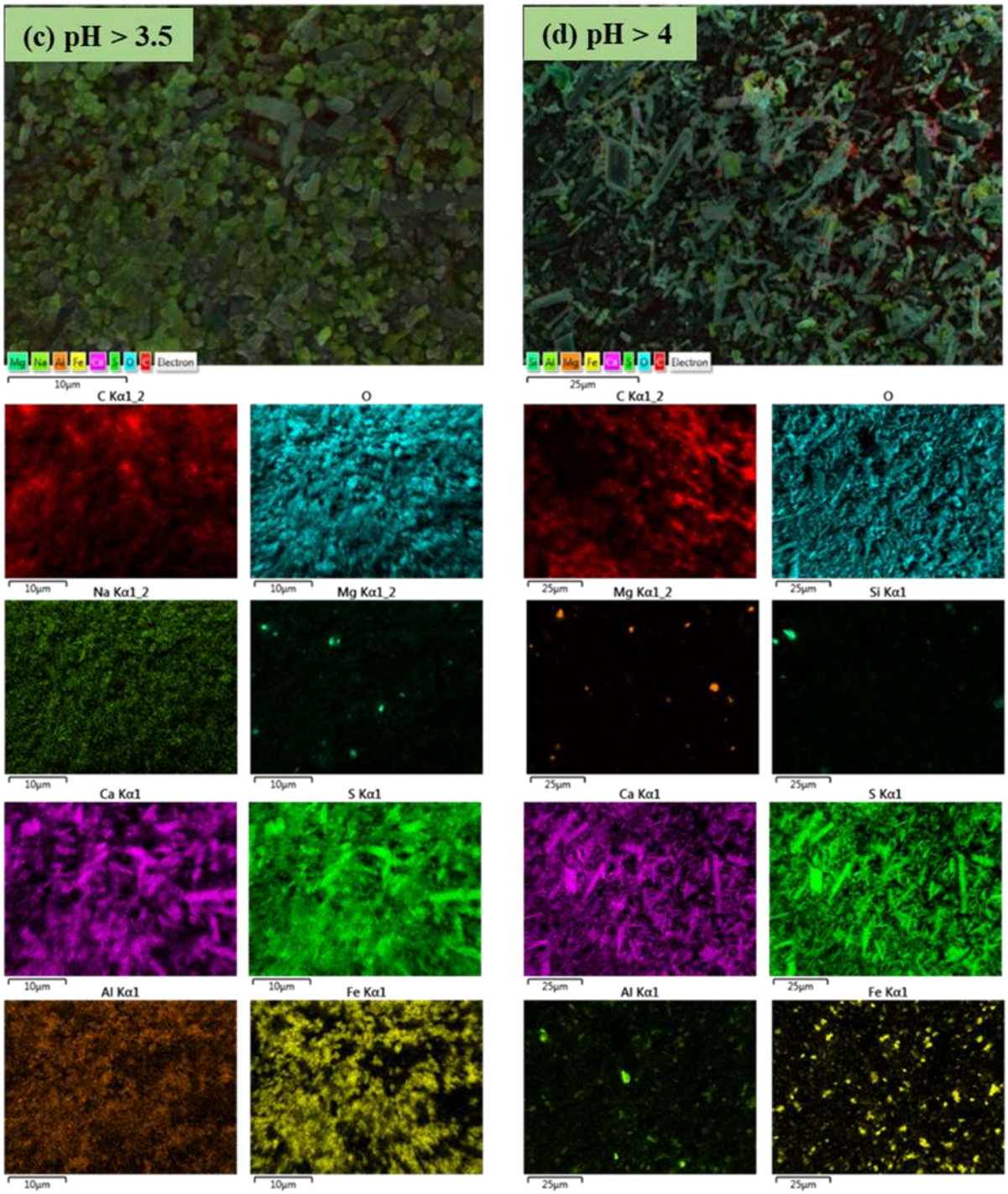


Figure 4.8: The FESEM image and mapping of (c) material recovered at pH = 3.5 and (d) product mineral recovered at pH = 4.

As shown in **Figure 4.8 [(c) – (d)]**, the recovered minerals were predominated by Ca, S, O, Fe, and Al. Specifically, pH≤3.5 was dominated by spherical and rod-like particles (Figure 4.8c). The rod-like particles were representing Ca, O, and S whilst the spherical particles were representing Fe, O, and Al. This denotes that there is high possibility of precipitating Fe-O-Al hydroxides and hydrated gypsum at pH≤3.5. Similar results were observed at pH≤4 but the predominant particles were rod-like structures (**Figure 4.8d**). The system was deficient of Al and Fe at pH <4, hence confirming that they were recovered at pH≤3.5. Mg and Na were not dominating the recovered materials hence denoting the possibility of them dissolving into aqueous solution. The morphological properties and elemental mapping of minerals recovered at pH ≤6 and ≤8 are shown in **Figure 4.9**.

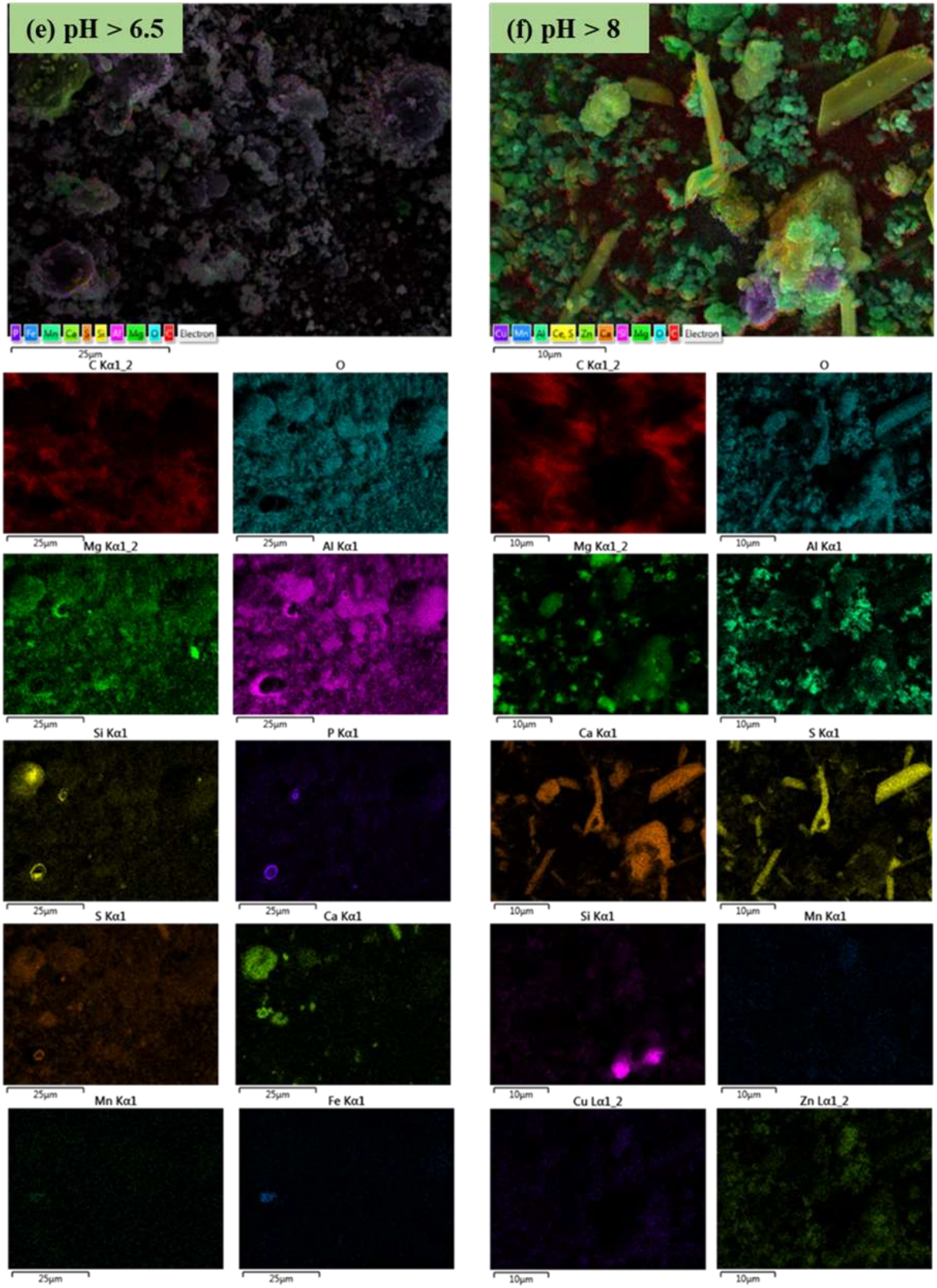


Figure 4.9: The FESEM image and mapping of (e) material recovered at pH≤6.5 and (f) product mineral recovered at pH ≤ 8.

As shown in **Figure 4.9** (e-f), the recovered minerals were predominated by Ca, S, O, Mg, and Al. Specifically, pH≤6.5 was dominated by spherical-like particles (Figure 4.9e). The spherical particles represent Mg, O, and Al. However, the Al-O was observed to be dominant hence demonstrating that this is the element that is mainly recovered at this pH range. Other elements such as Fe, S, and Ca were not predominant. Interestingly, Mn was observed to be present in the recovered minerals. This denotes that at pH ≤6.5, Mn commences to precipitate from aqueous solution as activated magnesite continues to be dosed into the system. Furthermore, Mg was observed to be high, thence denoting that it is precipitating or approaching saturation in the system (**Figure 4.9e**). The presence of Al-O denotes the formation of Al-hydroxides as predicted by PHREEQC geochemical modelling. The deficiency of Fe denotes that it has been fully depleted from aqueous solution whilst the deficiency of Ca and S denotes that these elements hardly precipitate at this pH range. The deficiencies of different elements could further be explained by their levels in product water quality from the sequential recovery process. Thenceforth, at pH≤8, a mixture of rod-like and spherical particles and nano-sheets were observed (Figure 4.9f).

As shown in **Figure 4.9** (f), the recovered minerals were predominated by Ca, S, O, Mg, and Al. Specifically, pH ≤8 was dominated by a sandwich of spherical and rod-like particles (Figure 4.9e). The spherical particles were representing Mg, O, and Al whilst the rod-like structures were representing Ca, S, and O. Interestingly, there was an emergence of Mn and Zn, although Mn commenced at pH ≤6.5. However, the Al-O-Mg were observed to be dominant hence demonstrating that this is the element that is highly recovered at this pH range. Other elements such as S, and Ca were not predominant. The presence of O further confirms and attests that the product minerals are hydroxides and hydrated minerals. Moreover, the presence of Mn was detected in the recovered minerals hence confirming the potential formation of manganese hydroxide and rhodochrosite. This denotes that at pH ≤8, Mn precipitation further intensifies from aqueous solution as the dose of activated magnesite increases on a step-wise fashion. Furthermore, Mg was observed to be high, thence denoting that it is precipitating or approaching in saturation in the system (**Figure 4.9e**). The presence of Al-O-Mg denotes the formation of Al-Mg-hydroxides as predicted by PHREEQC geochemical model. The deficiency of Fe denotes that it has been fully depleted from aqueous solution whilst the presence of Ca and S denotes that gypsum forms at this pH range. The morphological properties and elemental mapping of minerals recovered at pH ≤9.5 and ≤10.5 are shown in **Figure 4.10.**

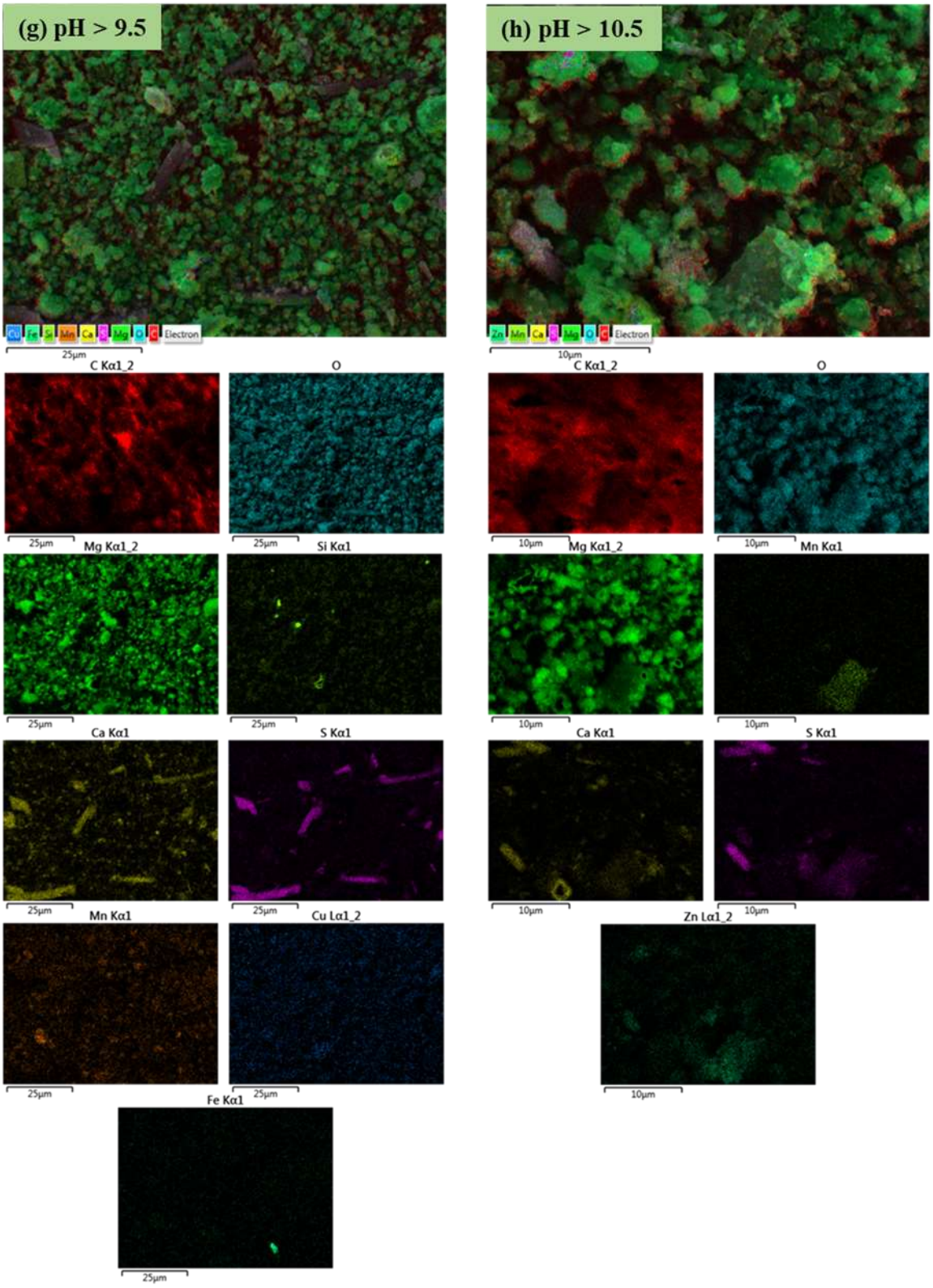


Figure 4.10: The FESEM image and mapping of (g) material recovered at pH≤9.5 and (h) mineral recovered at pH ≤ 10.5.

As shown in **Figure 4.10** (g-h), the image for pH≤9.5 (Figure 4.10g) showed particles with spherical structure mixed with scattered particles with rod-shaped structures. Mg and O were observed to be dominant in this stage hence denoting the feasibility of $Mg(OH)_2$ precipitating which is in agreement with the PHREEQC geochemical modelling. Scattered rods of Ca, O, and S were also observed and this denotes the formation of hydrated gypsum at this pH range. Furthermore, Si was observed to be present in the recovered sludge. Interestingly, Cu and Mn were observed to be present and these are miniscule elements which were removed from AMD during the metal's recovery process. This confirms that this pH favours the precipitation of Cu and Mn from aqueous solution. PHREEQC geochemical modelling predicted Cu, Mn, Fe, and Mg to precipitate as metals hydroxide. Furthermore, Mn was also predicted to precipitate as rhodochrosite ($MnCO_3$). The presence of Ca, O and S confirms the formation of hydrated gypsum from the chemical interaction.

As shown in **Figure 4.10** (h), the image for pH≤10.5 showed particles with spherical structure mixed with particles with rod-shaped structures. Mg and O were observed to be dominant in this stage hence denoting the feasibility of $Mg(OH)_2$ precipitating in agreement with the PHREEQC geochemical modelling results. Scattered rods of Ca, O, and S were also observed and this denotes the formation of hydrated gypsum at this pH range. Furthermore, C was observed to be present in the recovered sludge and this could be indicating the formation of carbonates. Interestingly, Al, Fe, and Mn were not present in the recovered minerals and this confirms that these elements were completely removed from AMD during the metal's recovery process. This confirms that pH≤10.5 favours the precipitation of metals from aqueous solution. The water quality results further confirms the findings which were reported in this study. PHREEQC geochemical modelling predicted Mg to precipitate as metal hydroxides. Furthermore, Mn was also predicted to precipitate as rhodochrosite ($MnCO_3$) while the presence of Ca, O and S confirms the formation of hydrated gypsum from the chemical interaction.

4.7.4 Spot analysis using HR-SEM-EDS

To further corroborate the results of the elemental composition, EDS spot-analysis was employed. The morphological properties and spot-analysis with elemental distribution of raw and the recovered minerals are shown in **Figure 4.11 (a-h)**. The morphological property and spot-analysis with elemental distribution of the feedstock is shown in **Figure 4.11 (a)**.

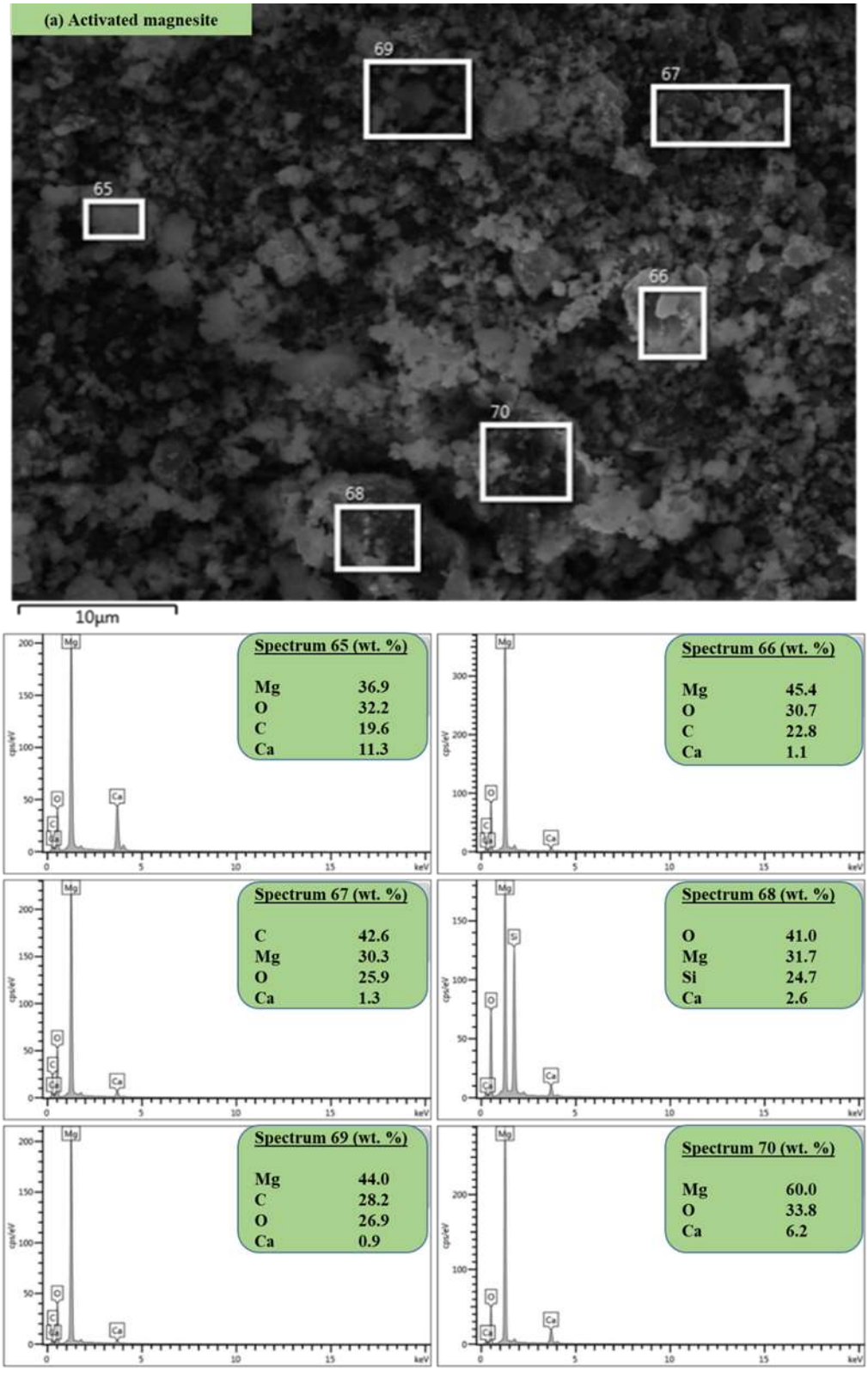


Figure 4.11 (a): The SEM-EDS showing the spot analysis image, and the relevant EDS spectra (Wt. %) of the feedstock which was used for minerals recovery.

As shown in **Figure 4.11 (a),** activated magnesite was observed to be dominated by Mg, C, O, and Ca. The observed elements were distributed across the surface in varying levels. This denotes that these chemical species could play a significant role in AMD neutralisation. The morphological property and spot-analysis with elemental distribution of the recovered material is shown in **Figure 4.11b for pH≤3**.

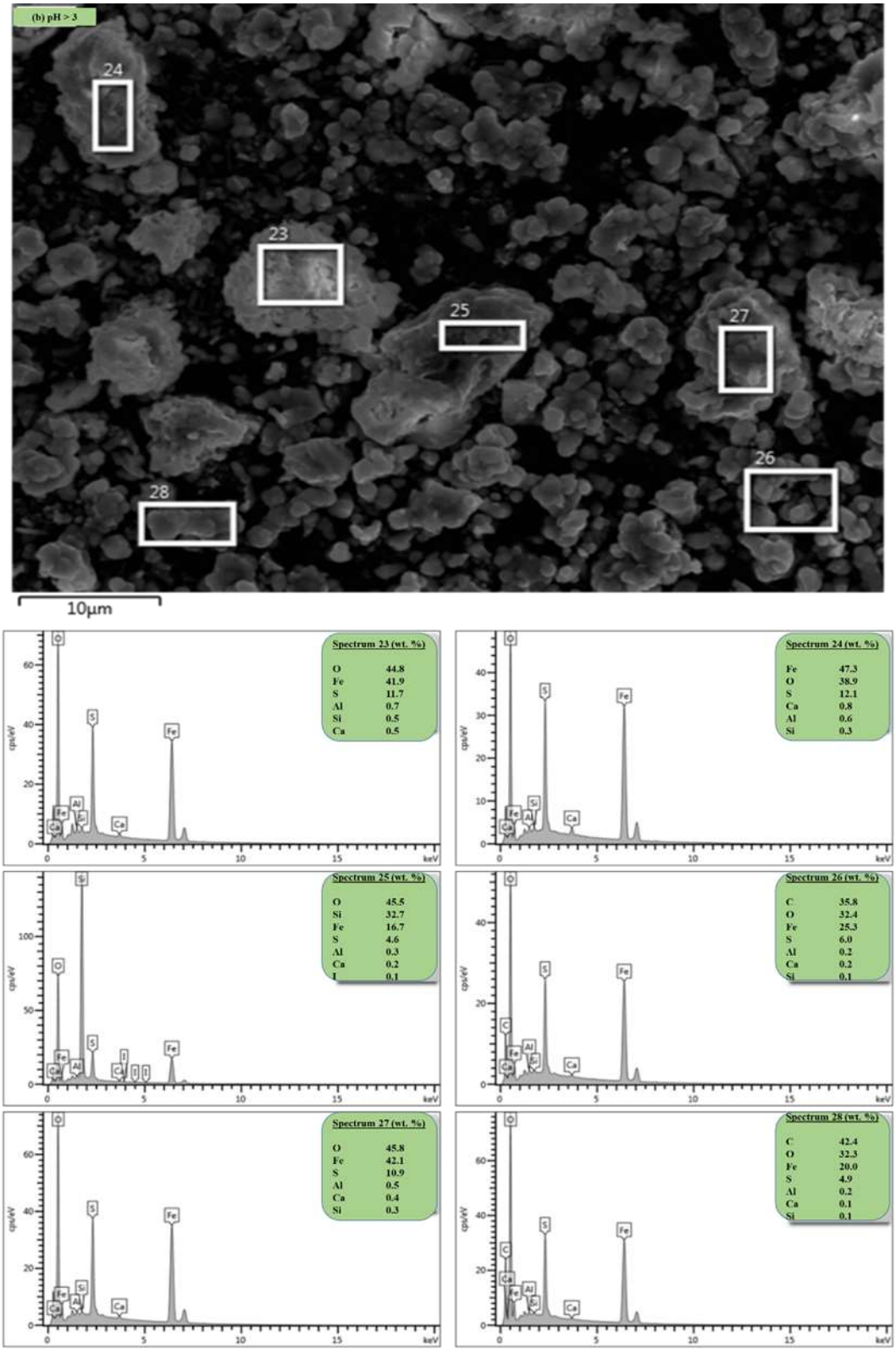


Figure 4.11 (b): The SEM-EDS showing the spot analysis image, and the relevant EDS spectra (Wt. %) of the recovered mineral at pH = 3.

As shown in **Figure 4.11 (b),** the mineral recovered at pH≤3 comprised of O, Fe, S, and C as major elements and traces of Al, Si, Ca, and S. The observed elements were distributed across

the surface in varying levels. The presence of Fe and S denotes the possible formation of Fe-oxy-hydro-sulphates as predicted by PHREEQC. The morphological and spot-analysis with elemental distribution of the recovered material is shown in **Figure 4.11c for pH≤3.5**.

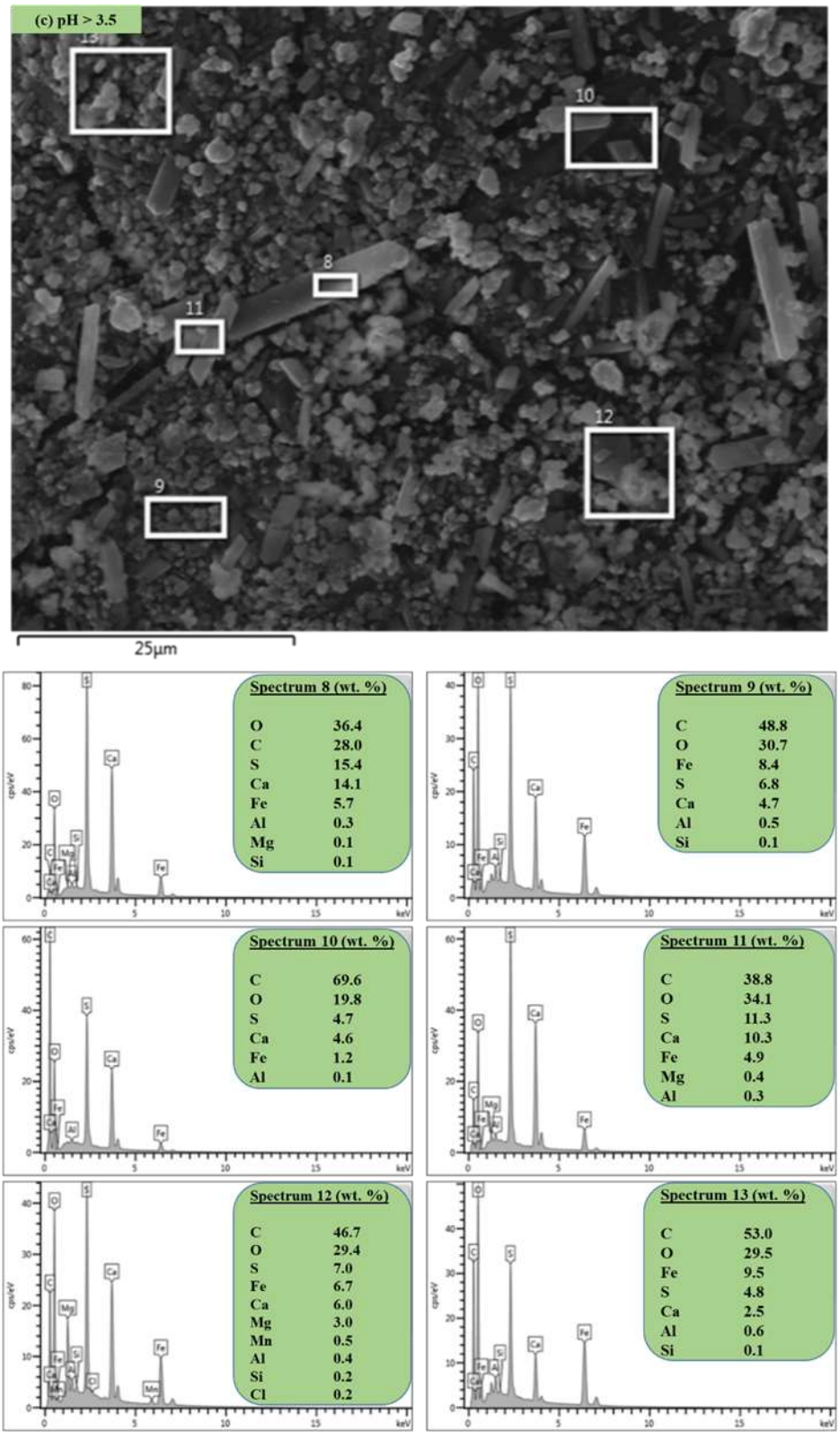


Figure 4.11 (c): The SEM-EDS showing the spot analysis image, and the relevant EDS spectra (Wt. %) of the recovered mineral at pH≤3.5.

As shown in **Figure 4.11 (c),** the mineral recovered at pH≤3.5 comprised of Ca, O, Fe, S, and C as major elements and traces of Al and Si. The observed elements were distributed across the surface in varying levels. The presence of Fe, Ca and S denotes the possible formation of Fe-oxy-hydro-sulphates and gypsum as predicted by PHREEQC. The morphological and spot-analysis with elemental distribution of the recovered material is shown in **Figure 4.11d** for pH≤4.

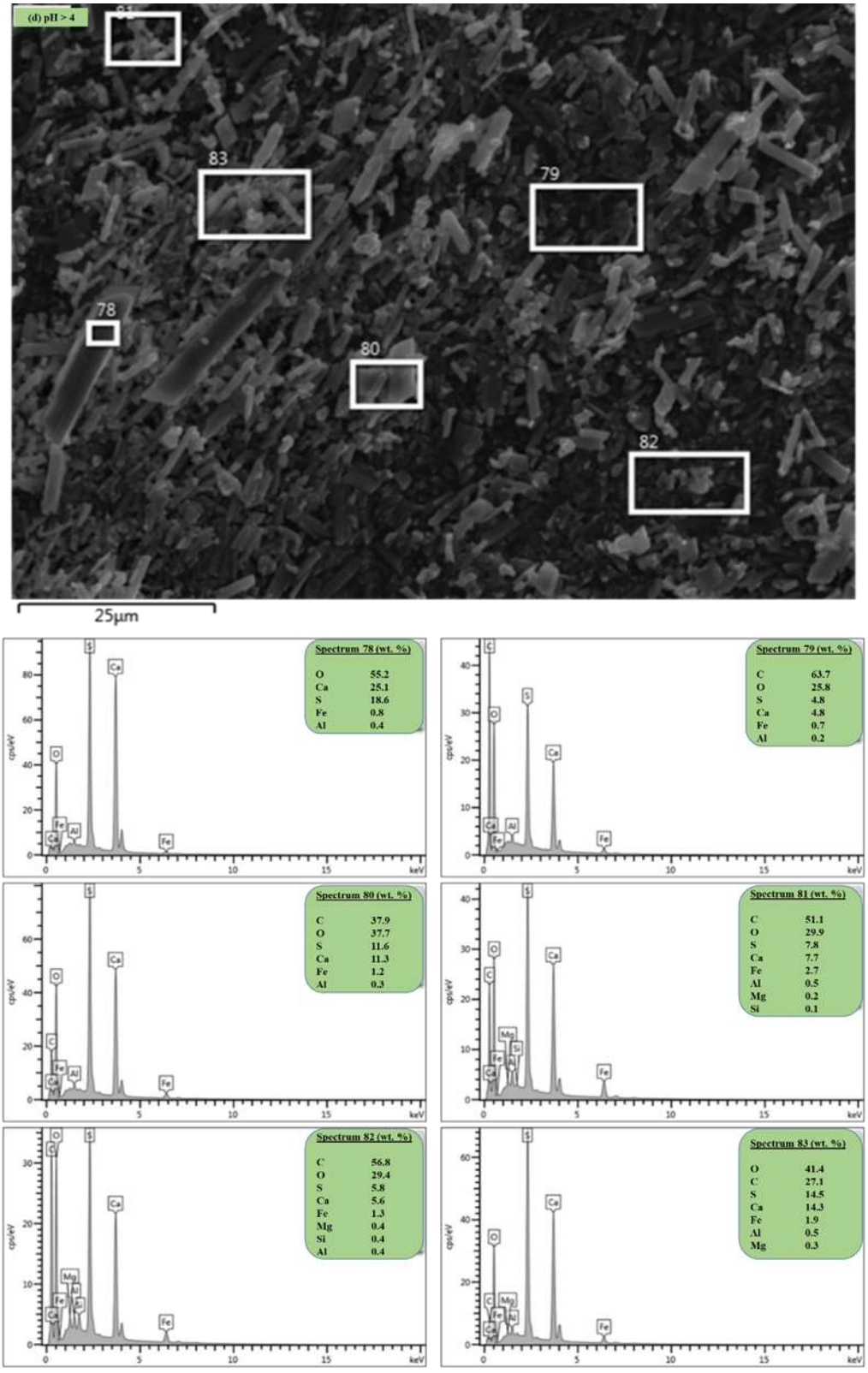


Figure 4.11 (d): The SEM-EDS showing the spot analysis image, and the relevant EDS spectra (Wt. %) of the recovered mineral at pH≤4.

As shown in **Figure 4.11 (d),** the mineral recovered at pH≤4 comprised of O, Fe, Ca, S, and C as major elements and traces of Al and Si. The observed elements were distributed across the surface in varying levels. The presence of Fe and S denotes the possible formation of Fe-oxy-hydro-sulphates as predicted by PHREEQC. Furthermore, the Ca and S rods confirm the presence of gypsum in the matrices of the recovered minerals. The morphological and spot-analysis with elemental distribution of the recovered material is shown in **Figure 4.11e for** pH≤6.5.

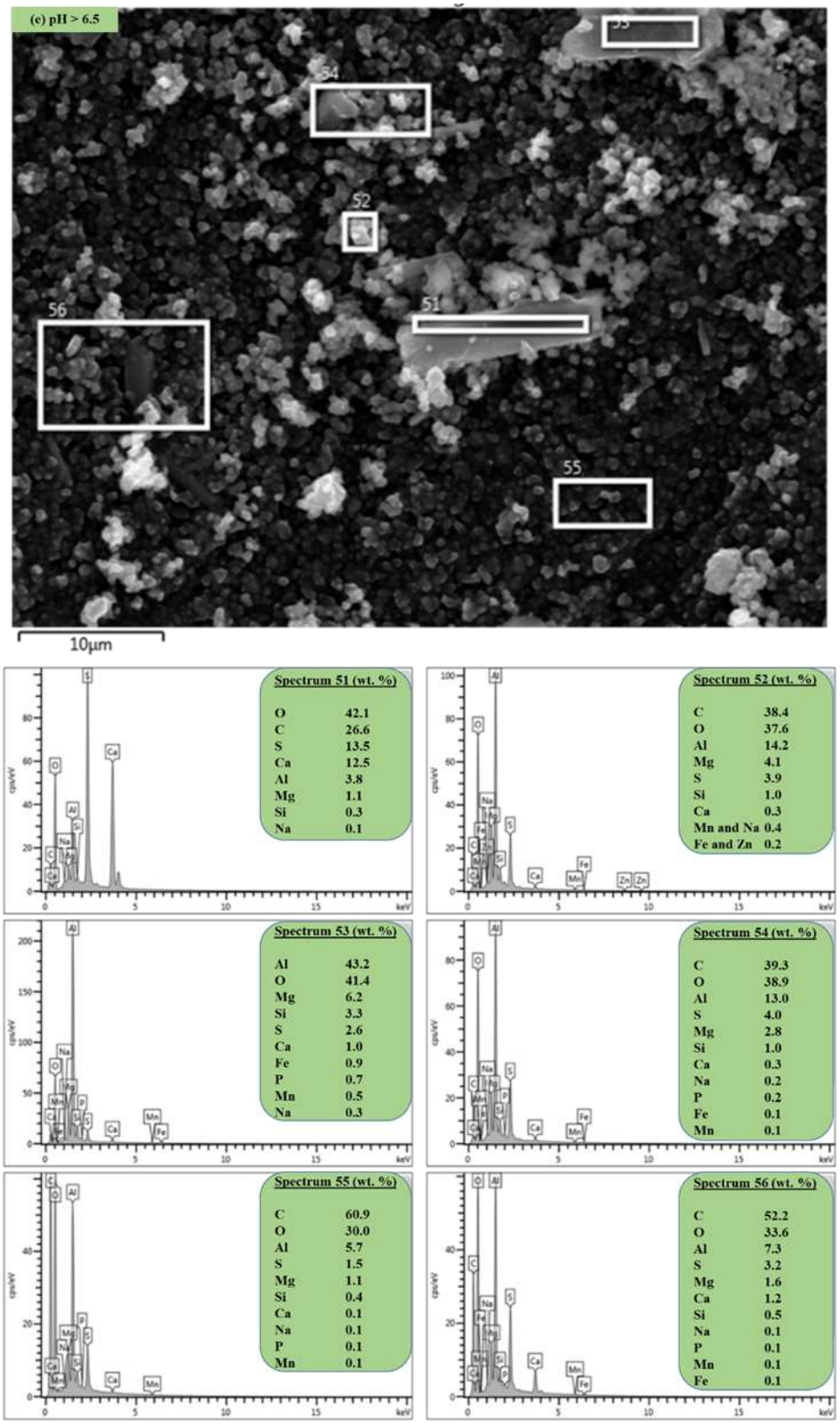


Figure 4.11 (e): The SEM-EDS showing the spot analysis image, and the relevant EDS spectra (Wt. %) of the recovered mineral at pH≤6.5.

As shown in **Figure 4.11 (e),** the mineral recovered at pH≤6.5 comprised of O, Al, Ca, S, and C as major elements and traces of Fe, Mn, Mg, Si, P, and Na. The observed elements were

distributed across the surface in varying levels. The presence of Al and S denotes the possible formation of Al-oxy-hydro-sulphates whilst Ca and S demonstrate gypsum (seen as rods) as predicted by PHREEQC geochemical modelling. The morphological and spot-analysis with elemental distribution of the recovered material is shown in **Figure 4.11f for** pH≤8.

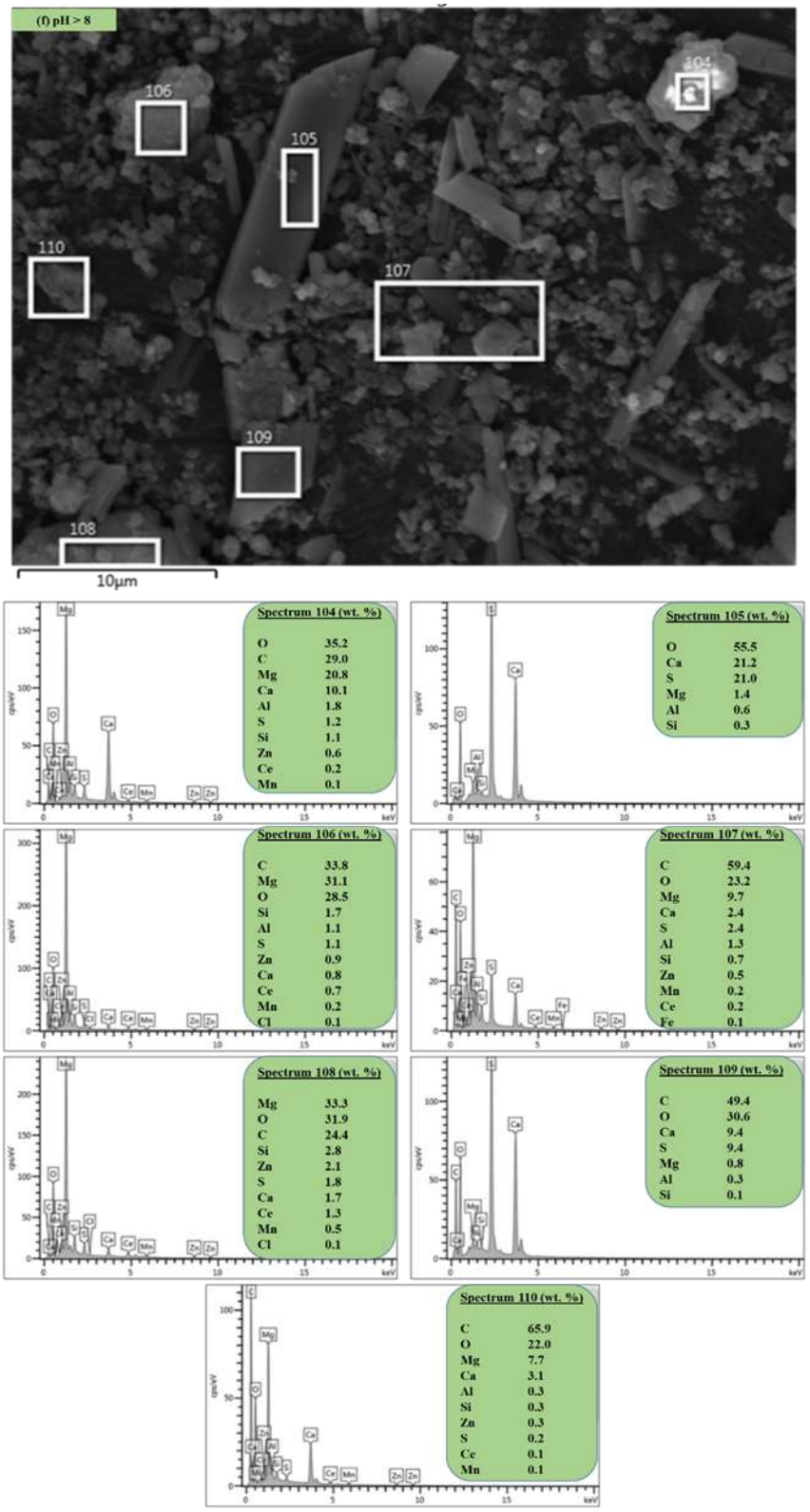


Figure 4.11 (f): The SEM-EDS showing the spot analysis image, and the relevant EDS spectra (Wt. %) of the recovered mineral at pH≤8.

As shown in **Figure 4.11 (f),** the minerals recovered at pH≤8 comprised of Mg, O, Al, Ca, S, and C as major elements and traces of Zn, Mn, Si, Fe, and Ce. The observed elements were distributed across the surface in varying levels. The presence of Al and S denotes the possible formation of Al-oxy-hydro-sulphates whilst Ca and S demonstrate gypsum as predicted by PHREEQC geochemical model. The morphological and spot-analysis with elemental distribution of the recovered material is shown in **Figure 4.11g for pH≤9.5**.

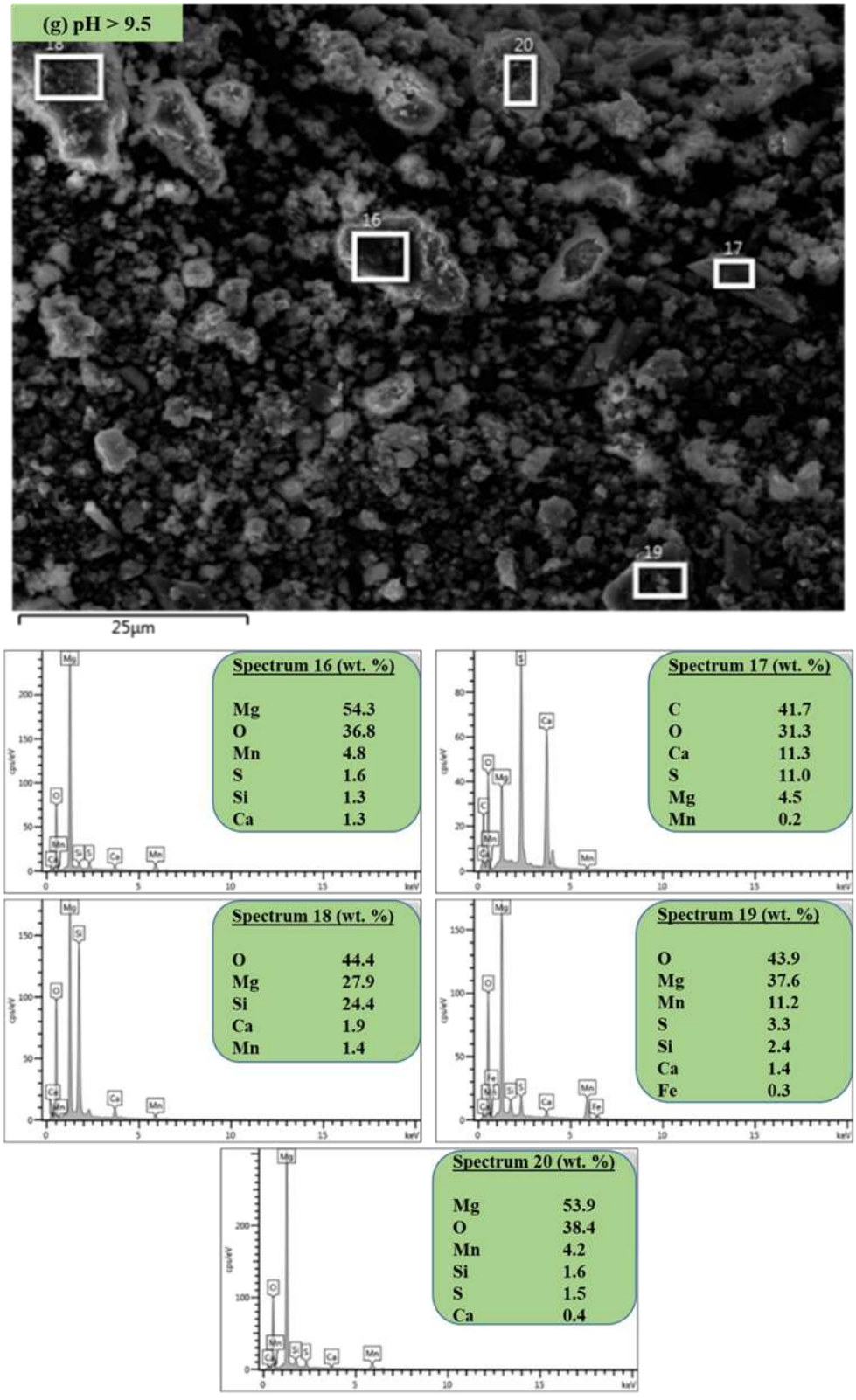


Figure 4.11 (g): The SEM-EDS showing the spot analysis image, and the relevant EDS spectra (Wt. %) of the recovered mineral at pH≤9.5.

As shown in **Figure 4.11 (g),** the minerals recovered at pH≤9.5 comprised of O, Mn, and Mg as major elements and traces of Ca, Fe, Ce, and S. The observed elements were distributed

across the surface in varying levels. The presence of Ca and S denotes the possible formation of calcium sulphates as predicted by PHREEQC. Ce denotes the possible recovery of rare-earth metal. The predominance of Mn and Mg confirms their immense recovery at this pH range. The morphological and spot-analysis with elemental distribution of the recovered material is shown in **Figure 4.11h for** pH≤10.5.

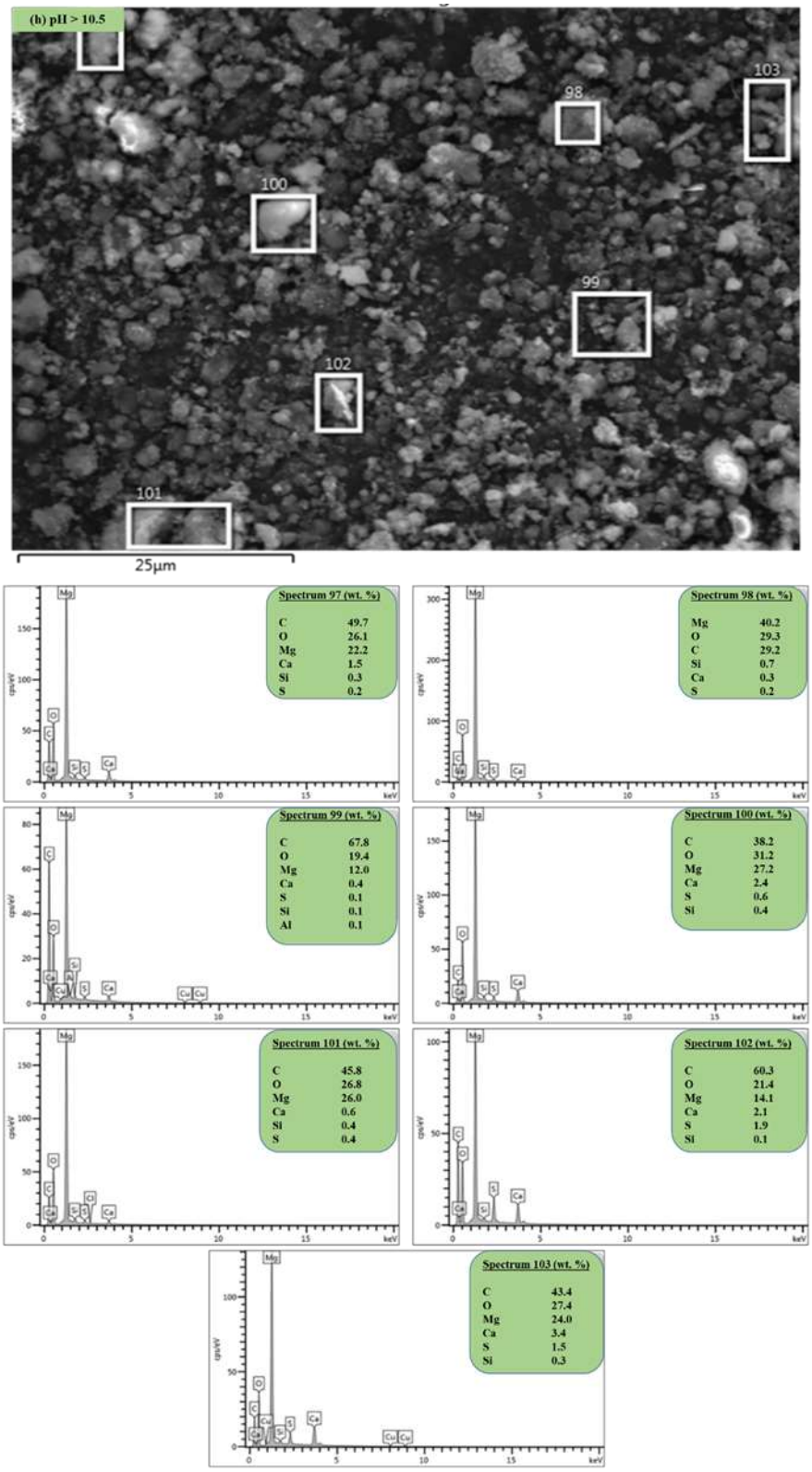


Figure 4.11 (h): The SEM-EDS showing the spot analysis image, and the relevant EDS spectra (Wt. %) of the recovered mineral at pH≤10.5.

As shown in **Figure 4.11 (h),** the mineral recovered at pH ≤10.5 comprised of O, Mg, and C as major elements and traces of Ca, Si, and S. The observed elements were distributed across

the surface in varying levels. The presence of Ca, Mg, and S denotes the possible formation of calcium sulphates and brucite as predicted by PHREEQC. These results confirm the attenuation of heavy metals from AMD and this could be confirmed by their reduced level in the water quality results.

4.8 Mineralogical composition

The mineral composition of minerals recovered at different pH ranges (pH ≤3 to pH≤10.5) are shown in **Figure 4.12**. The advanced X-ray diffraction (XRD) was used to ascertain the mineralogical properties of the raw feedstock and recovered minerals.

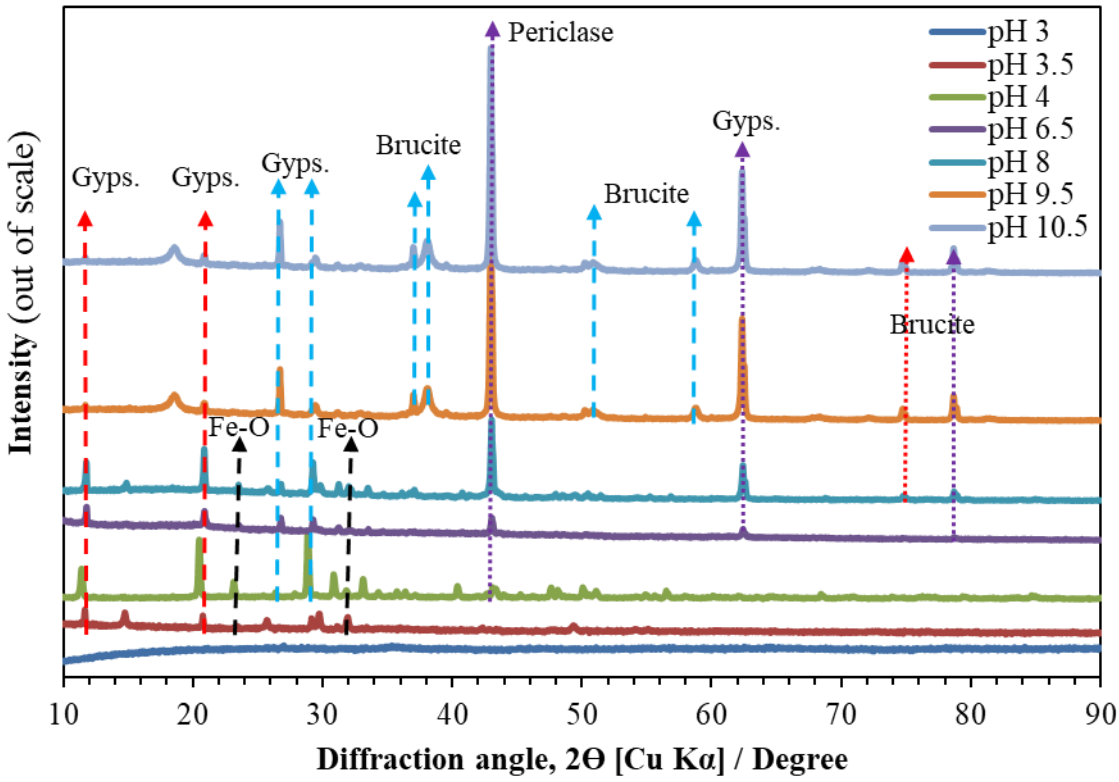


Figure 4.12: The mineral composition of minerals recovered at different pH ranges (pH ≤3 to pH≤10.5).

As shown in **Figure 4.12**, the identified peaks at 2 theta degrees suggest that different mineral phases were recovered at different pH ranges. The feedstock was mainly amorphous but this could be mainly due to the calcination effect. Furthermore, minerals recovered at different pH ranges also demonstrated crystalline and amorphous nature of the material. This corroborates what has been reported in literature (Muedi et al., 2021). At pH≤3, the material was rich in Fe-based minerals and gypsum. This confirms the water quality results and the HR-SEM-EDS

mappings. Furthermore, at pH ≤ 3.5, the crystalline peaks of Fe-minerals were observed at 2Θ = 11, 14, 25, 29, 30, 31 and 49. This was in-line to what has been reported from the PHREEQC geochemical simulation and HR-SEM-EDS. Thenceforth, at pH ≤ 4, the peaks of Al and Fe were noted at 2Θ = 11, 28, 31, 33, 41, and 20, 23 and 57. The findings grossly confirm the HR-SEM-EDS results. The peaks from pH≤ 4 to ≤8 confirmed the presence of hydrated gypsum at 2Θ = 12, 29.5, 43 and 63 whilst the peaks at pH ≤9.5 – 10 confirmed the gypsum peaks at 2Θ = 42 and 63. Overall, the obtained results were in agreement with the HR-SEM-EDS analysis and the PHREEQC geochemical simulations. As confirmed in the SEM-EDS mapping, similar results are observed for manganese where the peaks are observed at 2Θ = 27, 38 and 59. Finally, the peaks of brucite as Mg-mineral were noted at 2Θ = 19 and 63. The obtained results corroborate results which were reported in high resolution (HR)-SEM-EDS. This also confirms the fate of chemical species from AMD during the sequential interaction of activated cryptocrystalline magnesite and AMD. The findings confirm the recovery of different minerals at different pH ranges.

4.9 Chemical species-functional groups using FTIR

The information on the chemical species-functional groups of feedstock and recovered materials are shown in **Figure 4.13**.

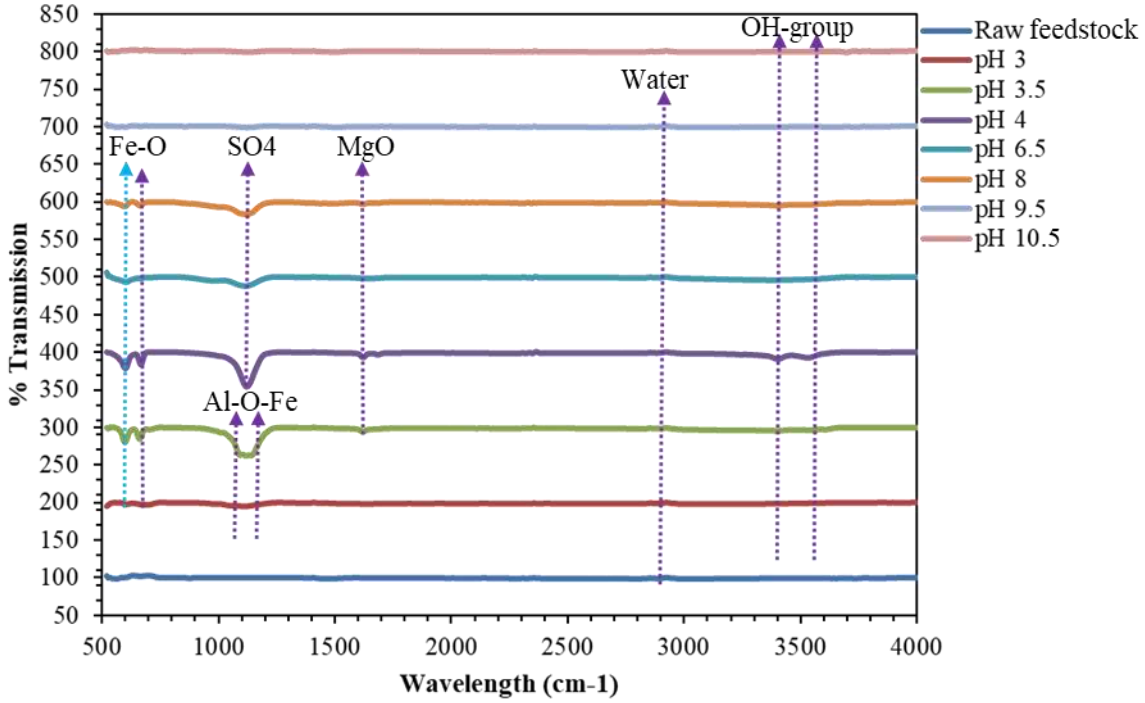


Figure 4.13: The information on the functional groups of feedstock and recovered materials.

As shown in **Figure 4.13**, the peaks for the feedstock comprised the Mg bending which is relative to 3702 cm^{-1}, the Mg-O stretches corresponding to band 1500 and 950 cm^{-1} and carbonates bending corresponding to bands 1680, 1450, 850 cm^{-1} (Dhal et al., 2015, Chamack et al., 2018). Thenceforth, the doublet at 1490, 1419 cm^{-1} corresponds to asymmetric stretching vibrations of carbonate hence confirming the formation of carbonate minerals. Specifically, the split denotes the presence of $CaCO_3$ and $MgCO_3$. The stretches at 1117, 886, and 795 cm^{-1} corresponds to in-plane and out-of-plane bending vibrations of the carbonate ion in the matrices hence confirming the presence of magnesite and calcite (Wu et al., 2020). The hydroxyl group and water molecules were observed at Peak at 3698 and 3450 cm^{-1} respectively. The Al-OH-Al bending was noted at 917 cm^{-1}. The peaks at 875 cm^{-1} and 836 cm^{-1} correspond to $Fe^{2+/3+}$ and Mg^{2+} (Tabelin et al., 2017a). These are attributed to the precipitation of those chemical species with an increase in pH. The peaks at 1000 – 1300 represent the Fe and Al species (Gypser et al., 2017, Liu et al., 2017, Tabelin et al., 2017b). This further confirms the fate of Al and Fe which were attenuated from AMD to the resultant product. The obtained results are in agreement with results which were reported in high resolution SEM-EDS and X-ray diffraction (XRD) including the water quality analysis.

4.10 PHREEQC modelling of saturation index of all the chemical components

The saturation indices (SI) of recovered chemical species at varying pH ranges as modelled by PHREEQC are shown in **Figure 4.14 (a-d).**

Figure 4.14 (a-d), reveals that different mineral phases were predicted as pH changed. Specifically, at pH between ≤3-6 boehmite, alunite and Alum-K were observed to precipitate whilst brucite was observed to precipitate at ≥6 - 10. This corroborates what has been reported in HR-SEM-EDS mapping and the XRD results. Furthermore, the diaspore and gibbsite were observed to be more likely to precipitate from pH ≥3 – 10.5 and this corroborates with what has been reported in EDS mapping results. Thenceforth, jarosite (ss) and jarosite-K were observed to be more likely to precipitate at pH < 4, whilst Jurbanite at pH ≥2 – 7 except for Jarosite-H which precipitated at pH ≥3. Manganese was observed to precipitate as pyrochroite at pH≥8. Moreover, other species of manganese which were predicted to more likely precipitate were manganite, melanterite, mirabilite and thenardite. The results obtained from PHREEQC geochemical model are consistent with what has been reported in the characterisation using XRD, FTIR, and HR-SEM-EDS as presented in sections 4.7-4.9.

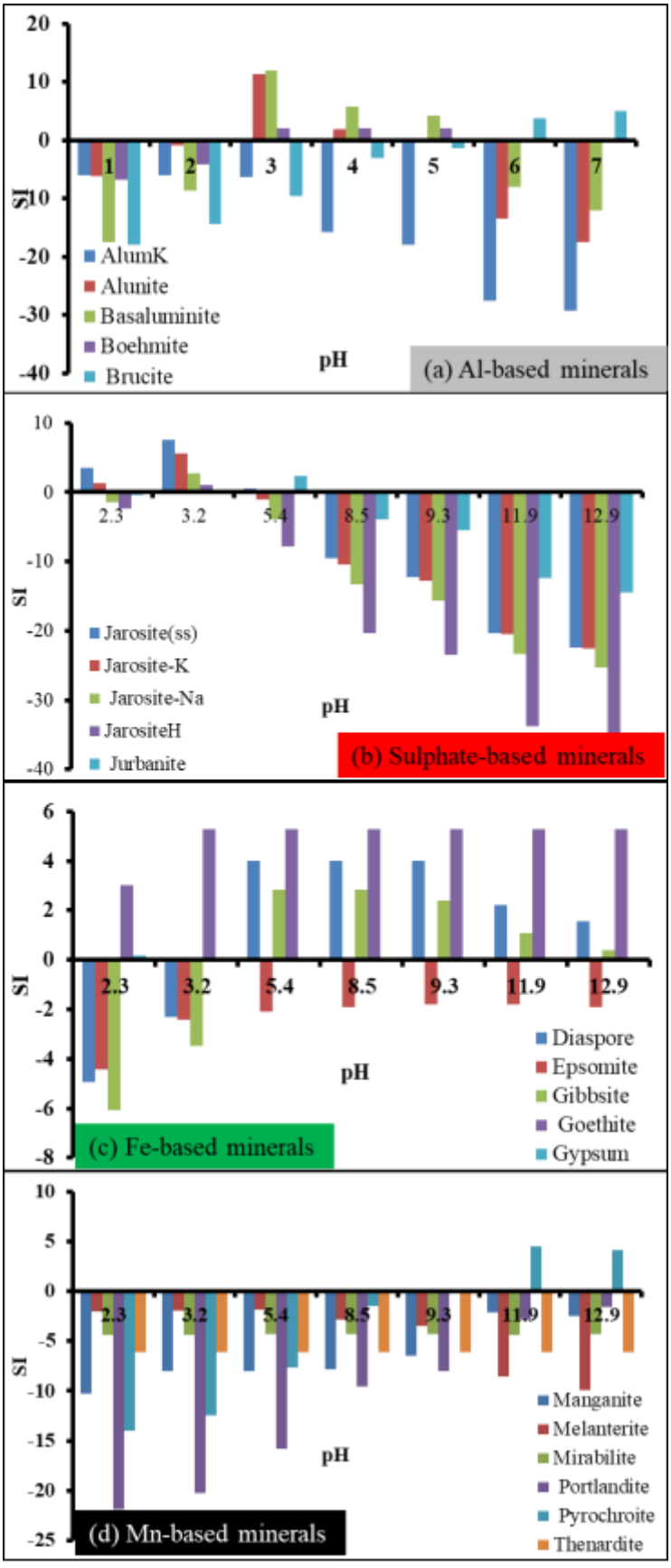


Figure 4.14: The saturation indices (SI) of mineral phases which were recovered from AMD at different pH ranges using PHREEQC geochemical model.

CHAPTER FIVE

RECOMMENDATION AND CONCLUSIONS

In this chapter, the concluding remarks and recommendations pertaining the objectives are described in detail. This also includes the gaps, challenges, and future research avenues based on the findings of this research.

The objectives of this study were:

- To assess the chemical characteristics of acid mine drainage before and after contacting different dosages of calcined cryptocrystalline magnesite;
- To determine the physicochemical properties of calcined cryptocrystalline magnesite and the recovered mineral resources using different analytical techniques;
- To optimise the optimum dosage for fractional and sequential recovery of metals and minerals from AMD;
- To use PHREEQC geochemical model to numerically model the process to complement the laboratory tests and to inform about the mechanisms thereof; and
- To assess the quality of product water against different water quality guidelines, standards, and specifications.

5.1 Conclusions and lessons learnt

The findings from this study confirmed the feasibility of recovering Al, Fe, Mn and sulphate from real AMD and their relativity to solution pH. PHREEQC modelling confirmed that prevalent species existed as di-valents, tri-valents, and oxyanions in aqueous solution. The optimisation study showed Fe to be recovered at pH ≥ 3 - 3.5, gypsum at pH ≥ 4 - 9, Al at pH ≥ 6.5, Mn at pH ≥ 9.5, Cu at pH ≥ 7, Zn at pH ≥ 8, Pb at pH ≥ 8 and Ni at pH ≥ 9. Simulation using the PHEEQC model obtained broadly similar results thus validating the experimental results. Essentially, greater than 99% removal efficiency was achieved for all the metals (Al Fe and Mn) for given pH regimes. The highest removal efficiency for sulphate was 40% at a pH of 10.5. Other metals such as Zn, Cu, Ni, and Pb were also removed from AMD. The reduction of chemical species in the treated AMD further confirmed the attenuation of chemical species and this was corroborated with the chemical characterisation of the product sludge. The fate of chemical species were verified using a synergy of HR-SEM equipped with EDS amongst other

analytical techniques. Lastly, but not least, the PHREEQC geochemical modelling suggested that chemical species were removed as (oxy)-hydroxides, (oxy)-hydro-sulphates, and metals hydroxides. Ca and SO_4^{2-} were removed as gypsum ($CaSO_4 \cdot 2H_2O$) and Pb, Fe, and Al as hydroxyl sulphate minerals. Mg formed a complex of $MgSO_4$ in solution and it was removed as $Mg(OH)_2$ at pH ≥ 9.5. Overall, this study demonstrated the pragmativity and feasibility of recovering valuable minerals from AMD. Finally, feasible and practical avenues for minerals harvesting from AMD for potential valorisation and beneficiation were confirmed and scientifically proven. Future research studies should focus on the enhancement of the purity of minerals recovered from AMD and the beneficiation of the product water for drinking purposes. The costs of mineral recovery and the associated environmental, ecological and other impacts however need to also be considered and future research also needs to focus in this direction. Moreover, cross contamination and lack of efficacy was the main challenge that could be linked to minerals recovery from AMD. In addition, some of the mineral phases that are identified using PHREEQC geochemical model could not be detected using advanced techniques such XRD and this could be attributed to the type of mineral phases being synthesized, i.e., crystalline and amorphous. Thus, it could be concluded that these techniques are complementary.

5.2 Recommendations

The findings from this study revealed various avenues that need future research to refine the conclusions which were drawn from this study. The main recommendations are to:

- Undertake research to enhance the purity of the recovered minerals and minimize cross contamination.
- Explore the effect of pre-concentration on the purity of recovered minerals and their economic values.
- Perform a techno-economic evaluation for the developed technology including a market analysis of the recovered minerals.
- Employ different techniques such as reverse osmosis, membrane distillation and forward osmosis to reclaim drinking water or water fit-for-purpose from the product water generated from the recovery process.
- Perform life cycle assessment of the proposed technology and approach in a quest to assess its sustainability and ecological footprints.

- Demonstrate the feasibility of sequential recovery of minerals at pilot scale using the developed optimum conditions.
- Assess the efficacy of this approach to AMD from different sources, e.g. coal and gold mining, and variations thereof.

REFERENCES

Aaron, G. L., Griffith, E. M. & Hacker, D. B. 2014. Geochemical and Hydrologic Assessment of Drainage from Cherry Valley Coal Mine, Ohio. Environmental & Engineering Geoscience, 20**,** 257-272.

Abdrakhmanova, R. N., Orehkova, N. N. & Gorlova, O. E. 2019. Adaptation of the SAVMIN process for mine water treatment. IOP Conference Series: Materials Science and Engineering, 687**,** 066077.

Adam, M. R., Othman, M. H. D., Abu Samah, R., Puteh, M. H., Ismail, A. F., Mustafa, A., A. Rahman, M. & Jaafar, J. 2019. Current trends and future prospects of ammonia removal in wastewater: A comprehensive review on adsorptive membrane development. Separation and Purification Technology, 213**,** 114-132.

Agboola, O. 2019. The role of membrane technology in acid mine water treatment: a review. Korean Journal of Chemical Engineering, 36**,** 1389-1400.

Agboola, O., Maree, J., Kolesnikov, A., Mbaya, R. & Sadiku, R. 2014. Theoretical performance of nanofiltration membranes for wastewater treatment. Environmental Chemistry Letters, 13**,** 37-47.

Aguiar, A., Andrade, L., Grossi, L., Pires, W. & Amaral, M. 2018. Acid mine drainage treatment by nanofiltration: A study of membrane fouling, chemical cleaning, and membrane ageing. Separation and Purification Technology, 192**,** 185-195.

Ahokpossi, D. P., Atangana, A. & Vermeulen, P. D. 2018. Hydro-geochemical characterizations of a platinum group element groundwater system in Africa. Journal of African Earth Sciences, 138**,** 348-366.

Akcil, A. & Koldas, S. 2006. Acid Mine Drainage (AMD): causes, treatment and case studies. Journal of Cleaner Production, 14**,** 1139-1145.

Akinwekomi, V., Kefeni, K. K., Maree, J. P. & Msagati, T. a. M. 2016. Integrated acid mine drainage treatment using $Mg(OH)_2$ or $Mg(HCO_3)_2$ and $Ca(OH)_2$: Implications for separate removal of metals and sulphate. International Journal of Mineral Processing, 155**,** 83-90.

Akinwekomi, V., Maree, J. P., Masindi, V., Zvinowanda, C., Osman, M. S., Foteinis, S., Mpenyana-Monyatsi, L. & Chatzisymeon, E. 2020. Beneficiation of acid mine drainage (AMD): A viable option for the synthesis of goethite, hematite, magnetite, and gypsum – Gearing towards a circular economy concept. Minerals Engineering, 148**,** 106204.

Akinwekomi, V., Maree, J. P., Zvinowanda, C. & Masindi, V. 2017a. Synthesis of magnetite from iron-rich mine water using sodium carbonate. Journal of Environmental Chemical Engineering.

Akinwekomi, V., Maree, J. P., Zvinowanda, C. & Masindi, V. 2017b. Synthesis of magnetite from iron-rich mine water using sodium carbonate. Journal of Environmental Chemical Engineering, 5**,** 2699-2707.

Al-Zoubi, H., Rieger, A., Steinberger, P., Pelz, W., Haseneder, R. & Härtel, G. 2010. Nanofiltration of acid mine drainage. Desalination and Water Treatment, 21**,** 148-161.

Ali, H., Khan, E. & Sajad, M. A. 2013. Phytoremediation of heavy metals—Concepts and applications. Chemosphere, 91**,** 869-881.

Amaya-Vías, D., Tataru, L., Herce-Sesa, B., López-López, J. A. & López-Ramírez, J. A. 2019. Metals removal from acid mine drainage (Tinto River, SW Spain) by water gap and air gap membrane distillation. Journal of Membrane Science, 582**,** 20-29.

Amos, R. T., Blowes, D. W., Bailey, B. L., Sego, D. C., Smith, L. & Ritchie, A. I. M. 2015. Waste-rock hydrogeology and geochemistry. Applied Geochemistry, 57**,** 140-156.

Anawar, H. M. 2015. Sustainable rehabilitation of mining waste and acid mine drainage using geochemistry, mine type, mineralogy, texture, ore extraction and climate knowledge. Journal of Environmental Management, 158**,** 111-121.

Andrade, L. H., Aguiar, A. O., Pires, W. L., Grossi, L. B. & Amaral, M. C. S. 2017. Comprehensive bench- and pilot-scale investigation of NF for gold mining effluent treatment: Membrane performance and fouling control strategies. Separation and Purification Technology, 174**,** 44-56.

Andrić, I., Jamali-Zghal, N., Santarelli, M., Lacarrière, B. & Le Corre, O. 2015. Environmental performance assessment of retrofitting existing coal fired power plants to co-firing with biomass: carbon footprint and emergy approach. Journal of Cleaner Production, 103**,** 13-27.

Asad, S. A., Farooq, M., Afzal, A. & West, H. 2019. Integrated phytobial heavy metal remediation strategies for a sustainable clean environment - A review. Chemosphere, 217**,** 925-941.

Baker, B. J. & Banfield, J. F. 2003. Microbial communities in acid mine drainage. FEMS Microbiology Ecology, 44**,** 139-152.

Balistrieri, L. S., Seal Ii, R. R., Piatak, N. M. & Paul, B. 2007. Assessing the concentration, speciation, and toxicity of dissolved metals during mixing of acid-mine drainage and

ambient river water downstream of the Elizabeth Copper Mine, Vermont, USA. Applied Geochemistry, 22**,** 930-952.

Basu, H., Singhal, R. K., Pimple, M. V. & Reddy, A. V. R. 2015. Arsenic removal from groundwater by goethite impregnated calcium alginate beads. Water, Air, and Soil Pollution, 226, 2(22-45).

Ben Ali, H. E., Neculita, C. M., Molson, J. W., Maqsoud, A. & Zagury, G. J. 2019. Performance of passive systems for mine drainage treatment at low temperature and high salinity: A review. Minerals Engineering, 134**,** 325-344.

Bhateria, R. & Singh, R. 2019. A review on nanotechnological application of magnetic iron oxides for heavy metal removal. Journal of Water Process Engineering, 31**,** 100845.

Blais, J. F., Djedidi, Z., Cheikh, R. B., Tyagi, R. D. & Mercier, G. 2008. Metals precipitation from effluents: Review. Practice Periodical of Hazardous, Toxic, and Radioactive Waste Management, 12**,** 135-149.

Blowes, D. W., Ptacek, C. J., Jambor, J. L., Weisener, C. G., Paktunc, D., Gould, W. D. & Johnson, D. B. 2003. The Geochemistry of Acid Mine Drainage. Treatise on Geochemistry: Second Edition, Volume 9. Editor: Barbara Sherwood Lollar. Executive Editors: Heinrich D. Holland and Karl K. Turekian. pp. 612. ISBN 0-08-043751-6. Elsevier, 2003., p.149-204.

Bologo, V., Maree, J. P. & Carlsson, F. 2012. Application of magnesium hydroxide and barium hydroxide for the removal of metals and sulphate from mine water. Water SA, 38**,** 23-28.

Bui, T. Q., Ngo, H. T. M. & Tran, H. T. 2018. Surface-protective assistance of ultrasound in synthesis of superparamagnetic magnetite nanoparticles and in preparation of mono-core magnetite-silica nanocomposites. Journal of Science: Advanced Materials and Devices, 3**,** 323-330.

Buzzi, D. C., Viegas, L. S., Rodrigues, M. a. S., Bernardes, A. M. & Tenório, J. a. S. 2013. Water recovery from acid mine drainage by electrodialysis. Minerals Engineering, 40**,** 82-89.

Bwapwa, J. K., Jaiyeola, A. T. & Chetty, R. 2017. Bioremediation of acid mine drainage using algae strains: A review. South African Journal of Chemical Engineering, 24**,** 62-70.

Chalkley, R., Child, F., Al-Thaqafi, K., Dean, A. P., White, K. N. & Pittman, J. K. 2019. Macroalgae as spatial and temporal bioindicators of coastal metal pollution following

remediation and diversion of acid mine drainage. Ecotoxicology and Environmental Safety, 182**,** 109458.

Chamack, M., Mahjoub, A. & Hosseinian, A. 2018. Facile Synthesis of Nanosized MgO as Adsorbent for Removal of Congored Dye from Wastewate. Nanochemistry Research, 3**,** 85-91.

Chen, T., Yan, B., Lei, C. & Xiao, X. 2014. Pollution control and metal resource recovery for acid mine drainage. Hydrometallurgy, 147–148**,** 112-119.

Cheng, H., Hu, Y., Luo, J., Xu, B. & Zhao, J. 2009. Geochemical processes controlling fate and transport of arsenic in acid mine drainage (AMD) and natural systems. Journal of Hazardous Materials, 165**,** 13-26.

Chu, W.-L., Dang, N.-L., Kok, Y.-Y., Ivan Yap, K.-S., Phang, S.-M. & Convey, P. 2018. Heavy metal pollution in Antarctica and its potential impacts on algae. Polar Science.

Department of Water Affairs and Forestry 1996. South African Water Quality Guidelines (first edition), Field Guide. Department of Water Affairs and Forestry, Volume 8.

Dhal, J. P., Sethi, M., Mishra, B. G. & Hota, G. 2015. MgO nanomaterials with different morphologies and their sorption capacity for removal of toxic dyes. Materials Letters, 141**,** 267-271.

Doyi, I., Essumang, D., Gbeddy, G., Dampare, S., Kumassah, E. & Saka, D. 2018. Spatial distribution, accumulation and human health risk assessment of heavy metals in soil and groundwater of the Tano Basin, Ghana. Ecotoxicology and Environmental Safety, 165**,** 540-546.

Duuring, P., Hagemann, S. G., Banks, D. A. & Schindler, C. 2018. A synvolcanic origin for magnetite-rich orebodies hosted by BIF in the Weld Range District, Western Australia. Ore Geology Reviews, 93**,** 211-254.

EPA 2017. Water Quality Standards Handbook. Chapter 3: Water Quality Criteria. EPA-823-B-17-001. EPA Office of Water, Office of Science and Technology, Washington, DC,https://www.epa.gov/sites/production/files/2014-10/documents/handbook-chapter3.pdf.

Equeenuddin, S. M., Tripathy, S., Sahoo, P. K. & Panigrahi, M. K. 2010. Hydrogeochemical characteristics of acid mine drainage and water pollution at Makum Coalfield, India. Journal of Geochemical Exploration, 105**,** 75-82.

Favas, P. J. C., Sarkar, S. K., Rakshit, D., Venkatachalam, P. & Prasad, M. N. V. 2016. Chapter 17 - Acid Mine Drainages From Abandoned Mines: Hydrochemistry, Environmental

Impact, Resource Recovery, and Prevention of Pollution. Environmental Materials and Waste. Academic Press. (pp. 413-462). Elsevier Inc.. https://doi.org/10.1016/B978-0-12-803837-6.00017-2

Fernando, W. a. M., Ilankoon, I. M. S. K., Syed, T. H. & Yellishetty, M. 2018. Challenges and opportunities in the removal of sulphate ions in contaminated mine water: A review. Minerals Engineering, 117**,** 74-90.

Figueiredo, J., Vila, M. C., Góis, J., Biju, B. P., Futuro, A., Martins, D., Dinis, M. L. & Fiúza, A. 2019. Bi-level depth assessment of an abandoned tailings dam aiming its reprocessing for recovery of valuable metals. Minerals Engineering, 133**,** 1-9.

Fosso-Kankeu, E., Wolkersdorfer, C. & Burgess, J. 2020. Recovery of Byproducts from Acid Mine Drainage Treatment, Wiley. Elvis Fosso-Kankeu (Editor), Christian Wolkersdorfer (Editor), Jo Burgess (Editor), ISBN: 978-1-119-62013-6, September 2020, 384 Pages

Foureaux, A. F. S., Moreira, V. R., Lebron, Y. a. R., Santos, L. V. S. & Amaral, M. C. S. 2019. Direct contact membrane distillation as an alternative to the conventional methods for value-added compounds recovery from acidic effluents: A review. Separation and Purification Technology**,** 116251.

Frost, R., Yong Zhu, H., Wu, P. & Bostrom, T. 2005. Synthesis of acicular goethite with surfactants. Materials Letters, 59**,** 2238-2241.

Fu, F. & Wang, Q. 2011. Removal of heavy metal ions from wastewaters: A review. Journal of Environmental Management, 92**,** 407-418.

Garrido, A., Condori, J., Strosnider, W. & Nairn, R. 2009. Acid mine drainage impacts on irrigation water resources, agricultural soils, and potatoes in potosí, Bolivia. 26th Annual Meetings of the American Society of Mining and Reclamation and 11th Billings Land Reclamation Symposium 2009, 1.

Gazea, B., Adam, K. & Kontopoulos, A. 1996. A review of passive systems for the treatment of acid mine drainage. Minerals Engineering, 9**,** 23-42.

Geldenhuys, A. J., Maree, J. P., De Beer, M. & Hlabela, P. 2003. An integrated limestone/lime process for partial sulphate removal. Journal of the South African Institute of Mining and Metallurgy, 103**,** 345-354.

Gitari, W. M., Petrik, L. F., Etchebers, O., Key, D. L., Iwuoha, E. & Okujeni, C. 2008. Passive neutralisation of acid mine drainage by fly ash and its derivatives: A column leaching study. Fuel, 87**,** 1637-1650.

Groudev, S., Georgiev, P., Spasova, I. & Nicolova, M. 2008. Bioremediation of acid mine drainage in a uranium deposit. Hydrometallurgy, 94**,** 93-99.

Gu, J.-D. 2018. Mining, pollution and site remediation. International Biodeterioration & Biodegradation. 128, 1-2. doi: 10.1016/j.ibiod.2017.11.006.

Gypser, S., Hirsch, F., Schleicher, A. M. & Freese, D. 2017. Impact of crystalline and amorphous iron- and aluminum hydroxides on mechanisms of phosphate adsorption and desorption. Journal of Environmental Sciences, 70, 175-189.

Haldar, S. K. 2018. Chapter 14 - Environmental System Management of Mineral Resources and Sustainable Development. In: HALDAR, S. K. (ed.) Mineral Exploration (Second Edition). Elsevier. eBook ISBN: 9780128140239

Hallberg, K. B. 2010. New perspectives in acid mine drainage microbiology. Hydrometallurgy, 104**,** 448-453.

Hatch, M. J. & Dillon, J. A. 1963. Acid Retardation. Simple Physical Method for Separation of Strong Acids from Their Salts. Industrial & Engineering Chemistry Process Design and Development, 2**,** 253-263.

Hedrich, S. & Johnson, D. B. 2014. Remediation and Selective Recovery of Metals from Acidic Mine Waters Using Novel Modular Bioreactors. Environmental Science & Technology, 48**,** 12206-12212.

Hengen, T. J., Squillace, M. K., O'sullivan, A. D. & Stone, J. J. 2014. Life cycle assessment analysis of active and passive acid mine drainage treatment technologies. Resources, Conservation and Recycling, 86**,** 160-167.

Hentati, O., Chaker, S., Wali, A., Ayoub, T. & Ksibi, M. 2014. Effects of long-term irrigation with treated wastewater on soil quality, soil-borne pathogens, and living organisms: Case study of the vicinity of El Hajeb (Tunisia). Environmental Monitoring and Assessment, 186**,** 2671-2683.

Hlabela, P., Maree, J. & Bruinsma, D. 2007. Barium carbonate process for sulphate and metal removal from mine water. Mine Water and the Environment, 26**,** 14-22.

Hobbs, P. J. & Cobbing, J. E. 2007. Hydrogeological Assessment of Acid Mine Drainage Impacts in the West Rand Basin, Gauteng Province. Hydrogeological Assessment of Acid Mine Drainage Impacts in the West Rand Basin, Gauteng Province. CSIR report.

Hogsden, K. L. & Harding, J. S. 2012. Consequences of acid mine drainage for the structure and function of benthic stream communities: A review. Freshwater Science, 31**,** 108-120.

Hong, S., Cannon, F. S., Hou, P., Byrne, T. & Nieto-Delgado, C. 2014. Sulfate removal from acid mine drainage using polypyrrole-grafted granular activated carbon. Carbon, 73**,** 51-60.

Hu, Y., Zhou, J., Du, B., Liu, H., Zhang, W., Liang, J., Zhang, W., You, L. & Zhou, J. 2019. Health risks to local residents from the exposure of heavy metals around the largest copper smelter in China. Ecotoxicology and Environmental Safety, 171**,** 329-336.

Hughes, T. A. & Gray, N. F. 2011. Effectiveness and sustainability of active and passive systems for the treatment of acid mine drainage and the recovery of metals: A review. Mine Drainage and Related Problems, 1-70, 2011.

Hughes, T. A. & Gray, N. F. 2013. Co-treatment of acid mine drainage with municipal wastewater: Performance evaluation. Environmental Science and Pollution Research, 20**,** 7863-7877.

Ivask, A., Titma, T., Visnapuu, M., Vaija, H., Käkinen, A., Sihtmäe, M., Pokhre, S., Mädler, L., Heinlaan, M., Kisand, V., Shimmo, R. & Kahru, A. 2015. Toxicity of 11 metal oxide nanoparticles to three mammalian cell types in vitro. Current Topics in Medicinal Chemistry, 15**,** 1914-1929.

Jain, R. K., Cui, Z. C. & Domen, J. K. 2016. Chapter 4 - Environmental Impacts of Mining. Environmental Impact of Mining and Mineral Processing. Boston: Butterworth-Heinemann, 322, eBook ISBN: 9780128040928.

Johnson, D. B., Dziurla, M. A., Kolmert, Å. & Hallberg, K. B. 2002. The microbiology of acid mine drainage: Genesis and biotreatment. South African Journal of Science, 98**,** 249-255.

Johnson, D. B. & Hallberg, K. B. 2005. Acid mine drainage remediation options: a review. Science of The Total Environment, 338**,** 3-14.

Jooste, S. & Thirion, C. 1999. An ecological risk assessment for a South African acid mine drainage. Water Science and Technology, 39**,** 297-303.

Jovanovic, N., Annandale, J., Westhuizen, A. M. & Steyn, J. 2004. Monitoring the effect of irrigation with gypsiferous mine wastewater on crop production potential as affected by soil water and salt balance. Journal of The South African Institute of Mining and Metallurgy, 104**,** 73-81.

Jung, S. P., Cheong, Y., Yim, G., Ji, S. & Kang, H. 2014. Performance and bacterial communities of successive alkalinity-producing systems (SAPSs) in passive treatment

processes treating mine drainages differing in acidity and metal levels. Environmental Science and Pollution Research, 21**,** 3722-3732.

Kalita, E. & Baruah, J. 2020. 16 - Environmental remediation. In: THOMAS, S., TRESA SUNNY, A. & VELAYUDHAN, P. (eds.) Colloidal Metal Oxide Nanoparticles. Elsevier, 608, eBook ISBN: 9780128133583.

Karakatsanis, E., Cogho, V.E., . Drinking Water from Mine Water Using the HiPrO® Process – Optimum coal Mine Water reclamation Plant. In: WOLKERSDORFER, C., FREUND , H.,, ed. "Mine Water and Innovative Thinking" 2010 Australia, Sydney. IMWA 2010.

Kastyuchik, A., Karam, A. & Aïder, M. 2016. Effectiveness of alkaline amendments in acid mine drainage remediation. Environmental Technology & Innovation, 6**,** 49-59.

Keefer, G. B. & Sack, W. A. 1983. Sludge recycle and reuse in acid mine drainage treatment. Journal of the Water Pollution Control Federation, 55**,** 278-284.

Kefeni, K. K. & Mamba, B. B. 2020. Evaluation of charcoal ash nanoparticles pollutant removal capacity from acid mine drainage rich in iron and sulfate. Journal of Cleaner Production, 251**,** 119720.

Kefeni, K. K., Mamba, B. B. & Msagati, T. a. M. 2017a. Magnetite and cobalt ferrite nanoparticles used as seeds for acid mine drainage treatment. Journal of Hazardous Materials, 333**,** 308-318.

Kefeni, K. K., Msagati, T. a. M. & Mamba, B. B. 2017b. Acid mine drainage: Prevention, treatment options, and resource recovery: A review. Journal of Cleaner Production, 151**,** 475-493.

Kefeni, K. K., Msagati, T. a. M., Nkambule, T. T. I. & Mamba, B. B. 2018. Synthesis and application of hematite nanoparticles for acid mine drainage treatment. Journal of Environmental Chemical Engineering, 6**,** 1865-1874.

Kefeni, K. K., Msagati, T. M. & Mamba, B. B. 2015a. Synthesis and characterization of magnetic nanoparticles and study their removal capacity of metals from acid mine drainage. Chemical Engineering Journal, 276**,** 222-231.

Kefeni, K. K., Msagati, T. M., Maree, J. P. & Mamba, B. B. 2015b. Metals and sulphate removal from acid mine drainage in two steps via ferrite sludge and barium sulphate formation. Minerals Engineering, 81**,** 79-87.

Kiiskila, J. D., Li, K., Sarkar, D. & Datta, R. 2020. Metabolic response of vetiver grass (Chrysopogon zizanioides) to acid mine drainage. Chemosphere, 240**,** 124961.

Kiiskila, J. D., Sarkar, D., Panja, S., Sahi, S. V. & Datta, R. 2019. Remediation of acid mine drainage-impacted water by vetiver grass (Chrysopogon zizanioides): A multiscale long-term study. Ecological Engineering, 129**,** 97-108.

Kim, S. D., Kilbane Ii, J. J. & Cha, D. K. 1999. Prevention of acid mine drainage by sulfate reducing bacteria: Organic substrate addition to mine waste piles. Environmental Engineering Science, 16**,** 139-145.

Kotsiopoulos, A. & Harrison, S. T. L. 2018. Co-disposal of benign desulfurised tailings with sulfidic waste rock to mitigate ARD generation: Influence of flow and contact surface. Minerals Engineering, 116**,** 62-71.

Langmuir, D. 1997. Aqueous Environmental Geochemistry, New Jersey, Prentice Hall.

Lèbre, É., Corder, G. D. & Golev, A. 2017. Sustainable practices in the management of mining waste: A focus on the mineral resource. Minerals Engineering, 107**,** 34-42.

Lewis, A. E. 2010. Review of metal sulphide precipitation. Hydrometallurgy, 104**,** 222-234.

Liao, J., Ru, X., Xie, B., Zhang, W., Wu, H., Wu, C. & Wei, C. 2017. Multi-phase distribution and comprehensive ecological risk assessment of heavy metal pollutants in a river affected by acid mine drainage. Ecotoxicology and Environmental Safety, 141**,** 75-84.

Liu, Z.-D., Wang, H.-C., Zhou, Q. & Xu, R.-K. 2017. Effects of adhesions of amorphous Fe and Al hydroxides on surface charge and adsorption of K+ and Cd2+ on rice roots. Ecotoxicology and Environmental Safety, 145**,** 207-213.

López, J., Reig, M., Gibert, O. & Cortina, J. L. 2019. Recovery of sulphuric acid and added value metals (Zn, Cu and rare earths) from acidic mine waters using nanofiltration membranes. Separation and Purification Technology, 212**,** 180-190.

Lopez, J., Reig, M., Gibert, O., Valderrama, C. & Cortina, J. L. 2018. Evaluation of NF membranes as treatment technology of acid mine drainage: metals and sulfate removal. Desalination, 440**,** 122-134.

Luo, C., Routh, J., Dario, M., Sarkar, S., Wei, L., Luo, D. & Liu, Y. 2020. Distribution and mobilization of heavy metals at an acid mine drainage affected region in South China, a post-remediation study. Science of The Total Environment**,** 138122.

Madzivire, G., Gitari, W. M., Vadapalli, V. R. K., Ojumu, T. V. & Petrik, L. F. 2011. Fate of sulphate removed during the treatment of circumneutral mine water and acid mine drainage with coal fly ash: Modelling and experimental approach. Minerals Engineering, 24**,** 1467-1477.

Madzivire, G., Petrik, L. F., Gitari, W. M., Ojumu, T. V. & Balfour, G. 2010. Application of coal fly ash to circumneutral mine waters for the removal of sulphates as gypsum and ettringite. Minerals Engineering, 23**,** 252-257.

Magagane, N., Masindi, V., Ramakokovhu, M. M., Shongwe, M. B. & Muedi, K. L. 2019. Facile thermal activation of non-reactive cryptocrystalline magnesite and its application on the treatment of acid mine drainage. Journal of Environmental Management, 236**,** 499-509.

Maila, M. D., Maree, J. P. & Cele, L. M. 2014. Acid mine water neutralisation with ammonium hydroxide and desalination with barium hydroxide. Water SA, 40**,** 521-528.

Maree, J. P. & Du Plessis, P. 1994. Neutralization of acid mine water with calcium carbonate. Water Science and Technology, 29**,** 285-296.

Maree, J. P., Greben, H. A. & De Beer, M. 2004a. Treatment of acid and sulphate-rich effluents in an integrated biological/chemical process. Water SA, 30**,** 183-189.

Maree, J. P., Hlabela, P., Nengovhela, R., Geldenhuys, A. J., Mbhele, N., Nevhulaudzi, T. & Waanders, F. B. 2004b. Treatment of mine water for sulphate and metal removal using barium sulphide. Mine Water and the Environment, 23**,** 195-203.

Maree, J. P., Mujuru, M., Bologo, V., Daniels, N. & Mpholoane, D. 2013. Neutralisation treatment of AMD at affordable cost. Water SA, 39**,** 245-250.

Maree, J. P., Streydom, W. F., Adlem, C. J. L., De Beer, M., Van Tonder, G. J. & Van Dijk, B. J. 2004c. Neutralization of acid mine water and sludge disposal. WRC Report No. 1057/1/04, Water Research Commission.

Maree, J. P., Strydom, W. F. & De Beer, M. 1999. Integrated iron(II) oxidation and limestone neutralisation of acid mine water. Water Science and Technology.

Martí-Calatayud, M. C., Buzzi, D. C., García-Gabaldón, M., Ortega, E., Bernardes, A. M., Tenório, J. a. S. & Pérez-Herranz, V. 2014. Sulfuric acid recovery from acid mine drainage by means of electrodialysis. Desalination, 343**,** 120-127.

Masindi, V. 2016. A novel technology for neutralizing acidity and attenuating toxic chemical species from acid mine drainage using cryptocrystalline magnesite tailings. Journal of Water Process Engineering, 10**,** 67-77.

Masindi, V. 2017a. Integrated treatment of acid mine drainage using cryptocrystalline magnesite and barium chloride. Water Practice and Technology, 12**,** 727-736.

Masindi, V. 2017b. Recovery of drinking water and valuable minerals from acid mine drainage using an integration of magnesite, lime, soda ash, CO_2 and reverse osmosis treatment processes. Journal of Environmental Chemical Engineering, 5**,** 3136-3142.

Masindi, V. 2018. Testing and upscaling treatment technologies for mine wastewater and metal recovery. CSIR Science Scope, 13**,** 64-65.

Masindi, V. 2020. Conversion of cryptocrystalline magnesite to MgO nanosheets: Insights into microstructural properties. Materials Today: Proceedings.

Masindi, V., Akinwekomi, V., Maree, J. P. & Muedi, K. L. 2017a. Comparison of mine water neutralisation efficiencies of different alkaline generating agents. Journal of Environmental Chemical Engineering, 5**,** 3903-3913.

Masindi, V., Foteinis, S. & Chatzisymeon, E. 2021. Co-treatment of acid mine drainage and municipal wastewater effluents: Emphasis on the fate and partitioning of chemical contaminants. Hazardous Materials, 126677**,** 1-12.

Masindi, V., Gitari, M. W., Tutu, H. & De Beer, M. 2014. Neutralization and attenuation of metal species in acid mine drainage and mine leachates using magnesite: a batch experimental approach. An Interdisciplinary Response to Mine Water Challenges**,** 640-644.

Masindi, V., Gitari, M. W., Tutu, H. & De Beer, M. 2015a. Passive remediation of acid mine drainage using cryptocrystalline magnesite: A batch experimental and geochemical modelling approach. Water SA, 41**,** 677-682.

Masindi, V., Gitari, M. W., Tutu, H. & De Beer, M. 2016a. Fate of inorganic contaminants post treatment of acid mine drainage by cryptocrystalline magnesite: Complimenting experimental results with a geochemical model. Journal of Environmental Chemical Engineering, 4**,** 4846-4856.

Masindi, V., Gitari, M. W., Tutu, H. & Debeer, M. 2015b. Efficiency of ball milled South African bentonite clay for remediation of acid mine drainage. Journal of Water Process Engineering, 8**,** 227-240.

Masindi, V., Gitari, M. W., Tutu, H. & Debeer, M. 2017b. Synthesis of cryptocrystalline magnesite–bentonite clay composite and its application for neutralization and attenuation of inorganic contaminants in acidic and metalliferous mine drainage. Journal of Water Process Engineering, 15**,** 2-17.

Masindi, V., Gitari, W. M. & Tutu, H. 2017c. Simultaneous sorption of as, b, cr, mo and se from coal fly ash leachates by Al3+-pillared bentonite clay: Implication for the

construction of activated geo-synthetic clay liner. Water Practice and Technology, 12**,** 186-201.

Masindi, V., Madzivire, G. & Tekere, M. 2018a. Reclamation of water and the synthesis of gypsum and limestone from acid mine drainage treatment process using a combination of pre-treated magnesite nanosheets, lime, and CO_2 bubbling. Water Resources and Industry, 20**,** 1-14.

Masindi, V., Madzivire, G. & Tekere, M. 2018b. Reclamation of water and the synthesis of gypsum and limestone from acid mine drainage treatment process using a combination of pre-treated magnesite nanosheets, lime, and CO_2 bubbling. Water Resources and Industry, 20**,** 1-14.

Masindi, V., Ndiritu, J. G. & Maree, J. P. 2018c. Fractional and step-wise recovery of chemical species from acid mine drainage using calcined cryptocrystalline magnesite nano-sheets: An experimental and geochemical modelling approach. Journal of Environmental Chemical Engineering, 6**,** 1634-1650.

Masindi, V., Osman, M. S. & Abu-Mahfouz, A. M. 2017d. Integrated treatment of acid mine drainage using BOF slag, lime/soda ash and reverse osmosis (RO): Implication for the production of drinking water. Desalination, 424**,** 45-52.

Masindi, V., Osman, M. S., Mbhele, R. N. & Rikhotso, R. 2016b. Fate of pollutants post treatment of acid mine drainage with basic oxygen furnace slag: Validation of experimental results with a geochemical model. Journal of Cleaner Production, 172**,** 2899-2909.

Masindi, V., Osman, M. S. & Shingwenyana, R. 2019a. Valorization of acid mine drainage (AMD): A simplified approach to reclaim drinking water and synthesize valuable minerals - Pilot study. Journal of Environmental Chemical Engineering, 7**,** 103082.

Masindi, V., Osman, M. S. & Shingwenyana, R. 2019b. Valorization of acid mine drainage (AMD): A simplified approach to reclaim drinking water and synthesize valuable minerals – Pilot study. Journal of Environmental Chemical Engineering, 7**,** 103082.

Mavhungu, A., Masindi, V., Foteinis, S., Mbaya, R., Tekere, M., Kortidis, I. & Chatzisymeon, E. 2020. Advocating circular economy in wastewater treatment: Struvite formation and drinking water reclamation from real municipal effluents. Journal of Environmental Chemical Engineering**,** 103957.

Mirbagheri, S. A. & Hosseini, S. N. 2005. Pilot plant investigation on petrochemical wastewater treatmentfor the removal of copper and chromium with the objective of reuse. Desalination, 171**,** 85-93.

Mohan, D. & Chander, S. 2006. Removal and recovery of metal ions from acid mine drainage using lignite—A low cost sorbent. Journal of Hazardous Materials, 137**,** 1545-1553.

Mohan, D. & Pittman Jr, C. U. 2007. Arsenic removal from water/wastewater using adsorbents—A critical review. Journal of Hazardous Materials, 142**,** 1-53.

Moodley, I., Sheridan, C. M., Kappelmeyer, U. & Akcil, A. 2018. Environmentally sustainable acid mine drainage remediation: Research developments with a focus on waste/by-products. Minerals Engineering, 126**,** 207-220.

Motsi, T., Rowson, N. A. & Simmons, M. J. H. 2009. Adsorption of heavy metals from acid mine drainage by natural zeolite. International Journal of Mineral Processing, 92**,** 42-48.

Muedi, K. L., Brink, H. G., Masindi, V. & Maree, J. P. 2021. Effective removal of arsenate from wastewater using aluminium enriched ferric oxide-hydroxide recovered from authentic acid mine drainage. Journal of Hazardous Materials, 414**,** 125491.

Mulopo, J. 2015. Continuous pilot scale assessment of the alkaline barium calcium desalination process for acid mine drainage treatment. Journal of Environmental Chemical Engineering, 3**,** 1295-1302.

Mulopo, J. 2016. Direct elemental sulphur recovery from gold acid mine drainage streams. Journal of Environmental Chemical Engineering, 4**,** 4670-4679.

Naidoo, S. 2014. An assessment of the impacts of acid mine drainage on socio-economic development in the Witwatersrand: South Africa. Environment, Development and Sustainability, 17, 1045-1063.

Naidu, G., Ryu, S., Thiruvenkatachari, R., Choi, Y., Jeong, S. & Vigneswaran, S. 2019. A critical review on remediation, reuse, and resource recovery from acid mine drainage. Environmental Pollution, 247**,** 1110-1124.

Name, T. & Sheridan, C. 2014. Remediation of acid mine drainage using metallurgical slags. Minerals Engineering, 64**,** 15-22.

Natarajan, K. A. 2008. Microbial aspects of acid mine drainage and its bioremediation. Transactions of Nonferrous Metals Society of China, 18**,** 1352-1360.

Neculita, C. M. & Rosa, E. 2019. A review of the implications and challenges of manganese removal from mine drainage. Chemosphere, 214**,** 491-510.

Neculita, C. M., Vigneault, B. & Zagury, G. J. 2008. Toxicity and metal speciation in acid mine drainage treated by passive bioreactors. Environmental Toxicology and Chemistry, 27**,** 1659-1667.

Nengovhela, N. R., Strydom, C. A., Maree, J. P., Oosthuizen, S. & Theron, D. J. 2007. Recovery of sulphur and calcium carbonate from waste gypsum. Water SA, 33**,** 741-747.

Netto, E., Madeira, R. A., Silveira, F. Z., Fiori, M. A., Angioleto, E., Pich, C. T. & Geremias, R. 2013. Evaluation of the toxic and genotoxic potential of acid mine drainage using physicochemical parameters and bioassays. Environmental Toxicology and Pharmacology, 35**,** 511-516.

Nguegang, B., Masindi, V., Msagati, T. a. M. & Tekere, M. 2021. The Treatment of Acid Mine Drainage Using Vertically Flowing Wetland: Insights into the Fate of Chemical Species. Minerals, 11**,** 477.

Ngulube, T., Gumbo, J. R., Masindi, V. & Maity, A. 2017. An update on synthetic dyes adsorption onto clay based minerals: A state-of-art review. Journal of Environmental Management, 191**,** 35-57.

Nleya, Y., Simate, G. S. & Ndlovu, S. 2016. Sustainability assessment of the recovery and utilisation of acid from acid mine drainage. Journal of Cleaner Production, 113**,** 17-27.

Nordstrom, D. K., Blowes, D. W. & Ptacek, C. J. 2015a. Hydrogeochemistry and microbiology of mine drainage: An update. Applied Geochemistry, 57**,** 3-16.

Nordstrom, D. K., Blowes, D. W. & Ptacek, C. J. 2015b. Hydrogeochemistry and microbiology of mine drainage: An update. Applied Geochemistry, 57**,** 3-16.

Obenaus-Emler, R., Falah, M. & Illikainen, M. 2020. Assessment of mine tailings as precursors for alkali-activated materials for on-site applications. Construction and Building Materials, 246**,** 118470.

Oh, C., Han, Y.-S., Park, J. H., Bok, S., Cheong, Y., Yim, G. & Ji, S. 2016. Field application of selective precipitation for recovering Cu and Zn in drainage discharged from an operating mine. Science of the Total Environment, 557–558**,** 212-220.

Oliveira, C. M., Machado, C. M., Duarte, G. W. & Peterson, M. 2016. Beneficiation of pyrite from coal mining. Journal of Cleaner Production, 139**,** 821-827.

Omotehinse, A. O. & Ako, B. D. 2019. The environmental implications of the exploration and exploitation of solid minerals in Nigeria with a special focus on Tin in Jos and Coal in Enugu. Journal of Sustainable Mining, 18**,** 18-24.

Osman, M. S., Masindi, V. & Abu-Mahfouz, A. M. 2019. Computational and experimental study for the desalination of petrochemical industrial effluents using direct contact membrane distillation. Applied Water Science, 9**,** 29.

Parbhakar-Fox, A. & Lottermoser, B. G. 2015. A critical review of acid rock drainage prediction methods and practices. Minerals Engineering, 82**,** 107-124.

Park, I., Tabelin, C. B., Jeon, S., Li, X., Seno, K., Ito, M. & Hiroyoshi, N. 2019. A review of recent strategies for acid mine drainage prevention and mine tailings recycling. Chemosphere, 219**,** 588-606.

Park, J. H., Edraki, M., Mulligan, D. & Jang, H. S. 2014. The application of coal combustion by-products in mine site rehabilitation. Journal of Cleaner Production, 84**,** 761-772.

Park, S.-M., Shin, S.-Y., Yang, J.-S., Ji, S.-W. & Baek, K. 2015. Selective Recovery of Dissolved Metals from Mine Drainage Using Electrochemical Reactions. Electrochimica Acta, 181**,** 248-254.

Park, S. M., Yoo, J. C., Ji, S. W., Yang, J. S. & Baek, K. 2013. Selective recovery of Cu, Zn, and Ni from acid mine drainage. Environmental Geochemistry and Health, 35**,** 735-743.

Parkhurst, D. L. 1995. User's guide to PHREEQC - A computer program for speciation, reaction-path, advective-transport, and inverse geochemical calculations. User's Guide to PHREEQC (Version 2) - A Computer Program for Speciation, Batch-Reaction, One-Dimensional Transport, and Inverse Geochemical Calculations. Water-Resources Investigations Report 99-4259.

Parkhurst, D. L. & Appelo, C. a. J. 1999. Users guide to Phreeqc (Version 2) - A computer program for speciation, batch-reactions, one-dimensional transport and inverse geochemical calculations. Water-Resources Investigations Report 99-4259.

Peretyazhko, T., Zachara, J. M., Boily, J. F., Xia, Y., Gassman, P. L., Arey, B. W. & Burgos, W. D. 2009. Mineralogical transformations controlling acid mine drainage chemistry. Chemical Geology, 262**,** 169-178.

Petrilakova, A., Balintova, M. & Holub, M. 2014. Precipitation of heavy metals from acid mine drainage and their geochemical modeling. Selected Scientific Papers - Journal of Civil Engineering, 9(1), 79-86.

Phuan, Y. W., Ong, W.-J., Chong, M. N. & Ocon, J. D. 2017. Prospects of electrochemically synthesized hematite photoanodes for photoelectrochemical water splitting: A review. Journal of Photochemistry and Photobiology C: Photochemistry Reviews, 33**,** 54-82.

Pope, J. & Trumm, D. 2015. Controls on Zn Concentrations in Acidic and Neutral Mine Drainage from New Zealand's Bituminous Coal and Epithermal Mineral Deposits. Mine Water and the Environment, 34**,** 455-463.

Potgieter-Vermaak, S. S., Potgieter, J. H., Monama, P. & Van Grieken, R. 2006. Comparison of limestone, dolomite and fly ash as pre-treatment agents for acid mine drainage. Minerals Engineering, 19**,** 454-462.

Pozo-Antonio, S., Puente-Luna, I., Lagüela-López, S. & Veiga-Ríos, M. 2014. Techniques to correct and prevent acid mine drainage: A review. DYNA (Colombia), 81**,** 73-80.

Qu, D., Wang, J., Wang, L., Hou, D., Luan, Z. & Wang, B. 2009. Integration of accelerated precipitation softening with membrane distillation for high-recovery desalination of primary reverse osmosis concentrate. Separation and Purification Technology, 67**,** 21-25.

Ramakokovhu, M. M., Masindi, V. & Tekere, M. 2020. Evaluating the efficacy of thermo-mechano-activated cryptocrystalline magnesite nanosheets for the removal of chromium ions from wastewater. Materials Today: Proceedings. 38, 1006-1017

Rambabu, K., Banat, F., Pham, Q. M., Ho, S.-H., Ren, N.-Q. & Show, P. L. 2020. Biological Remediation of Acid Mine Drainage: Review of Past Trends and Current Outlook. Environmental Science and Ecotechnology**,** 100024.

Ramontja, T., Eberle, D., Coetzee, H., Schwarz, R. & Juch, A. Critical challenges of acid mine drainage in South Africa's Witwatersrand gold mines and mpumalanga coal fields and possible research areas for collaboration between South African and German researchers and expert teams. The New Uranium Mining Boom: Challenge and Lessons Learned, 2011. 389-400.

Ricci, B. C., Ferreira, C. D., Aguiar, A. O. & Amaral, M. C. S. 2015. Integration of nanofiltration and reverse osmosis for metal separation and sulfuric acid recovery from gold mining effluent. Separation and Purification Technology, 154**,** 11-21.

Ristić, M., Opačak, I. & Musić, S. 2013. The synthesis and microstructure of goethite particles precipitated in highly alkaline media. Journal of Alloys and Compounds, 559**,** 49-56.

Rojas, C., Martínez, C. E. & Bruns, M. A. 2014. Fe biogeochemistry in reclaimed acid mine drainage precipitates—Implications for phytoremediation. Environmental Pollution, 184**,** 231-237.

Ryu, S., Naidu, G., Hasan Johir, M. A., Choi, Y., Jeong, S. & Vigneswaran, S. 2019. Acid mine drainage treatment by integrated submerged membrane distillation–sorption system. Chemosphere, 218**,** 955-965.

Sabs 2015. South African National Standard (SANS). Drinking water - Part 2: Application of SANS 241-1

Sahoo, P. K., Kim, K., Equeenuddin, S. M. & Powell, M. A. 2013. Current approaches for mitigating acid mine drainage. Reviews of environmental contamination and toxicology, 226**,** 1-32.

Schug, B., Mandel, K., Schottner, G., Shmeliov, A., Nicolosi, V., Baese, R., Pietschmann, B., Biebl, M. & Sextl, G. 2017. A mechanism to explain the creep behavior of gypsum plaster. Cement and Concrete Research, 98**,** 122-129.

Sen Gupta, S. & Bhattacharyya, K. G. 2012. Adsorption of heavy metals on kaolinite and montmorillonite: A review. Physical Chemistry Chemical Physics, 14**,** 6698-6723.

Seo, E. Y., Cheong, Y. W., Yim, G. J., Min, K. W. & Geroni, J. N. 2017. Recovery of Fe, Al and Mn in acid coal mine drainage by sequential selective precipitation with control of pH. CATENA, 148, Part 1**,** 11-16.

Seo, J., Kwon, D., Yoon, T. H. & Jung, J. 2010. Potential risks of the natural nanoparticles from the acid mine drainage and a novel approach for their toxicity assessment. Toxicology and Environmental Health Sciences, 2**,** 215-220.

Shahrin, S., Lau, W.-J., Kartohardjono, S., Jamshidi Gohari, R., Goh, P.-S., Jaafar, J. & Ismail, A. F. 2019. Chapter 1 - Development of adsorptive ultrafiltration membranes for heavy metal removal. In: LAU, W.-J., ISMAIL, A. F., ISLOOR, A. & AL-AHMED, A. (eds.) Advanced Nanomaterials for Membrane Synthesis and its Applications. Elsevier.

Shengo, M. L., Kime, M.-B., Mambwe, M. P. & Nyembo, T. K. 2019. A review of the beneficiation of copper-cobalt-bearing minerals in the Democratic Republic of Congo. Journal of Sustainable Mining, 18**,** 226-246.

Sheoran, A. S. & Sheoran, V. 2006. Heavy metal removal mechanism of acid mine drainage in wetlands: A critical review. Minerals Engineering, 19**,** 105-116.

Sheoran, A. S., Sheoran, V. & Choudhary, R. P. 2010. Bioremediation of acid-rock drainage by sulphate-reducing prokaryotes: A review. Minerals Engineering, 23**,** 1073-1100.

Sheoran, A. S., Sheoran, V. & Choudhary, R. P. 2011a. Geochemistry of acid mine drainage: A review. Perspectives in Environmental Research. 217-243

Sheoran, V., Sheoran, A. & Choudhary, R. P. 2011b. Biogeochemistry of acid mine drainage formation: A review. Mine Drainage and Related Problems**,** 119-154.

Sheoran, V., Sheoran, A. S. & Choudhary, R. P. 2011c. Biogeochemistry of acid mine drainage formation: A review. Mine Drainage and Related Problems, 119-154

Shu, X.-H., Zhang, Q., Lu, G.-N., Yi, X.-Y. & Dang, Z. 2017. Pollution characteristics and assessment of sulfide tailings from the Dabaoshan Mine, China. International Biodeterioration & Biodegradation, 119-154.

Sierra, C., Álvarez Saiz, J. R. & Gallego, J. L. R. 2013. Nanofiltration of acid mine drainage in an abandoned mercury mining area. Water, Air, and Soil Pollution, 224.

Silva, R. D. A., Castro, C. D., Vigânico, E. M., Petter, C. O. & Schneider, I. a. H. 2012. Selective precipitation/UV production of magnetite particles obtained from the iron recovered from acid mine drainage. Minerals Engineering, 29**,** 22-27.

Silva, R. D. A., Secco, M. P., Lermen, R. T., Schneider, I. a. H., Hidalgo, G. E. N. & Sampaio, C. H. 2019. Optimizing the selective precipitation of iron to produce yellow pigment from acid mine drainage. Minerals Engineering, 135**,** 111-117.

Simate, G. S. & Ndlovu, S. 2014. Acid mine drainage: Challenges and opportunities. Journal of Environmental Chemical Engineering, 2**,** 1785-1803.

Simunika, N., Broadhurst, J. L., Petersen, J. & Franzidis, J. P. 2013. Predicting the time-related generation of acid rock drainage from mine waste: A copper case study.

Singh, S., Sukla, L. B. & Goyal, S. K. 2020. Mine waste & circular economy. Materials Today: Proceedings.

Skandrani, A., Demers, I. & Kongolo, M. 2019. Desulfurization of aged gold-bearing mine tailings. Minerals Engineering, 138**,** 195-203.

Skousen, J. 2014. Overview of Acid Mine Drainage Treatment with Chemicals. Acid Mine Drainage, Rock Drainage, and Acid Sulfate Soils: Causes, Assessment, Prediction, Prevention, and Remediation, 105-118, Online ISBN:9781118749197 |DOI:10.1002/9781118749197

Skousen, J., Zipper, C. E., Rose, A., Ziemkiewicz, P. F., Nairn, R., Mcdonald, L. M. & Kleinmann, R. L. 2017. Review of Passive Systems for Acid Mine Drainage Treatment. Mine Water and the Environment, 36**,** 133-153.

Skousen, J. G., Ziemkiewicz, P. F. & Mcdonald, L. M. 2019. Acid mine drainage formation, control and treatment: Approaches and strategies. The Extractive Industries and Society, 6**,** 241-249.

Sobral, O., Marin-Morales, M. A. & Ribeiro, R. 2013. Could contaminant induced mutations lead to a genetic diversity overestimation? Ecotoxicology, 22**,** 838-846.

Sparks, D. L. 1995. Environmental Soil Chemistry, Academic Press.USA

Sracek, O., Choquette, M., Gélinas, P., Lefebvre, R. & Nicholson, R. V. 2004. Geochemical characterization of acid mine drainage from a waste rock pile, Mine Doyon, Québec, Canada. Journal of Contaminant Hydrology, 69**,** 45-71.

Stolzenburg, P., Capdevielle, A., Teychené, S. & Biscans, B. 2015. Struvite precipitation with MgO as a precursor: Application to wastewater treatment. Chemical Engineering Science, 133**,** 9-15.

Strosnider, W., Winfrey, B. & Nairn, R. 2011. Novel Passive Co-Treatment of Acid Mine Drainage and Municipal Wastewater. Journal of environmental quality, 40**,** 206-13.

Strydom, C. A., Hudson-Lamb, D. L., Potgieter, J. H. & Dagg, E. 1995. The thermal dehydration of synthetic gypsum. Thermochimica Acta, 269-270**,** 631-638.

Syranidou, E., Christofilopoulos, S. & Kalogerakis, N. 2017. Juncus spp.—The helophyte for all (phyto)remediation purposes? New Biotechnology, 38**,** 43-55.

Tabelin, C. B., Veerawattananun, S., Ito, M., Hiroyoshi, N. & Igarashi, T. 2017a. Pyrite oxidation in the presence of hematite and alumina: I. Batch leaching experiments and kinetic modeling calculations. Science of The Total Environment, 580**,** 687-698.

Tabelin, C. B., Veerawattananun, S., Ito, M., Hiroyoshi, N. & Igarashi, T. 2017b. Pyrite oxidation in the presence of hematite and alumina: II. Effects on the cathodic and anodic half-cell reactions. Science of The Total Environment, 581-582**,** 126-135.

Taha, Y., Benzaazoua, M., Hakkou, R. & Mansori, M. 2017. Coal mine wastes recycling for coal recovery and eco-friendly bricks production. Minerals Engineering, 107**,** 123-138.

Talukdar, B., Kalita, H. K., Baishya, R. A., Basumatary, S. & Sarma, D. 2016. Evaluation of genetic toxicity caused by acid mine drainage of coal mines on fish fauna of Simsang River, Garohills, Meghalaya, India. Ecotoxicology and Environmental Safety, 131**,** 65-71.

Talukdar, B., Kalita, H. K., Basumatary, S., Saikia, D. J. & Sarma, D. 2017. Cytotoxic and genotoxic affects of acid mine drainage on fish Channa punctata (Bloch). Ecotoxicology and Environmental Safety, 144**,** 72-78.

The United Nations. 2018. The Sustainable Development Goals Report. In: THE UNITED NATIONS & DEPARTMENT OF ECONOMIC AND SOCIAL AFFAIRS. (eds.).

Tiruta-Barna, L. 2008. Using PHREEQC for modelling and simulation of dynamic leaching tests and scenarios. Journal of Hazardous Materials, 157**,** 525-533.

Tolonen, E. T., Rämö, J. & Lassi, U. 2015. The effect of magnesium on partial sulphate removal from mine water as gypsum. Journal of Environmental Management, 159**,** 143-146.

Torres, E., Ayora, C., Jiménez-Arias, J. L., García-Robledo, E., Papaspyrou, S. & Corzo, A. 2014. Benthic metal fluxes and sediment diagenesis in a water reservoir affected by acid mine drainage: A laboratory experiment and reactive transport modeling. Geochimica et Cosmochimica Acta, 139**,** 344-361.

Tran, H. N., Tomul, F., Nguyen, H. T. H., Nguyen, D. T., Lima, E. C., Le, G. T., Chang, C.-T., Masindi, V. & Woo, S. H. 2020. Innovative spherical biochar for pharmaceutical removal from water: Insight into adsorption mechanism. Journal of Hazardous Materials**,** 122255.

Tran, H. N., You, S.-J., Hosseini-Bandegharaei, A. & Chao, H.-P. 2017a. Mistakes and inconsistencies regarding adsorption of contaminants from aqueous solutions: A critical review. Water Research, 120**,** 88-116.

Tran, H. N., You, S. J., Hosseini-Bandegharaei, A. & Chao, H. P. 2017b. Mistakes and inconsistencies regarding adsorption of contaminants from aqueous solutions: A critical review. Water Research, 120**,** 88-116.

Tripathy, D. P. 2014. Prevention and treatment of acid mine drainage: An overview. Recent Trends in Modelling of Environmental Contaminants.

Truter, J. C., Wyk, J. H. V., Oberholster, P. J. & Botha, A. M. 2014. The impacts of neutralized acid mine drainage contaminated water on the expression of selected endocrine-linked genes in juvenile Mozambique tilapia Oreochromis mossambicus exposed in vivo. Ecotoxicology and Environmental Safety, 100**,** 209-217.

Tutu, H., Mccarthy, T. S. & Cukrowska, E. 2008. The chemical characteristics of acid mine drainage with particular reference to sources, distribution and remediation: The Witwatersrand Basin, South Africa as a case study. Applied Geochemistry, 23**,** 3666-3684.

Vardhan, K. H., Kumar, P. S. & Panda, R. C. 2019. A review on heavy metal pollution, toxicity and remedial measures: Current trends and future perspectives. Journal of Molecular Liquids, 290**,** 111197.

Viadero, R., Wei, X. & Buzby, K. 2006. Characterization and Dewatering Evaluation of Acid Mine Drainage Sludge from Ammonia Neutralization. Environmental Engineering Science - ENVIRON ENG SCI, 23**,** 734-743.

Vigneri, R., Malandrino, P., Gianì, F., Russo, M. & Vigneri, P. 2017. Heavy metals in the volcanic environment and thyroid cancer. Molecular and Cellular Endocrinology, 457**,** 73-80.

Villain, L., Alakangas, L. & Öhlander, B. 2013. The effects of backfilling and sealing the waste rock on water quality at the Kimheden open-pit mine, northern Sweden. Journal of Geochemical Exploration, 134**,** 99-110.

Wang, L., Ji, B., Hu, Y., Liu, R. & Sun, W. 2017. A review on in situ phytoremediation of mine tailings. Chemosphere, 184**,** 594-600.

Wang, L. P., Ponou, J., Matsuo, S., Okaya, K., Dodbiba, G., Nazuka, T. & Fujita, T. 2013. Integrating sulfidization with neutralization treatment for selective recovery of copper and zinc over iron from acid mine drainage. Minerals Engineering, 45**,** 100-107.

Wang, N., Chen, M., Li, Y. Y. & Ni, H. W. 2011. Preparation of MgO whisker from magnesite tailings and its application. Transactions of Nonferrous Metals Society of China (English Edition), 21**,** 2061-2065.

Wei, X. & Viadero Jr, R. C. 2007. Synthesis of magnetite nanoparticles with ferric iron recovered from acid mine drainage: Implications for environmental engineering. Colloids and Surfaces A: Physicochemical and Engineering Aspects, 294**,** 280-286.

Westholm, L. J., Repo, E. & Sillanpää, M. 2014. Filter materials for metal removal from mine drainage—a review. Environmental science and pollution research international, 21**,** 9109-9128.

Who 2017. Guidelines for drinking-water quality: fourth edition incorporating first addendum, Geneva, World Health Organization.

Wissmeier, L. & Barry, D. A. 2010. Implementation of variably saturated flow into PHREEQC for the simulation of biogeochemical reactions in the vadose zone. Environmental Modelling and Software, 25**,** 526-538.

Wu, H.-L., Du, Y.-J., Yu, J., Yang, Y.-L. & Li, V. C. 2020. Hydraulic conductivity and self-healing performance of Engineered Cementitious Composites exposed to Acid Mine Drainage. Science of The Total Environment, 716**,** 137095.

Xenidis, A., Mylona, E. & Paspaliaris, I. 2002. Potential use of lignite fly ash for the control of acid generation from sulphidic wastes. Waste Management, 22**,** 631-641.

Xingyu, L., Zou, G., Wang, X., Zou, L., Wen, J., Ruan, R. & Wang, D. 2013. A novel low pH sulfidogenic bioreactor using activated sludge as carbon source to treat acid mine drainage (AMD) and recovery metal sulfides: Pilot scale study. Minerals Engineering, 48**,** 51-55.

Yadav, S. K. 2010. Heavy metals toxicity in plants: An overview on the role of glutathione and phytochelatins in heavy metal stress tolerance of plants. South African Journal of Botany, 76**,** 167-179.

Yadav, V. B., Gadi, R. & Kalra, S. 2019. Clay based nanocomposites for removal of heavy metals from water: A review. Journal of Environmental Management, 232**,** 803-817.

Yan, B., Mai, G., Chen, T., Lei, C. & Xiao, X. 2015. Pilot test of pollution control and metal resource recovery for acid mine drainage. Water Science and Technology, 72**,** 2308-2317.

Yuan, Y., Wu, Y., Ge, X., Nie, D., Wang, M., Zhou, H. & Chen, M. 2019. In vitro toxicity evaluation of heavy metals in urban air particulate matter on human lung epithelial cells. Science of The Total Environment, 678**,** 301-308.

Zeng, Z., Xie, Y., Hu, X. J. & Lu, Q. 2009. Determination of antimony and bismuth in caustic calcined magnesite by microwave digestion-hydride generation atomic fluorescence spectrometry. Yejin Fenxi/Metallurgical Analysis, 29**,** 65-67.

Zhang, H. & Luo, S. 2007. Modeling the leaching behavior of simulated HLW-glass using PHREEQC. Nuclear Science and Techniques/Hewuli, 18**,** 150-153.

Zhang, M. 2011. Adsorption study of Pb(II), Cu(II) and Zn(II) from simulated acid mine drainage using dairy manure compost. Chemical Engineering Journal, 172**,** 361-368.

Zhang, W.-J., Huo, C.-F., Feng, G., Li, Y.-W., Wang, J. & Jiao, H. 2010. Dehydration of goethite to hematite from molecular dynamics simulation. Journal of Molecular Structure: THEOCHEM, 950**,** 20-26.

Zhang, X., Zhang, K., Lv, W., Liu, B., Aikawa, M. & Wang, J. 2019. Characteristics and risk assessments of heavy metals in fine and coarse particles in an industrial area of central China. Ecotoxicology and Environmental Safety, 179**,** 1-8.

Zhao, H., Xia, B., Qin, J. & Zhang, J. 2012. Hydrogeochemical and mineralogical characteristics related to heavy metal attenuation in a stream polluted by acid mine drainage: A case study in Dabaoshan Mine, China. Journal of Environmental Sciences, 24**,** 979-989.

Zhou, Y., Lu, J., Zhou, Y. & Liu, Y. 2019. Recent advances for dyes removal using novel adsorbents: A review. Environmental Pollution, 252**,** 352-365.

Zhu, C., Wang, Q., Pang, W., Wang, Z., Cao, J., Hu, W., Tang, J., Huang, J. & Wu, Z. 2017. Mechanisms of phosphorus removal from wastewater by ion exchange resin. Desalination and Water Treatment, 79**,** 347-355.

Zipper, C. & Skousen, J. 2014. Passive Treatment of Acid Mine Drainage. Acid Mine Drainage, Rock Drainage, and Acid Sulfate Soils: Causes, Assessment, Prediction, Prevention, and Remediation.

Zumarán Farfán, J. R. J., Barbosa Filho, O. & De Souza, V. P. Environment impacts of the acid drainage of soil waste in the mineral industria. 58th Congresso Anual da ABM (ASSociacao Brasileira de Metalurgia e Materiais), 2003. 1171-1181.

Zvinowanda, C. M., Zikalala, N. N., Mtombeni, T., Maree, J. P., Louw, W. J. & Oosthuizen, F. 2014. Process optimization of freeze desalination of brine using HybridICE^{TM} pilot plant. Desalination and Water Treatment, 52**,** 6315-6324.